University of Alberta

Implementing a UV Disinfection System in a Low-Income Area of Bolivia, South America

by

Mario Alberto Zapata Peláez

A thesis submitted to the Faculty of Graduate Studies and Research
in partial fulfillment of the requirements for the degree of

Master of Science in Environmental Engineering

Department of Civil and Environmental Engineering

Spring 2011
Edmonton, Alberta

To my beloved wife, my loving mother and my courageous brother for all their support in this adventure. In loving memory of my father and my little sister.

ABSTRACT

Microbial pollution of water is one of the principal causes of life-threatening diarrheal diseases in the developing world. Ultraviolet (UV) light is increasingly recognized as a viable alternative for the disinfection of drinking water and wastewater in developed countries, but its feasibility in low-income areas has to be assessed further. The rural community of Cerro Grande, in Bolivia, has been hit by outbreaks of gastrointestinal diseases, so two UV-based disinfection systems were implemented there. One of them was a fabricated unit, with materials available locally, whereas the other was a commercially-available unit. The fabricated unit was validated following USEPA procedures and was modeled using computational fluid dynamics. It was observed that a UV-based disinfection system can be sustainable for as few as 20 users, and even for 48 users in areas with poor feed water quality and lacking an electrical grid and distribution network, with a monthly cost of US$2.

ACKNOWLEDGMENTS

It is almost impossible to list all the individuals and entities that contributed in one or another way to the successful completion of this project. However, I want to extend my deepest appreciation to the following individuals and entities:

My supervisors, Dr. James R. Bolton and Dr. Mohamed Gamal El-Din, for their invaluable support and input throughout all the stages of this process.
Our lab technician Maria Demeter for all her constant and unconditional help.
Mr. Brendan Mulligan, Mr. David Bethune and Ms. Brianna Ball from the University of Calgary.
Mr. Julio Torres from the Universidad San Francisco Xavier in Sucre, Bolivia.
Mr. Trevor Hirsche, Mr. Roberto Salas and Mr. Ernesto Durán from COBAGUAL (Bolivian-Canadian cooperation for clean water).
Trojan Technologies and, especially, Dr. Linda Gowman, for the gift of the Trojan UV disinfection units.
And the community of Cerro Grande for their endless cooperation, especially Mr. Lino Barrientos and Mrs. Narcisa Telegüé.

Furthermore, this project would have not been possible without the grants and financial assistance provided by the following institutions, all of which are greatly appreciated.

The Natural Sciences and Engineering Research Council of Canada (NSERC), Ottawa, Canada
The International Development Research Centre (IDRC), Ottawa, Canada
The Canadian International Development Agency (CIDA), Gatineau, Canada
The Foundation for the Future of Colombia (COLFUTURO), Bogotá, Colombia

TABLE OF CONTENTS

LIST OF TABLES

LIST OF FIGURES

LIST OF COMMON ABBREVIATIONS

AC	Alternate current
ATCC	American Type Culture Collection
BSF	Bio-Sand filter
CFD	Computational fluid dynamics
DC	Direct current
FC	Fecal coliforms
HDI	Human development index
HRT	Hydraulic retention time
LCC	Life cycle cost
LP	Low pressure (mercury lamp)
LPHO	Low pressure high output (mercury lamp)
MP	Medium pressure (mercury lamp)
MUVI	Coefficient of maximum UV inactivation
O&M	Operation and maintenance
OCC	Off-line chemical cleaning
PV	Photovoltaic
PVC	Poly(vinyl chloride)
SD	Standard deviation
SODIS	Solar disinfection
SS	Stainless steel
TC	Total coliforms
UA	University of Alberta
USEPA	United States Environmental Protection Agency
UTALAB	Technical unit of support to laboratories
UV	Ultraviolet
UVT	UV percent transmittance

1. INTRODUCTION

Water is unarguably a fundamental element for the preservation and health of life on Earth, especially that of humans. Nevertheless, polluted water can be the cause of several life-threatening petulancies, including diarrhoeal diseases, which kill over 2.2 million children annually under the age of 5 (WHO, 2000). Although the world coverage of improved drinking water sources was about 86% as of 2006, the gap between the global coverage in urban areas and that in rural areas was 18%. Furthermore, the gap in the access to improved drinking water sources between high-income and low-income countries was about 22%. Consequently, rural areas in low income countries present the lowest access percentage to improved drinking water sources, at only 58% (WHO, 2008). Providing safe potable water is of paramount importance, since safe water, sanitation and hygiene practices may reduce diarrhoeal disease on average between 25% and 33% (WHO, 2000).

Bolivia, which is located in the Andean region of South America, is ranked 113th out of 182 countries (as of 2007) according to the human development index (HDI) of the United Nations (UN). It is also positioned as 117th out of 177 countries (as of 2007) regarding the gross domestic product (GDP) per capita (UNDP, 2009). In 2006, the access of Bolivian population in urban areas to improved water sources was about 96%, whereas in rural areas it was only about 69%; the overall access was about 86% (WHO, 2008). According to Reid (1998), the estimated percentage of disinfected water supplied by the water agencies is 72%, but it decreases to 52% when the rural sector is taken into account. For the

majority of water systems in Bolivia, chlorine is the disinfectant of choice to provide safe potable water, although some attempts have been made in order to implement point-of-use chlorination (Sobsey *et al*., 2003).

The sustainability of water supply projects in low-income regions may be put into jeopardy by many factors, such as poor financial management, lack of ownership by the community, and high capital and recurrent costs (Haysom, 2006). Considering this, disinfection by ultraviolet (UV) light becomes an attractive alternative because it may be implemented with locally available materials, renewable energy sources (sunlight), and with affordable capital and operation & maintenance (O&M) costs.

The research summarised below attempts to carry out an assessment of the implementation of an UV disinfection system in a low-income area of Bolivia, providing answers to questions such as:

- Is it feasible to introduce a UV-based disinfection system into a low-income community of a developing country?
- If feasible, what does it take to implement the system in terms of costs, technical requirements, operation and maintenance, and sustainability?
- What are the benefits of this technology in comparison with other existing technologies, some of which have been already implemented in the study area?

1.1 Organization of this document

This thesis is divided into five chapters, as described below.

- Background literature: this chapter provides a concise survey of the available literature on the topic of this study including UV system components and economic considerations.
- Design and validation of the UV unit: this chapter details all the engineering and experimental procedures carried out in the design and validation of the UV unit, as well as in the design of the electrical and structural systems.
- Computational fluid dynamics (CFD) modeling of the UV unit: this is a chapter devoted to the theory of the CFD modeling, its application to the UV reactor and its coupling with a fluence-rate distribution model.
- Implementing UV disinfection in a low-income community: this chapter deals with all the economic and technical considerations when implementing the UV disinfection system in a low-income community of Bolivia. Its findings may be extrapolated to low-income communities elsewhere.
- Conclusions and recommendations: this chapter provides insights on the results achieved by this study, suggestions for its replication in other places and needs for further research.

2. BACKGROUND LITERATURE

2.1 Definitions

In order to obtain a better understanding of the present document, some useful definitions are presented below. Unless stated otherwise, these terms are adapted from Bolton and Cotton (2008).

Absorbance (*A*) is the common logarithm ($\log_{10}$) of the ratio of the incident to the transmitted irradiance for a light beam, with a wavelength centered at λ, passing through a medium with a path length *l*.

Absorption is the physical process by which the photons are removed from a beam as it passes through a medium containing absorbing substances.

Biodosimetry is a test that assesses the performance of a UV reactor, by comparing the number of viable challenge (or target) microorganisms before and after UV exposure. This test is undertaken in a full-scale UV reactor and a bench-scale setup (*collimated beam apparatus*).

Challenge microorganism is a non-pathogenic microorganism that is used as a surrogate organism for pathogenic organisms in the biodosimetry test.

Collimated beam apparatus is a setup comprised of an enclosed UV lamp and a collimating tube which makes the beam quasi-collimated (parallel). A UV dose-response curve is obtained by exposing the challenge microorganisms to specific UV doses.

Computational Fluid Dynamics (CFD) is a compiled computing code that is able to solve the set of complex Navier-Stokes equations, applied to a given fluid in a limited physical space, through mathematical techniques (Hirsch, 2007).

Concentration is the quantity of a substance per unit of volume or mass. In the case of microorganisms, concentration (or *titre*) is usually referred to as the number of CFU (colony forming units) per unit of volume (usually one or 100 mL).

Disinfection is the process by which water or air is rendered virtually free of pathogenic organisms, whether by physical restraining (filtration), elimination (chemical/physical disinfection) or inactivation (UV light) of such organisms.

DNA and *RNA* stand for deoxyribonucleic acid and ribonucleic acid, respectively. These structures carry the genetic information of a cell and are self-replicable.

Fluence (*F*) is equal to the product of the fluence rate and time, that is, the total amount of UV energy received by a small sphere of cross-sectional area d*A* divided by d*A*. It has units of J/m^2 or mJ/cm^2. It is synonymous with *UV dose*.

Fluence rate (E_o) is the total incident radiant power, coming from all directions, onto a very small sphere of cross-sectional area d*A*. It should not be confused with *irradiance*, as they are conceptually different.

Fouling/aging are the principal factors that reduce the fluence rate inside a UV reactor. Fouling is the accumulation of sediments on the quartz sleeve surface whereas aging is the normal decrease of the UV lamp output over the time.

Irradiance (*E*) is the total incident radiant power, coming from all directions, onto a very small surface of area d*A* divided by d*A*. Its units are W/m^2 or mW/cm^2.

Light is a type of electromagnetic radiation that has properties of a wave and a particle. Its spectrum is usually divided into three ranges, ultraviolet (UV), visible (vis) and infrared (IR), depending on the wavelength.

Low-income communities are those communities where the most of the inhabitants live close to or below a poverty level adopted by a nation. They are also defined as communities lacking essential infrastructure and adequate access to services, such as health and sanitation (Chen and Ravallion, 2008).

Path length is the distance (m or cm) through which a UV light beam passes.

Photon is the smallest 'particle' of electromagnetic radiation, which has energy but no mass.

Photovoltaic cells are devices made of light-sensitive materials (semiconductors) where photons are absorbed, collected and converted to an electrical current (Luque and Hegedus, 2003).

Reduction equivalent dose (RED) is the UV dose (fluence) delivered inside a reactor to achieve a certain level of microbial inactivation, as determined by a biodosimetry test.

Target microorganism is the microorganism that it is intended to be inactivated by a UV system. However, since this is usually a pathogenic organism, it is risky to handle it and, therefore, a surrogate (challenge) organism must be used instead.

Transmittance (*T*) is the ratio of the incident to the transmitted irradiance for a UV beam passing through a medium with a path length *l*.

Ultraviolet (UV) is the portion of the electromagnetic spectrum lying between the wavelengths of 100 and 400 nm.

UV intensity is synonymous with fluence rate, and it is the term used by the USEPA (2006).

Validation is the process by which a UV reactor is guaranteed to deliver a UV dose that successfully achieves a certain log inactivation of a target microorganism.

Wavelength (λ) is the distance (nm) between successive peaks in a light wave.

2.2 A brief overview of UV disinfection

Since the discovery of the waterborne source of the 1853 cholera epidemic in England by Dr. John Snow, much has been accomplished to control waterborne diseases, including shifting water sources or employing different filtration techniques (MWH, 2005). However, it was not until the bacteriological disease-causing agents were clearly identified [1908 (McGuire, 2006)] that disinfection, mainly chemical, became an integral component of every water treatment facility, especially in United States. Chlorine is, and has been, the disinfectant of choice in water treatment facilities in US and Canada for over 80 years. Nevertheless, it was demonstrated in 1974 that trihalomethanes (THMs) – which have been proven to be carcinogenic or mutagenic – are formed by the chlorination of water containing natural organic matter (NOM) (McGuire, 2006). The U.S. Environmental Protection Agency (USEPA) then urged all water facilities to evaluate the implementation of alternative disinfectants in those sites where the formation of THMs would pose a serious health risk for the population (USEPA, 1999). These alternatives include UV disinfection, which is a physical method (unlike other technologies which are chemical in nature), does not produce any harmful by-products and has been proven very effective in the inactivation of highly chlorine-resistant organisms, such as protozoa. With a history of almost

100 years, UV disinfection is increasingly being used as a primary treatment system in many water utilities over North America and Europe (Bolton and Cotton, 2008). It is expected that in the coming years the percentage of large water utilities in the US using UV will increase to over 10% (McGuire, 2006).

UV disinfection is defined as the absorption of light by microorganisms in the 200 – 300 nm wavelength range ('germicidal' range), which causes changes in the DNA and RNA of such microorganisms thus rendering them unviable. UV light is usually emitted by mercury discharge lamps. Among the advantages of UV disinfection are the aforementioned features of being a physical method not producing any harmful by-products, highly effective against protozoa, such as *Cryptosporidium* and *Giardia*, along with being a relatively inexpensive process with a small footprint and fast operation. However, it has some disadvantages, such as a lack of a residual after treatment, difficulty in monitoring the applied UV dose, and high dependence on a continuous electrical supply (Bolton and Cotton, 2008).

2.3 Current status of UV-based disinfection systems in low-income regions

Despite the success of UV disinfection in the countries where it is currently being applied in North America and Europe, it is not widely available in areas with lower incomes, such as in Asia, Africa, and Latin America or, at least, at a municipal or community-centralized water system level (Linden, 2008; Gadgil, 1998). Instead, there have been some attempts to implement UV disinfection at the household level as a point-of-use technology, namely, the solar water

disinfection (SODIS) approach and the UV tube device. The SODIS approach is based on the synergetic action of UVA and UVB and heat acting on water stored in clear bottles sitting on household rooftops, for several hours (Dejung *et al*., 2007).

The UV-tube device is a 65-cm long, 10 cm (4") diameter tube sealed with 10-cm diameter poly(vinyl chloride) (PVC) end caps, containing a General Electric germicidal G15T8 lamp and stainless steel (SS) lining. An average reduction of 4.5 logs was achieved in the MS2 coliphage counts, with a mean UV dose of 900 J/m^2, and a standard error of 80 J/m^2, in field experiments performed in two rural communities in the state of Baja California Sur, Mexico (Brownell *et al*., 2008).

Another UV disinfection system studied in developing countries is described by Gadgil *et al*. (1998). This consists of a semi-cylindrical cross-section aluminum reactor where the UV lamp is held on top and the water underneath flows by gravity. Various field experiments carried out in a water supply of a hospital in South Africa showed average reductions of 3 logs in the number of total coliforms (TC), *E. coli*, *Salmonellae*, and other enterobacteria with this system. Larsen and Brownell (2001) also developed a UV treatment system to be installed in a Haitian clinic. During the first six months of operation of the UV unit, which is preceded by a 1-3 micron industrial filter bag, there was a reported drop in the incidence of diarrheal diseases for the people living near the clinic.

2.4 Economic considerations regarding implementation of UV disinfection systems in low-income regions

The relatively low cost of UV disinfection is a factor making it attractive to be installed in low-income communities. For instance, Solsona and Méndez (2002) and Gadgil (1998) have established estimated operation and maintenance (O&M) costs of US$0.02 per cubic meter ($m^3$), for water treated with UV disinfection. Burch and Thomas (1998) estimated the O&M costs to be US$0.14/$m^3$ for UV disinfection in off-grid locations, and US$0.04/$m^3$ where an electrical supply was available; Vidal and Díaz (2000) estimated these costs as US$0.19/$m^3$. Other estimates are US$10 to US$100 as the O&M costs per family per year (Solsona and Méndez, 2002) and US$0.03 per family per week (Larsen and Brownell, 2001).

As for the capital costs, some reported values of community systems are US$300 (Solsona and Méndez, 2002), US$500 (Burch and Thomas, 1998; Gadgil and Shown, 1995), US$900 (Gadgil *et al*., 1998) and US$86,419 (Vidal and Díaz, 2000). RAEL (2006) and Brownell *et al*. (2008) claim that the UV-tube technology can have an initial cost as low as US$41, though it is to be installed at the household level only. Burch and Thomas (1998) established the life cycle cost of water disinfection with UV-based technologies (capital and O&M costs over their lifetimes) to be in a low to medium place in the scale of processes (from US$0.14 to US$2.35 per m^3). The lowest costs corresponded to slow sand and roughing filtration (US$0.03/$m^3$) and the highest corresponded to water boiling (US$20.83/$m^3$).

2.5 Equipment used in UV disinfection systems – UV reactor chamber

The equipment used in UV disinfection usually includes key components, such as UV lamps, sleeves, and UV sensors. However, one important component is the reactor casing that encloses all of the previously mentioned elements. Commercially, the preferred material used to build UV reactor chambers is stainless steel (SS) (Bolton and Cotton, 2008). It should be noted that this kind of closed-pipe reactor is commonly used for the disinfection of drinking water, whereas open-channel reactors are used mostly in the disinfection of wastewater.

2.5.1 Physical characteristics of the UV reactor chamber

Independent of the material that the chamber is made of, or the way the flow is directed inside it, a UV reactor to be installed in a low-income area must provide durability, reliability and affordability.

2.5.2 Hydraulic characteristics of the UV reactor

A key factor for the performance of a UV reactor is its hydraulics. Only by evaluating the hydraulic behaviour of the UV reactor is it possible to determine the path microorganisms will follow, so that they obtain a sufficient exposure to the UV source acquiring, in turn, a UV dose that renders them inactive. Therefore, in addition to evaluating the hydraulic behaviour of the reactor, it is necessary to assess the UV dose that is delivered across the entire reactor. This can be estimated by coupling a fluence-rate distribution model, which determines the fluence rate at any position in the UV reactor for a given UVT, with a program modeling fluid dynamics. As a consequence, the approximate position of a

particle, and the UV dose that is receiving (resulting from the fluence-rate model), can be modeled (Bolton and Cotton, 2008).

In low-income sites, where the objective is to keep costs as low as possible, yet be functional, the design should favour a gravity installation, so intermediate booster pumps do not have to be used. The inlet/outlet piping configuration is particularly important when performing the validation of the UV reactor, since this configuration can affect the UV dose delivery (Bolton and Cotton, 2008).

2.5.3 Validation of the UV reactor

This is a procedure used to determine the performance of a UV reactor under some given conditions of water quality, flow rate, lamp performance and reactor hydraulics (Bolton and Cotton, 2008). Currently, the only approach for UV reactor validation accepted by the USEPA is biodosimetry, which consists in measuring the log inactivation of a challenge microorganism during full-scale reactor testing for specific operating conditions of flow rate, UVT and UV sensor reading. The measured log inactivation is then determined for the challenge microorganism by obtaining a UV dose-response curve – derived from bench-scale experiments – in order to estimate the reduction equivalent dose (RED). The RED, in turn, is adjusted to include uncertainties and biases [See Figure 5.1 in USEPA (2006)]. Given the risk and difficulty of handling actual pathogenic microorganisms, it is necessary to employ challenge microorganisms to estimate the RED. This RED must then be adjusted to account for the uncertainty in the challenge microorganism UV response when compared to that of the target organism (USEPA, 2006).

The validation factor (*VF*) takes account of uncertainties and biases including, for example, the UV sensitivity of the challenge organism with respect to that of the target organism. The validated dose is then obtained by dividing the RED by the *VF*. Determination of *VF* (unitless) is given by Equation 5.13 in USEPA (2006), shown below as Equation 2-1.

$$VF = B_{\mathrm{RED}} \times \left(1 + \frac{U_{\mathrm{Val}}}{100}\right) \tag{2-1}$$

where *VF* is the validation factor (unitless), B_{RED} is the RED bias factor (unitless) and U_{Val} is the uncertainty in the validation determination (expressed as %).

The two UV dose-monitoring strategies currently accepted by the USEPA are the *UV intensity set-point* approach and the *calculated-dose* approach (USEPA, 2006). The UV intensity set point approach deals with determining one or more 'set points' for the UV sensor, so that the UV intensity meets or exceeds these set points and in turn the validated UV dose to be delivered. This approach is usually recommended for small water utilities (USEPA, 2006).

2.6 Equipment used in UV disinfection systems – UV lamps

UV lamps are the most important components of UV disinfection systems (Bolton and Cotton, 2008). The most common types of UV lamps are low pressure (LP), low pressure high output (LPHO), and medium pressure (MP); a complete description of the various types of UV lamps can be found in Bolton and Cotton (2008) and USEPA (2006). Previously, the assessment of sustainable technologies in low-income communities was discussed. From this, two specifications of UV lamps stand out: estimated lamp life and input power. This is because both

features have a strong impact on the capital and O&M costs of a UV facility. A comparison chart for these specifications is presented in Table 2-1.

Table 2-1 Estimated lamp life and input power of UV lamps

Characteristic	Lamp Type			Reference
	LP	LPHO	MP	
Estimated lamp life (h)	8000-12000	7000-10000	3000-6000	Bolton and Cotton (2008)
	8000-10000	8000-12000	4000-8000	USEPA (2006)
	8000-10000	8000-10000	3000-5000	MWH (2005)
Input power* (W/cm)	0.2-0.4	0.6-1.2	125-200	Bolton and Cotton (2008)
	0.5	1.5-10	50-250	USEPA (2006)
	0.3-0.8	1.7-4.2	8.3-83	MWH (2005)

* Based on a 120 cm-long UV lamp

From Table 2-1, the best option for a UV-disinfection system in a low-income community would be a LP lamp because of its longer lifetime and lower power consumption. Moreover, its germicidal efficiency is higher than that of MP lamps, since its principal emission (82%) is at 253.7 nm (Bolton and Cotton, 2008).

2.6.1 UV lamp aging

As lamps age, they undergo processes (e.g., solarisation and deposition of tungsten and mercury on the interior of the lamps) that affect their output. Solarisation is defined as the change in quartz transmittance caused by photo-thermal damage while the deposition of tungsten and mercury arises principally from electrode sputtering during start-up (First *et al*., 2007; USEPA, 2006). Although First *et al*. (2007) established one year as a safe period for the

replacement of UV lamps, the best reference for the adequate frequency of lamp change should be provided by the manufacturer itself (USEPA, 2006). Under operating conditions, lamp aging may be detected when sensor readings are consistently below those corresponding to the validated UV dose, even if sleeve cleaning has already taken place.

2.7 Equipment used in UV disinfection systems – Sleeves

Sleeves enclose UV lamps, so that they will not come into contact with the surrounding water, in order to keep a proper working temperature of about 40 ºC [for LP lamps (USEPA, 2006)]. Sleeves are usually made of good quality quartz, which is one of the few materials that transmits UV in the 200–300 nm range. The USEPA (2006) provides some of the most important characteristics of sleeve materials, as well as actions to be undertaken when installing and operating UV lamps to avoid or minimize the effects of lamp breakage and mercury spills.

2.7.1 Sleeve fouling

Sleeve fouling arises principally from precipitation reactions that usually take place under moderate concentrations of iron and hardness coupled with thermal activation (USEPA, 2006; Lin *et al*. 1999). Fouling, however, is a very complex process and the composition of the deposits has been found to be completely heterogeneous, without a clear predominant element (Lin *et al*., 1999). Fouling decreases the quartz UVT, and thus the lamp output to the water (Bolton and Cotton, 2008; USEPA, 2006), so a cleaning strategy should be implemented.

On the other hand, depending on the cleaning system used, that is, off-line chemical cleaning (OCC), on-line mechanical cleaning (OMC) or on-line

mechanical-chemical cleaning (OMCC), some type of 'permanent' fouling may arise. For example, Peng *et al*. (2005) showed that sleeves subject to mechanical cleaning only were more prone to undergo permanent fouling than those exposed to mechanical-chemical routines. As a consequence, the lamp sleeve fouling should be cleaned periodically (2–3 times per month) by rinsing it with an acid solution (OCC) (Bolton and Cotton, 2008). Acetic acid (vinegar) is an affordable acid solution that can be used in the lamp OCC. Both lamp aging and sleeve fouling have to be considered when calculating the operational set point in the UV intensity set point approach. See a detailed description of the testing in USEPA (2006).

2.8 Equipment used in UV disinfection systems – UV sensors

UV sensors are devices used to measure the irradiance at a given point inside the UV reactor, usually consisting of a photodetector, optical components and electrical connections (Bolton and Cotton, 2008; USEPA, 2006). Sensors are a vital component of the UV system, especially when the set point approach is used to monitor the UV dose. The position of the UV sensor is very important, since sensor readings are affected by the UV lamp output, sleeve transmittance, UVT and fouling of the sensor window (Bolton and Cotton, 2008). Ducoste and Linden (2005) state that the correct positioning of the UV sensor should be such that the variation in the sensor readings is proportional to the effectiveness of disinfection, regardless of changes in UVT or lamp output.

2.9 Equipment used in UV disinfection systems – Ballast

The ballast is a device used to provide regulated current to the lamp in order to ignite the discharge and operate smoothly. Currently, there are two types of commercially available ballasts: magnetic and electronic. The former is based on a magnetic choke working at line frequency (50–60 Hz) while the latter is based on solid-state electronic devices that regulate the output current and work at higher frequencies than line frequency (Rashid, 2007). As with other components, ballasts must provide durability, reliability and cost-effectiveness.

2.9.1 Power supply

The most frequent and inexpensive power supply for UV lamps in UV disinfection systems is the electrical grid. In household connections, the grid operates at a frequency between 50 and 60 Hz, with a voltage ranging from 100 to 240 V in alternate current (AC). The load, that is, the number and potency of appliances connected to the grid, defines the required power. The load in small UV disinfection systems would be the power required by the UV lamp(s) plus the additional power required by the other components and external devices, such as pumps. However, in some low-income regions, photovoltaic (PV) systems appear as a better choice for power; they even have been integrated into water pumping stations and water purification systems in order to preserve a continuous and safe operation (Luque and Hegedus, 2003).

Small PV systems, which function in a stand-alone manner (that is, not connected to the electrical grid), are comprised of a generator (module of PV cells), an accumulator (usually an electro-chemical battery), a charge controller

and an inverter [to convert direct current (DC) into AC]. The battery is regarded as the 'weakest link of the chain' because of its short life expectancy (about 3 years). To overcome this shortcoming, the UV system could include a reservoir. The generator would work during the day, when sunlight is available, and the water produced during this period would be stored in the reservoir. This way, there would be no need to provide a battery that works at night to power the UV lamp, and treated water would be available at all times. This scheme has been widely applied in solar-powered pumps for the extraction of groundwater (Argaw, 2003; Abu-Hamdeh, 2000; Alawaji *et al*., 1995).

2.10 Equipment used in UV disinfection systems – Alarm system

In UV-based water treatment systems, the alarm system is closely related to the UV sensor as this system provides a visual and/or audio signal that warns the operator about problems or conditions going on in the reactor. These conditions may include, for example, changes in the UV lamp output, as recorded by a UV sensor. In small water utilities, a single microprocessor (about US$100) is usually enough to translate the analog signal of a UV sensor into the digital signal of an alarm system (Bishop, 2002). The alarm might then be visual (LED), sound (buzzer) or dual-type 2008.

3. DESIGN AND VALIDATION OF THE UV UNIT

3.1 Installation site

Good engineering practice suggests that before undertaking any engineering project that intends to solve a problem, the context of the project should be described sufficiently and adequately, so that requirements and potential solutions can be envisaged at an early stage (Targýt, 2004). Therefore, a detailed description of a low-income community in Bolivia is presented first, including a brief history of its selection, current conditions, geographic location, and other relevant information.

3.1.1 Background of the site selection process

This study was conducted in Bolivia because a verbal agreement between the University of Alberta (UA) and the University of Calgary (UC) paved the way for the execution of this project in that country. Since 2007, the UC has been working in a project of water resources management in Bolivia, with funding from the Canadian International Development Agency (CIDA). So, with funds coming from the UA and the UC, and additional funding provided by a research grant of the Association of Universities and Colleges of Canada (AUCC), everything was set for field work. During the first trip, a Bolivian non-governmental organization (NGO), COBAGUAL (Cooperación Boliviana para agua limpia – Bolivian-Canadian cooperation for clean water) was contacted. COBAGUAL promotes the use of sand filters manufactured on site to treat water. This NGO is based in the municipality of Ascensión de Guarayos (Ascensión), in eastern Bolivia, and was

the ultimate link for contacting the leaders of the rural community of Cerro Grande.

3.1.2 Physical description of the study area

As mentioned, the community selected for this study was Cerro Grande, a rural community located about 60 km northwest of the urban area of Ascensión, province of Santa Cruz, Bolivia (Figure 3-1). Cerro Grande is a jurisdiction of the municipality of Ascensión which is in turn a jurisdiction, and the capital, of the county of Guarayos.

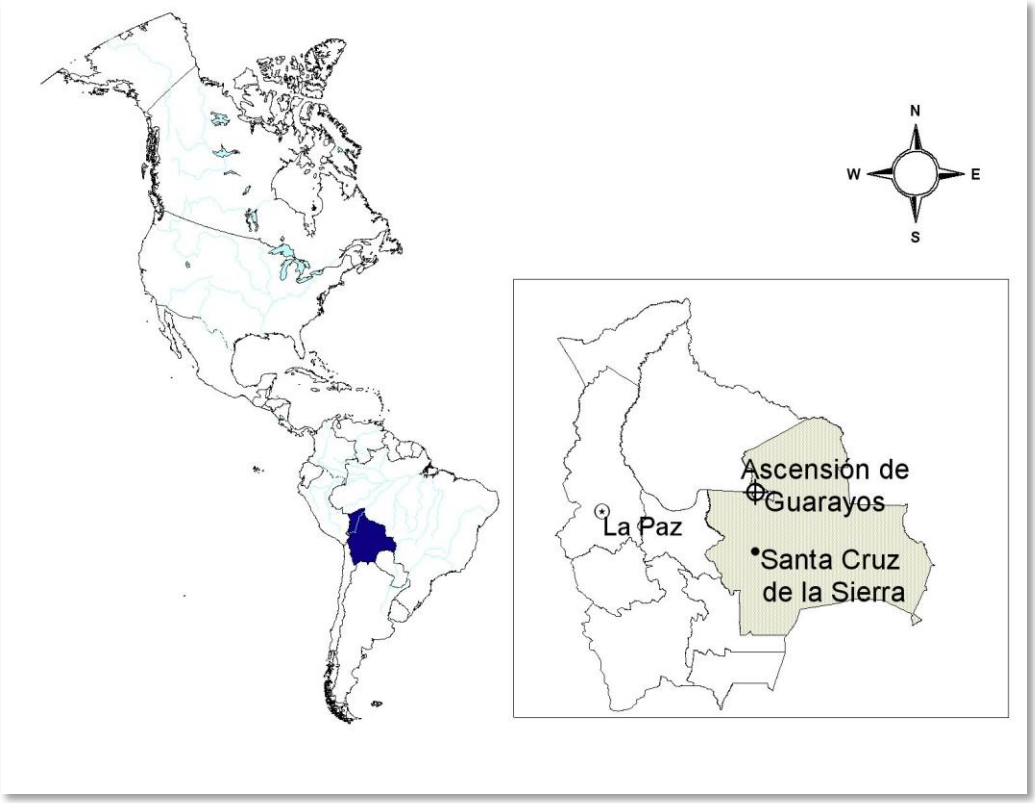

Figure 3-1 Location of Bolivia in the American continent and of Ascensión in Bolivia

This community is located at latitude 15º 37' 59" South and longitude 63º 34' 09" West (Garmin eTrex Vista C GPS, Olathe, KS), at the elementary

school, and at an altitude of 187 m above mean sea level. It is located next to National Route 9, which links the provinces of Santa Cruz and Beni. The mean annual temperature is about 25 ºC, with a cooler season in the months from May to September and a rainy season during the months of November through March, for an average annual precipitation of 1020 mm. The soils in this zone are of mainly clay composition (40% sandy clay loam and 50% clay) and are considered good for agriculture and livestock. Hydrographically, Cerro Grande is located in the San Pablo River basin, which in turn is contained in that of the Amazon River (GMAG, 2006).

3.1.3 Demographic and socioeconomic aspects

The population of Cerro Grande was estimated to be 413 inhabitants in 2005, 283 male and 130 female, comprising 100 families. There are no reports of specific age composition for this community, but for the whole rural population of Ascensión the age and gender breakdown is shown in Table 3-1 (GMAG, 2006). A substantial percentage (50%) of the rural population is aged 18 or younger, and from this segment almost half (42%) is aged 5 or younger.

Education in the community is provided at the elementary level in the local school while secondary-level education is provided in the urban area of Ascensión and post-secondary education is offered in the province's capital city (GMAG, 2006). No specific illiteracy rates are reported for the community, but the results of the 2001 census indicate a rate of 15% illiteracy in the rural area of the province of Santa Cruz, with a higher rate for women (22%) than for men (9%).

The average of years of study in rural Santa Cruz for population aged 19 or older is five (INE, 2009).

Table 3-1 Age and gender composition of the rural population in Ascensión (as of 2001)

Age range (years)	Inhabitants				Subtotal	%
	Male	%	Female	%		
0 – 5	509	10.8	472	10.0	981	20.9
6 – 18	789	16.8	594	12.6	1383	29.4
19 – 39	923	19.6	542	11.5	1465	31.2
40 – 64	498	10.6	240	5.1	738	15.7
65 and over	79	1.7	54	1.1	133	2.8
Totals	2798	59.5	1902	40.5	4700	100.0

Morbidity causes in children under the age of 5 have been identified as acute diarrheal infections (34%), acute respiratory infections (15%), and low weight at birth (3%). Statistics from 2001 reveal an infant mortality rate in Ascensión of 50.5 per 1000, or 5.1%; however, the results of a more profound and recent (2005) assessment in the rural zone (67% of the rural communities) indicate a higher mortality rate in this area, as much as double (10.2%). Currently, there is a nursery station (including a part-time male nurse) for the community, equipped with water and sanitation, some medical equipment, and two rooms (GMAG, 2006).

There are 1044 households in rural Ascensión. Several of these dwellings are made of adobe walls and thatch roofs, and some of them have separate, adequate spaces for kitchen and bathroom (35%), kitchen or bathroom (33%) or no spaces at all for kitchen and bathroom (22%) (GMAG, 2006). Households in the

community of Cerro Grande are not connected to any type of utility, such as running water or electrical grid. The number of inhabitants per household in rural Ascensión is estimated close to 5 (GMAG, 2006).

Agriculture and livestock are the principal economic activities in the municipality of Ascensión, employing 49% of the workforce, followed by low-skilled occupations (23%), and construction and manufacture trades (13%) (GMAG, 2006). Official records show that agriculture and livestock workers in rural areas of Bolivia earned an average monthly wage of Bs.$249 (US$35.60) in 2007; in the same year, the legal monthly minimum wage was Bs.$525 (US$75) (INE, 2009). Specific salary figures for Cerro Grande or rural Ascensión could not be found. According to official data, 88% of the population of Ascensión is considered to be poor, which includes people living in moderate poverty (56%) and indigence (32%), both in the urban and rural areas. The HDI numerical value for Ascensión was 0.629 in 2005, while the overall value of this index for Bolivia was 0.691 (INE, 2009). As a comparison, the reported 2007 HDI value for Canada was 0.966 (UNDP, 2009).

3.1.4 Current state of water supply, sanitation and electricity utilities

As noted above, the community of Cerro Grande lacks access to piped water, waste drainage and an electrical grid. Although the community households are dispersed, the bulk of the population is located somewhat close to the local school. For their water supply, they rely on 21 m-deep, hand-dug wells from which water is extracted with the help of manual pumps, so locals have to walk all the way to the well in order to collect water in 5-gallon jugs. There are three of

these pumps in the largest settlement, but only two of them are presently functional. Figure 3-2 shows the pump most frequently used by the residents.

Figure 3-2 Principal manual water pump in Cerro Grande

According to the residents, the water delivered by this pump has a slightly salty flavour, yet the water itself appears clear. A grab sample was taken from the pump in order to verify its water quality. Results of lab analyses are presented in Table 3-2. All of these parameters, excepting the UV percent transmittance and the total organic carbon (TOC), were analyzed by UTALAB (Unidad técnica de apoyo a laboratorios – Technical unit of support to laboratories). This is an ISO 9001:2000 accredited laboratory, and part of Universidad Gabriel René Moreno in Santa Cruz de la Sierra, Bolivia. The original report is shown in Appendix B. All UV percent transmittance (or absorbance) measurements were made using a spectrophotometer (Ultrospec 2100 pro, GE Healthcare Biosciences, Pittsburgh, PA) set at a 254 nm wavelength and a 10-mm path length. TOC was analyzed

using a TOC analyzer (Apollo 9000, Teledyne Tekmar, Mason, OH). Both pieces of equipment are located at the UA. These results will be further discussed later on.

Table 3-2 Laboratory results for a grab sample taken at the principal manual pump of Cerro Grande

Parameter	Units	Value	Method
Total alkalinity ($CaCO_3$)	mg/L	492	Titration
Total coliforms	CFU/100 mL	59	Membrane filter
Fecal coliforms	CFU/100 mL	< 2	Membrane filter
Total suspended solids	mg/L	7	Gravimetric
Total solids	mg/L	1336	Gravimetric
Turbidity	NTU	0.4	Nephelometric
UV transmittance	%	97.5	Spectrophotometry
Total organic carbon	mg/L	0.52	Oxidation by combustion

Since August 2009, a project has been underway to deliver running water to some communal taps and the local school and nurse station. To this end, a 5000-L reservoir tank was installed on top of a 6 m-tall wood tower. Water reaches the tank with the help of a submersible pump that is installed in a 90 m-deep, 4-inch diameter pumping well, which had been drilled since 2007 but had not yet been put into service. The pump is powered by a 8.1 kW gasoline generator. Both suction and impulsion pipes have a diameter of 1-1/2 in., this also being the diameter for the water main. Domestic tap connections will be completed on an on-demand basis, whereby the inhabitants have to provide for materials and labour in order for them to hook up to the water main.

Sanitation in the community is carried out through the use of latrines, which may or may not have an enclosure; this enclosure, if present, is usually a portable wooden cubicle that can be installed wherever is required. The mean depth of latrines is around 2 m. Neither national nor municipal interconnected systems cover the community yet, so a few households rely on electricity generated on site, mainly with gasoline generators. The local public phone is powered by a solar cell system.

3.2 Hydraulic design

The performance of a UV unit is strongly dependent on an adequate hydraulic design, which should in turn take into account all the constraints derived from a particular installation site. Below, the technical considerations for this process are listed.

- The equipment should function by gravity.
- The design should take into consideration the need for most materials to be purchased locally.
- The lack of water distribution mains forces the residents to collect water in containers, and store them at home, for the daily use.
- The levels of training and income in the community are not very high (see Section 3.1.3).

3.2.1 Design parameters

Accounting for the aforementioned factors, the following are the hydraulic design parameters chosen for the UV unit.

- *Flow rate*: the water consumption is usually lower when the source is not a residential tap, given the difficulty in fetching water from the source. Gadgil (1998) notes that a significant number of developing countries (within the ones under review) establish 20 L as the minimum quantity of water per person per day. Bolivian regulations establish that when communal taps are considered, the daily water consumption should be about 30 L/person/day maximum (MSOP, 2004).

Considering 24 families that regularly use the well (total population of about 150 persons) and 30 L as the daily quantity of water required per person, the total water volume that needs to be treated in a day is 4,500 L. The time period in which the most water-fetching takes place is about four hours (from around 8 am to noon), so this is the time used in the calculation of the flow rate, as shown in Equation 3-1.

$$Q = \frac{V}{t} = \frac{4500\,\mathrm{L} \times 1\,\mathrm{h}}{4\,\mathrm{h} \times 3600\,\mathrm{s}} = 0.312\,\mathrm{L\,s^{-1}} \qquad (3\text{-}1)$$

where Q is the flow rate (L/s), V is the volume (L) and t is the time (s).

- *Volume of reservoir*: the UV unit must include a reservoir because of the use of unreliable electricity sources. Since the residents collect water in a limited period of time, it would be advisable to reduce the size of the tank (down from 4,500 L). This way, the treated water is delivered more rapidly and capital and O&M costs are reduced. Therefore, considering a residence time in the tank of one hour, this yields a volume of 1,125 L (1.125 m^3). Since it is intended that the unit should work by gravity, a second tank must be devised. However, this tank is not to function as a reservoir but rather as an equalizer, that is, to be used to keep

a steady water level (head) at the inlet of the UV reactor. Further, this tank need not have the same size as the reservoir.

- *Diameter and length of the UV reactor*: since this is a system that is fed from a tank, the equation that best illustrates the resulting flow rate is given in Equation 3-2 (Nalluri and Featherstone, 2009).

$$Q = C_d \cdot a\sqrt{2gh} \tag{3-2}$$

where Q is the flow rate (m^3/s), C_d is the discharge coefficient (unitless), a is the cross-sectional area of the conduct (m^2), g is the acceleration of gravity (assumed as 9.80665 m/s^2) and h is the level of water (head) above the orifice (m).

An element affecting the sizing of the reactor is the UV lamp itself. Since this reactor will deal with somewhat fluctuating flow rates throughout the day, it is advisable to install a UV lamp that is robust enough to withstand these conditions. Although the design must be confirmed through biodosimetry tests – and fluence rate and CFD modeling – a first guess calls for a LP UVC lamp, with a nominal rating of 50 W. According to the input power shown in Table 2-1, such a power would be obtained for lamps at least 1.25 m long, using a power density of 0.4 W/cm. Consequently, the reactor should be at least 135 cm long. Considering this reactor length; a commercial diameter of 3" (7.62 cm) for the reactor and of 2" (5.08 cm) for the reactor inlet; a C_d of 0.5 (see Nalluri and Featherstone, 2009); and by substituting in Equation 3-2, a 5 cm hydraulic head is enough to deliver the required flow rate. A longer hydraulic retention time (HRT) would result in a longer exposure to UV light and, hence, a more effective disinfection. However, it should be noted that this is a preliminary hydraulic modeling of the reactor, as it is

assumed to be a plug-flow reactor (PFR), with a full cross-sectional area (*a*), and with an insignificant head loss by friction and accessories. A more sophisticated verification has to take place by using CFD modeling.

- *Materials*: it was considered in this study that a clear material for the reactor might increase people's acceptance for the technology, as they would actually get to see the device working. This leads to the option of a polymeric material, such as PVC or poly(methyl methacrylate) (PMMA), the latter commonly known as acrylic glass. Photodegradation of PVC takes place in the range of 280–500 nm because of the several additives in the PVC that absorb UV light, and the light-induced dehydrochlorination (Shi *et al*., 2008; Andrady *et al*., 1989). Photodegradation of PMMA, on the other hand, is not very well defined. Authors point out that it takes place at wavelengths from 320 nm and above (Torikai and Hasegawa, 1998), from 230 nm and above (Fox *et al*., 1963) or does not take place at all in the UV range (Nagai *et al*., 2005). There is general consensus, however, that at 254 nm PMMA, like PVC, strongly absorbs UV light, which makes it safe for installation and visual monitoring. The U.S. National Sanitation Foundation (NSF) deems health safe all those plastic products (PVC, PMMA and related) that are in compliance with the NSF/ANSI Standard 61, "Drinking water components – Health effects" (NSF, 2004).

3.2.2 Final prototype

After completing the drafting of the UV unit, it was taken to a workshop in order to build the prototype. PG Plastics (Edmonton, AB) was in charge of manufacturing the prototype. During the construction phase, it was decided to

build the top tank smaller than the bottom one in such way that it could be put away inside it when moving of the unit was required. Also, it was decided to use plastic bolted flanges instead of the end caps considered during the design to facilitate O&M. The material used to construct the UV reactor was ¼"-thick, clear PVC, compliant with the NSF/ANSI Standard 61, as PMMA was not readily available at the time. Another modification from the original design was the use of ball valves in both sides (inlet and outlet) to improve O&M. The unit was proven watertight with the use of O-rings in the union between the flange and the quartz sleeve and neoprene rubber in the flanges. The roof of the unit was made such that it could be tilted when installing the solar panel. The final prototype as completed is shown in Figure 3-3.

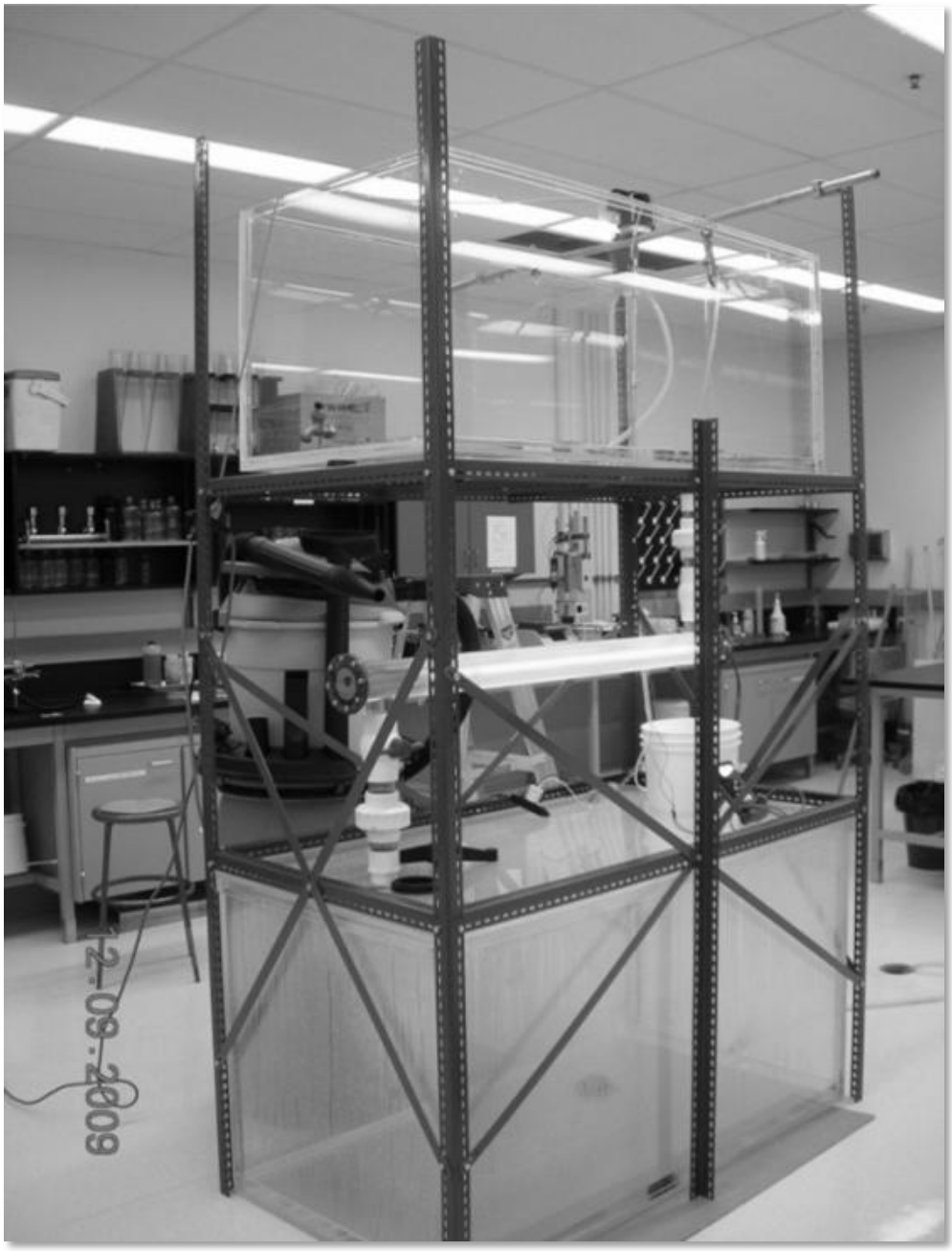

Figure 3-3 Final prototype of the UV unit displaying the steel framework and the lamp in operation

3.3 Electrical and structural design

3.3.1 Design of the PV system

The absence of an electrical supply makes it necessary to look at alternative energy sources. Being located between the parallels 9º 40' and 22º 53' South, Bolivia is one of the countries having the largest values of incident solar radiation. As a matter of fact, the lowlands (provinces of Beni, Pando and Santa Cruz) receive an average of 4900 W/m^2/day and 2000-2200 hours per year of solar light (Guzmán-Ortiz, 2010). This demonstrates a large potential for the implementation of PV systems in these areas.

PV systems are, as mentioned previously, those systems in which the light energy that comes from the sun (or any other light source) is converted into electrical energy through the use of solar cells. Materials for solar cells include mono-crystalline (c-Si), poly-crystalline (p-Si) and amorphous silicon (a-Si), GaAs, GaInP, Cu(InGa)Se_2, CdTe, among others, but silicon is the most common material (Luque and Hegedus, 2003). Overall efficiencies of PV modules in practice reach about 15%, with values often ranging between 8% and 12%. A typical value given by manufacturers is 10%. Equation 3-3 [referred to as Equation 20.80 in Luque and Hegedus (2003)] can be used to verify the size of a PV generator and an accumulator (battery) as a function of the installed load.

$$C_A = \frac{\eta_G \times A_G \times \overline{G_d}}{L} \text{ and } C_S = \frac{C_u}{L} \tag{3-3}$$

where C_A is the generator capacity (unitless), η_G is the conversion efficiency (unitless), A_G is the area of the PV generator (m^2), $\overline{G_d}$ is the average daily

irradiation on the generator surface (Wh/m^2), C_S is the battery capacity (unitless), C_u is the useful energy storage capacity of the battery (Wh) and L is the mean daily energy consumed by the load (Wh).

Technically, it is considered correct to use values for C_A and C_S that have been proven successful in hundreds of previous experiences. For installation in rural settings, values of $C_A = 1.1$ and $3 \leq C_S \leq 5$ have been widely employed (Luque and Hegedus, 2003); a value of 4 is a good guess for C_S. L can be computed from the load (the UV lamp potency or 55 W) operating during six hours, in order to keep an overestimate that accounts for unforeseen circumstances. Given this, L yields a value of 330 Wh. Considering regular commercial PV modules, an efficiency of 10% can be safely assumed.

The horizontal average daily radiation can be estimated from the clear-sky Page model as investigated by Tham *et al*. (2009), as there are no available records in the vicinity of Ascensión. This model considers the components of total solar radiation (direct-beam and diffuse irradiance) as being dependent on Linke turbidity factor and solar altitude, and it was proven adequate for semi-arid or mild climatic locations like Ascensión. In order to apply this model, ETRESH (2010) has a spreadsheet available programmed by Tham *et al*. (2009). The required Linke turbidity factor for a specific location assesses the effects of atmospheric gases, geography and time on the hourly irradiation and can be computed according to SODA (2004). Also, historical records of the required average daily standard atmospheric pressure are listed by TuTiempo.net (2010), along with other relevant climatic information. Historical records for Ascensión

date back from 1976. The Page model does not include the effects of albedo (ground reflection) irradiance, so a value of 0.2 times the average horizontal daily radiation was taken for this effect (Luque and Hegedus, 2003). Although the information available for the Ascensión station (latitude 15º 42' S, longitude 63º 06', altitude 247 m AMSL) spans over a number of years, only 2008 was considered for estimating solar radiation, since it was the most recent year with information for all of the 12 months. After applying the model, the month with the least average hourly radiation was August (548 Wh/m^2), and for this month the day having the least radiation was the 3rd (5918 Wh/m^2). This is the design value for average horizontal daily radiation, but it has to be further refined to account for a fixed inclined surface. An optimal orientation for the PV module in Ascensión is a north-facing tilt of 15º, as this is the approximate latitude of the site.

With this, and after solving the equations 20.39, 20.40 and 20.41 in Luque and Hegedus (2003), a daily irradiation on the generator surface ($\overline{G_d}$) of 4918 Wh/m^2 was found. By substituting this value in Equation 3-3, in addition to the values of C_A, η_G and L, and solving for A_G a value of 0.74 m^2 is obtained. By replacing C_S and L in Equation 3-3, a value of 1320 Wh results for C_u. Taking into account that power equals the product of voltage times current ($P = VI$), then the capacity of a regular 12 V battery, expressed in Ah, should be 110 Ah.

After having these values and with the advice of a retailer (Conergy, Edmonton, AB), a 125 W-rated solar panel (BP 3125J, BP p.l.c., London, UK) was selected (dimensions 1510 mm × 674 mm). Moreover, a 300 W inverter

(SureSine-300, Morningstar Corporation, Washington Crossing, PA) and a PV system (charge) controller (SunSaver SS-10L-12V, Morningstar Corporation, Washington Crossing, PA) were acquired from the same retailer. Given some import restrictions, a 65 Ah sealed lead-acid battery (NP 65-12I, Yuasa Battery Inc., Laureldale, PA) had to be purchased separately in Santa Cruz de la Sierra, Bolivia. The gross area of the solar panel is 1.01×10^6 mm^2 or 1.01 m^2, but BP Solar (2003) establishes that such module is comprised by 36 polycrystalline cells (156 mm×156 mm) in an array of 9×4. This results in a net area of 8.76×10^6 mm^2 or 0.88 m^2 that is still a larger area than that computed from Equation 3-3. The diagram for the electrical system setup is displayed in Figure 3-4.

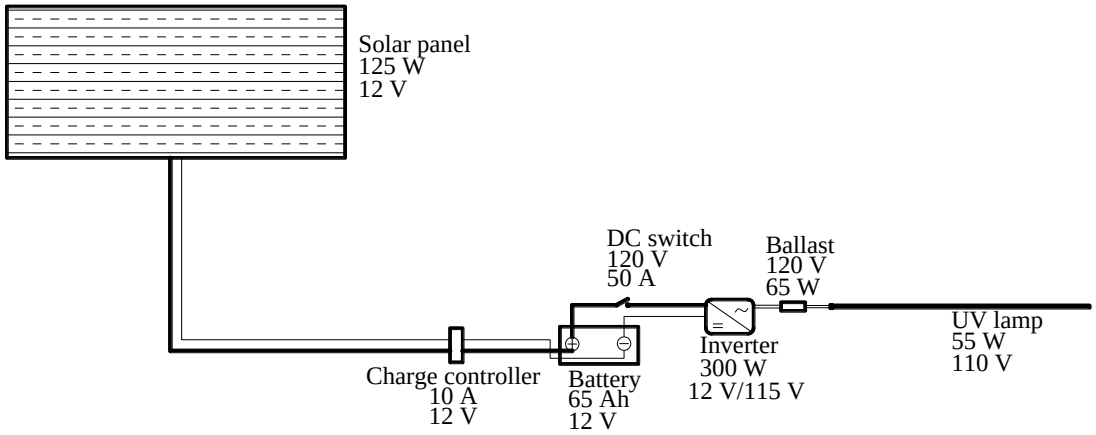

Figure 3-4 Diagram of the electrical system showing the relative size of components

Even though the battery nominal capacity calculated from Equation 3-3 is higher than the actual capacity of the battery, this is not an impediment for the normal performance of the system. For example, by applying the power-voltage-current relationship ($P = VI$) with the calculated value of $\overline{G_d}$, the actual values of A_G, V_{nom}, and inverter efficiency, and the assumed value of η_G, it is obtained a

charge of 33 Ah supplied daily by the generator. On the other hand, by applying the same relation, the amount of charge drawn by the load daily from the battery gives a value of 27.5 Ah. As a consequence, there is a daily surplus of 5.5 Ah that could be used for the recharge of the battery during cloudy days or for the consumption by the UV lamp.

3.3.2 Verifying the structural system

Figure 3-3 depicts the final prototype of the designed UV reactor and auxiliary tanks supported in a steel frame. In order to guarantee the stability of the structure in regard to not only its own weight and that of the elements supported by it, but also external actions such as wind or quakes, a structural verification of the frame must be performed. For this, a simple structural analysis using the stiffness method was performed. In this method, the stiffness matrix and force vector are determined for a particular frame in order to solve the equilibrium equation of that frame. The equilibrium equation has the form $F = KD$, where F is the force vector, K is the stiffness matrix and D is the displacement vector, which corresponds to the horizontal and vertical displacements, as well as the rotation angle caused by the bending moment (Wong, 2009). The force vector can be formed from the external loads applied to the frame, namely, own weight, tanks, wind, and combinations thereof. The stiffness matrix can be found through geometrical and structural properties of the steel beams, such as shape, inertia moment, and modulus of elasticity, among others. The displacement vector is then solved using linear algebra or finite element techniques, according to the coordinate system adopted (global or local). The frame was analyzed using

pcaFrame (Structurepoint, LLC, Skokie, IL), an older version of a proprietary software by the Portland Cement Association. The input to this program is listed below.

- *Geometric characteristics of the frame*: coordinates (*x*, *y*, *z*) of the joints of the frame, that is, those points where the beams connect.
- *Geometric characteristics of the steel beams*: cross-section shape and measures. In this case the profiles were taken as 'angles' with 2"-long flange and web and a thickness of 2 mm. The structural properties of steel were also defined.
- *Magnitude and direction of loads*: the loads defined for this run were self-weight, the top tank (amounting to 1.57 N/mm), the panel (0.18 N/mm), and a 100 km/h wind, resulting in a horizontal force of 0.62 N/mm. The location of the distributed loads can be observed in Figure 3-5a.
- *Fixities*: corresponding to those joints that have to be restrained in order to prevent their movement in any of the directions (*x*, *y* or *z*) or angle (θ). Only the joints in the base of the structure and those bearing the load of the top tank were fixed.

The deformed frame as a result of the applied load combinations is presented in Figure 3-5b. However, under the most critical case, that is, wind and steady loads combined, the maximum displacement is slightly over 0.5 mm, with bending moments generating rotations below 10^{-7} degrees. These displacements can be considered as acceptable and, therefore, the structure is stable under those load conditions.

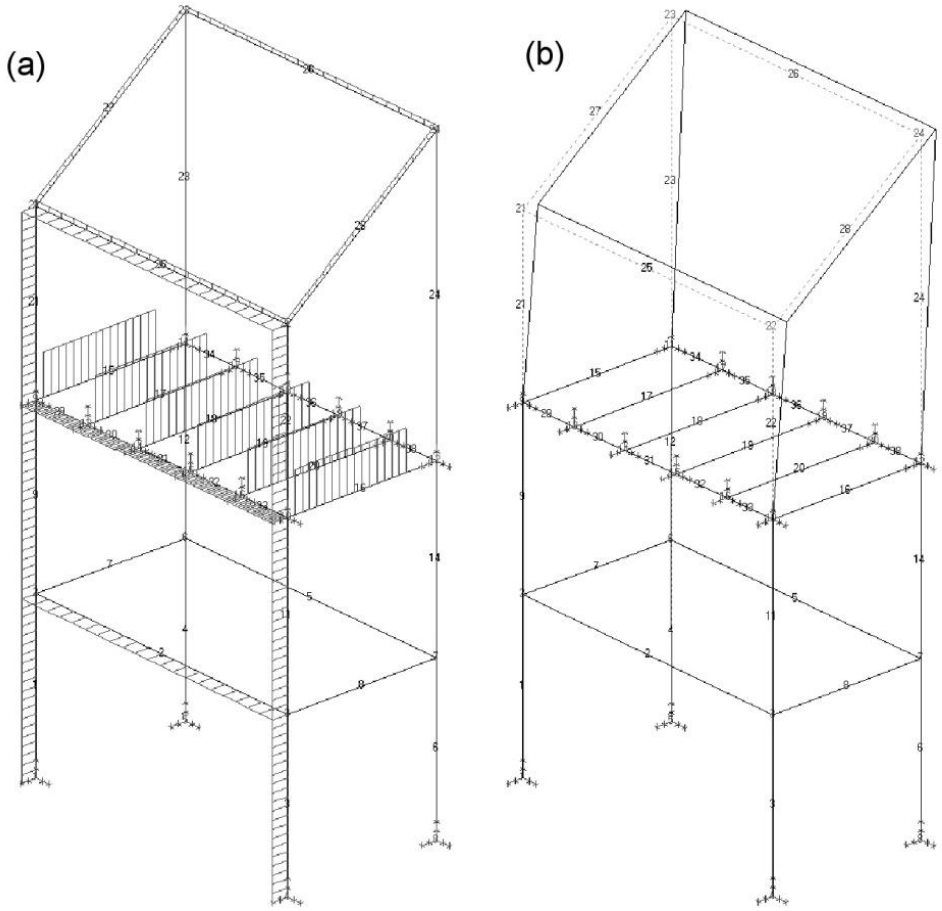

Figure 3-5 Estructural design: a) Location of the distributed loads ; b) Deformed structure

3.4 Modeling the fluence rate in the UV reactor

The software package UVCalc® (ver. 1.0, Bolton Photosciences Inc., Edmonton, AB) is able to obtain a good correlation with the measured values of the fluence rate, in addition to including the effects of refraction and reflection. Because of these features, UVCalc® was the model implemented in this study for modeling the fluence rate. Nevertheless, its results will be further refined when it is coupled with a CFD model, which is described later.

3.4.1 Influence of the water quality on the fluence rate

Bolton and Cotton (2008) established that a number of water quality parameters may impact the fluence rate delivered by a UV reactor. Among these are: UVT, turbidity, algae, organic matter, and soluble salts. The results of the lab analyses shown in Table 3-2 reveal a water quality that is acceptable for the implementation of a UV system without prior treatment. The turbidity is less than 1 NTU, which should not affect the effectiveness of the UV treatment. A high value of UVT does not have a significant effect on the system performance when dealing with drinking water (Bolton and Cotton, 2008). Therefore, the reported UVT value of 97.5% in Table 3-2 should not adversely affect UV treatment. Algae were not sampled, but their presence is unlikely in deep or even shallow wells (MWH, 2005). The very low TOC value indicates a low content of organic matter and thus an insignificant influence on the delivered fluence rate. The high hardness value suggests a high content of soluble salts, which do not impact on the delivered fluence rate per se, but do have an effect on fouling of the quartz sleeve. This content of soluble salts also agrees with the water's salty taste perceived by the community residents. In light of this salt content, which if deposited may foul the quartz sleeve, a shorter frequency of maintenance (OCC) should be advised.

3.4.2 Running UVCalc®

The graphic user interface (GUI) of UVCalc® is straightforward, comprising a single screen. Input parameters are defined in Bolton (2008) and a summary of these is presented in Table 3-3. It is worth mentioning that the lamp used in the

experiments with the reactor is a 1.15 m-long, containing a 55 W LP germicidal lamp (G48T6L/4, Atlantic Ultraviolet Corp., Hauppauge, NY) enclosed within a 1.2 m-long, 21.2 mm-diameter quartz sleeve closed in one end (Atlantic Ultraviolet Corp., Hauppauge, NY). According to the manufacturer, the lamp has a total UV output of 21 W, resulting in an efficiency of 38.2 % (AUC, 2009). The reactor also includes a UVC-selective SiC based UV sensor (SG01S-C18, **sg***lux*, Berlin, Germany) to be used during reactor validation.

Table 3-3 Numeric input data to UVCalc®

Power (W)	Efficiency (%)	Arc length (cm)	Sleeve diameter (cm)	Reactor length (cm)	Reactor diameter (cm)	Flow rate (L/min)	UVT* (%)
55	38.2	106.8	2.12	133.0	7.62	20.75	97.5
							85.0
							70.0

* According to the tests to be conducted during reactor validation

Other parameter inputs to UVCalc® include: lamp sleeve material, calculation type, experimental medium parameters, resolution and units. The numerical results are presented in Table 3-4, while the graphic results are depicted in Figure 3-6.

Table 3-4 Numerical results from the UVCalc® modeling

UVT (%)	Average fluence rate (mW/cm^2)	Estimated UV dose* (mJ/cm^2)
97.5	10.8	190.9
85.0	8.8	156.5
70.0	6.8	121.1

* based on a flow rate of 0.35 L/s with an HRT of 17.8 s

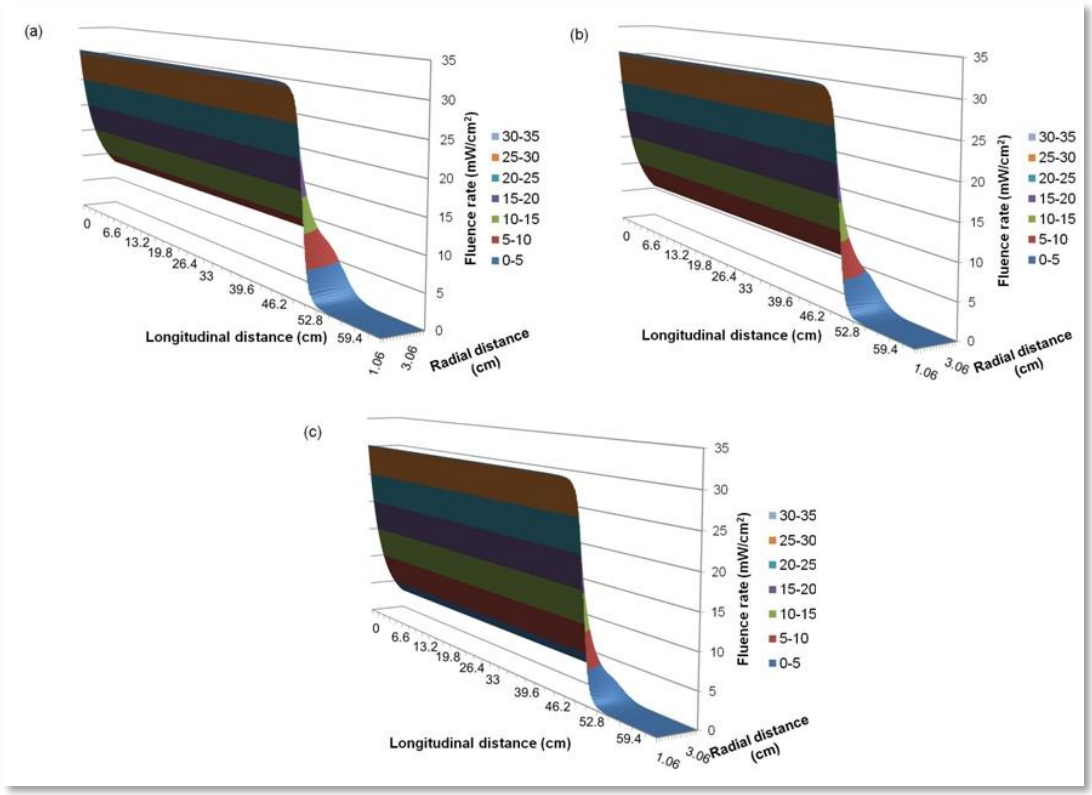

Figure 3-6 Results of the UVCalc® modeling for various UVT values: a) 97.5%; b) 85%; c) 70%. Only half the fluence-rate distribution is shown from the centre of the lamp to the reactor end

From Table 3-4, it is clear that a lower transmittance results in lower fluence rates in the reactor, and hence in a lower UV dose delivered to the microorganisms, for the same flow rate (0.35 L/s with an average HRT of 17.8 s). The lowest of the UV doses presented results in an expected virus removal of as much as 2.5 logs, as per the UV doses requirements given in Table 1.4 of USEPA (2006). Removals of more than 4 logs of both *Cryptosporidium* and *Giardia* would be safely achieved with all of these UV doses, according to the same table. It should also be pointed out that the farther from the lamp (both radially and longitudinally), the lower the fluence rates obtained. Coupling these results with

trajectories and cumulative UV doses derived from a CFD model should corroborate the results of biodosimetry. This will be explained later in this thesis.

3.4.3 Coefficient of maximum UV inactivation (MUVI)

The results shown in Table 3-4 and Figure 3-6 from the execution of the UVCalc® model for the UV dose correspond to the maximum theoretical values that can be achieved with this particular reactor, under those particular conditions of UVT and flow rate. This is because the reactor is assumed to be an 'ideal' plug-flow reactor, where there is a perfect mixing in the radial direction but no mixing in the longitudinal direction; therefore, all the particles in the same volume element would have the same velocity, the same HRT and the same average exposure to the UV. The UV dose would then be obtained by multiplying the average fluence rate times the HRT. However, in 'real-life' reactors this is seldom achieved because the reactor geometry, as well as fittings and piping configuration, modify the hydraulic pattern (Bolton and Cotton, 2008).

The coefficient of maximum UV inactivation (MUVI) gives an idea of the performance of the reactor as to both its hydraulic regime and the inactivation kinetics of the challenge microorganism. It is defined as the ratio between the measured (by biodosimetry) or modeled (by fluence-rate distribution/CFD models) RED and the maximum theoretical UV dose. For the same UVT, for example, the same reactor may yield different MUVIs depending, for example, on the flow rate; in other cases, for the same UVT and flow rate, two or more UV reactors may yield different MUVIs. The approximation of the mixing in a reactor to an ideal state might be indicated by the value of the MUVI for the same

challenge microorganism. Or, on the other hand, the inactivation kinetics of two or more microorganisms might be assessed for the same hydraulic configuration of the reactor. For example, the closer the value of the MUVI is to unity the closer the mixing is to an ideal state; also, the closer the MUVI is to unity the closer the inactivation coefficient of the microorganism is to the 'normal' state, as limited by the 90% confidence interval given by the USEPA (2006). Consequently, one could model the hydraulic behaviour a UV reactor by observing the changes in the MUVI, following changes in geometry, piping configuration or baffling of the reactor. An application of the MUVI concept is presented later in this document, based on the results of the biodosimetry tests.

3.5 Production of *Bacillus subtilis* spores

It was mentioned earlier that there are risks in handling pathogenic microorganisms when performing biodosimetry tests; hence the need to use non-pathogenic challenge microorganisms. The most widely used are *B. subtilis* spores and MS2 coliphage. For this study, it was decided to employ *B. subtilis* ATCC® 6633™ spores (American Type Culture Collection, Manassas, VA) as the surrogate microorganisms. The procedure followed to prepare and assay these spores is a modification of the procedure outlined by the USEPA (2006) and has been previously used at the UA (Guest, 2004). The procedure is described in Appendix A.1.

After the completion of some batches, the enumeration yielded a concentration of spores above 5×10^8 CFU/mL. With this titre, a concentration of

more than 10^3 CFU/mL was obtained during the validation of the UV unit, after diluting the stock solution in 40 L of demineralised (DM) water.

3.5.1 Low UV sensitivity *B. subtilis* ATCC® 6633™ spores

The procedure described in Appendix A.1 was followed for all batches of spores that were prepared in this study. However, only some of the samples that were exposed to a UV dose of 60 mJ/cm^2 had values of log inactivation located inside the 90% prediction interval outlined by the USEPA for *B. subtilis* spores (Figure 3-7). This raised questions as to whether some slight changes in the procedure of culture and harvest of *B. subtilis* spores yielded dramatic changes in the UV sensitivity of these organisms during all periods of time, with the exception of November 2010.

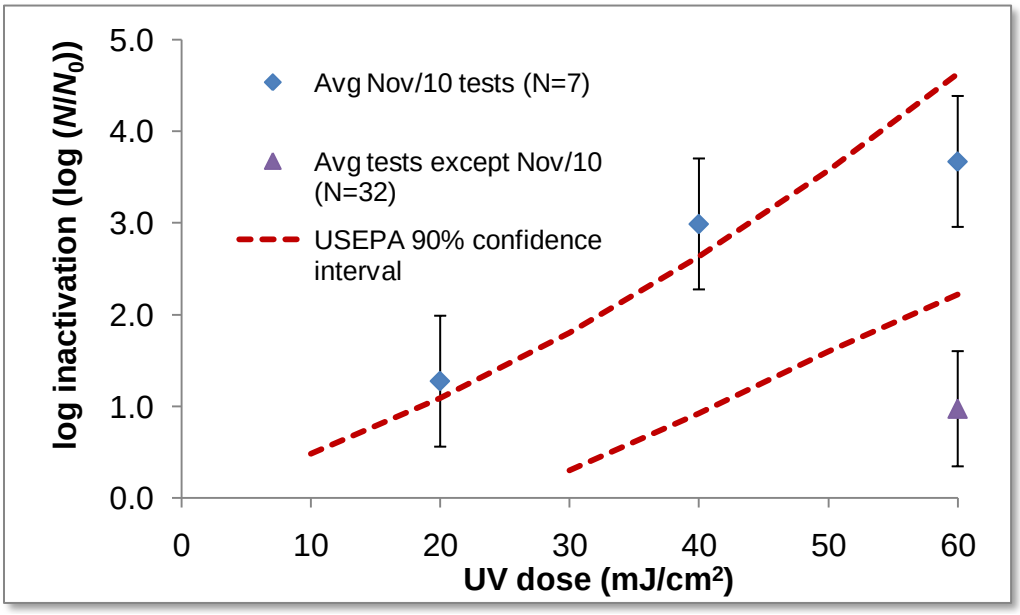

Figure 3-7 UV log inactivation of samples at different points in time

It should be noted that the principal guidelines for this process were based on the procedure by Guest (2004), which was followed previously by former

graduate students at the UA. This procedure is, however, slightly different in some points from the one outlined by the USEPA (2006) including, among others, the type of inoculum, the nutrient medium pH and the heat treatment for inactivation of vegetative cells. Changes in the exposure procedure, including size of the Petri dish, volume of the sample, type of stirrer, cell concentration of the solution, and type of solvent (water, phosphate-buffered water) did not affect the outcome dramatically. Furthermore, another experiment was performed for testing the exposure procedure, by using a different microorganism (*Escherichia coli* ATCC® 35218™); this test resulted in a UV dose-response curve for *E. coli* that agreed well with the values reported in literature (Chevefrils *et al.*, 2006). Therefore, it was decided to pinpoint the principal factor(s) affecting the UV sensitivity of the *B. subtilis* spores during the culture/harvest procedure, since factors in the UV exposure procedure were all ruled out.

At some point in time, before November 2010, the log inactivation for a UV dose of 60 mJ/cm^2 reached a value higher than usual. This was attributed to the heat of inactivation, so an older batch was re-harvested and heat-treated for 40 min at 75 °C but no significant changes were observed for this batch. In November 2010, an experiment involved culturing two batches of bacteria, one in a nutrient medium with pH = 7 and the other one with pH = 8, and monitoring their growth on a daily basis. Since the centrifuging procedure was onerous to carry out on a daily basis, it was decided to inactivate the vegetative cells by heat-treating the 20-mL vials in a boiling water bath (T > 98 °C) for 10 min. After several days of daily monitoring, no viable cells were observed in the planted

plates. Two new batches were set to grow, but their heat treatment was changed to 4 min. From the 12^{th} hour and onwards, a steady growth of viable cells was observed. The samples selected to be exposed to UV doses of 20, 40 and 60 mJ/cm^2 were collected at 48, 144 and 336 h. The averages of the values obtained from this experiment are those shown in Figure 3-7.

For all the growth times, the inactivation values given by all of the UV doses agreed very well with those reported in the literature, locating close to or within the 90% confidence interval given by the USEPA (2006). In general terms, the cells in the culture with the nutrient medium at pH = 8 developed a somewhat higher concentration than those with the medium at pH = 7. Also, the highest inactivations appeared for a collection time of 144 h (6 days). It should also be noted that the UV absorbance at 254 nm of the solutions containing samples with the nutrient medium at pH = 8 was higher than for their counterparts at pH = 7.

Retaking the assumption of heat-treatment as the centrepiece of the *B. subtilis* spores' UV sensitivity, a new batch was set out to grow for 6 days, with a nutrient medium pH of 7. Given the difference between the volume of the samples collected during the daily monitoring (4 mL) and those from the new batch to be heat-treated (at least 100 mL), a heat transfer model was devised. This model scaled-up the amount of heat energy that was transferred in the glass vials to the plastic bottles containing the larger sample, via equations of natural convection and transient conduction (Annaratone, 2010). The application of the model results to the plastic bottles resulted in longer times for the heat treatment of the bottles. However, significant changes in the UV sensitivity of the spores were not

detected in relation to the values reported before the daily monitoring. A combination of various temperatures and times of heat treatment still ended up in low UV sensitivity, which led to the conclusion that the heat treatment could be ruled out as the principal contributing factor for the spores' low UV sensitivity.

At this point, it is also important to mention that the time the *B. subtilis* spores remained suspended in a 50% ethanol solution affected their UV sensitivity. Guest (2004) recommended this stock solution to preserve such spores for an extended period of time. When samples prepared with this stock solution were exposed to UV at different points in time, the resulting UV inactivation was lower for the latter times, which means that the spores' UV sensitivity decreased over time. However, a definitive factor has not yet been found, although the focus has been directed at the seed for the culture. A common feature of the batches that had a 'normal' UV sensitivity was that they had to be re-inoculated after bacterial growth failed to show up 24 h after the first inoculation. It is a proven fact that the type of growth does have an effect on the UV susceptibility of *B. subtilis* spores. For example, it has been widely demonstrated that spores cultivated in agar plates (surface-cultivated spores) are more UV-sensitive than spores cultivated in liquid medium (Bohrerova *et al.*, 2006; Mamane *et al.*, 2005). In light of this, more research is suggested on the type of seed for the liquid culture (surface or liquid cultivated), the spore concentration of that seed, and the timing of the inoculation.

A final remark is that the UV resistance obtained for most of the batches of spores in this study could be very useful when performing the validation of UV reactors where the target organism is a highly UV-resistant one, such as

adenoviruses. Reported UV doses for a 4-log inactivation range from 100 to possibly more than 200 mJ/cm^2 (Yates, 2008; Hijnen *et al.*, 2006; Chevefrils *et al.*, 2006), while USEPA (2006) defines a 4-log virus inactivation credit for a dose of 186 mJ/cm^2. In this study, for a UV dose of 180 mJ/cm^2, the log inactivation was below the detection level but, in any case, was barely around 2 (see raw data in Appendix A.4).

3.6 Validation of the UV unit as designed

The preferred strategy for UV dose delivery in small water systems is the 'UV intensity set point approach' as defined by USEPA (2006). This is the strategy that was adopted for this particular UV reactor, since the other 'calculated-dose approach' results in high costs of UVT monitors, PLCs, and other ancillary equipment. The UVT was monitored with a spectrophotometer (Ultrospec 2100 pro, GE Healthcare Biosciences, Pittsburgh, PA) at 254 nm. The validation was considered as an 'off-site' validation.

Before starting the full-scale validation, the flow rate through the reactor was verified using a volumetric method. The inlet PVC ball valve was equalized such that various flow rates could be accommodated, while the outlet valve was left fully open. The flow rates obtained with this approach were 0.52 (±0.03 L/s with a 95% confidence), 1.01 (±0.03 L/s) and 1.32 L/s (±0.19 L/s), for respective apertures of the inlet valve of 3/8, 1/2, and 5/8. During the experiments, the 'in' and 'out' water samples were taken from a port set in the inlet and directly from the outlet pipe, respectively. The full-scale tests assessed combinations of these flow rates and UVTs. The UVT was modified by adding a coffee solution

(Maxwell House, Kraft Canada Inc., Toronto, ON) to the water, and was measured at 254 nm and a 1-cm path length using a spectrophotometer (Ultrospec 2100 pro, GE Healthcare Biosciences, Pittsburgh, PA). Three replicates were collected for each run. The *B. subtilis* stock solution was spiked into demineralised water in the top tank of the setup where it was thoroughly mixed using a mixing rotor.

The full-scale test was followed by the bench-scale one. For the bench-scale tests, a collimated beam apparatus equipped with a LP UV lamp (Calgon Carbon Corporation, Markham, ON) was utilized. This device complies with the technical requirements outlined in USEPA (2006). In order to derive the UV dose-response curve for *B. subtilis*, it was decided to apply UV doses of 0, 30, 60, 90, 120, 150 and 180 mJ/cm^2. These UV doses were selected because prior trials demonstrated a very low UV-sensitivity of the *B. subtilis* strain used in this study. Both bench-scale and full-scale experiments took place within 24 h of each other.

The UV doses in the bench-scale experiment were calculated following the procedure outlined in the spreadsheet programmed by Bolton (2004), which is based on the protocol by Bolton and Linden (2003). This program includes the divergence factor and calculates the Petri factor required by the USEPA (2006). A 15 mL sample of the suspension to be irradiated was placed in a 50 mm-diameter Petri dish, resulting in a depth less than 2 cm, so the spreadsheet "Fluence-LP-shallow" was used. The measurements required for the estimation of the Petri factor were undertaken with the help of a radial 5 mm-grid pictured in a plastic

screen on top of a magnetic stirrer (Isotemp, Fisher Scientific) and a calibrated radiometer (IL1400A, International Light Inc., Newburyport, MA).

The two water samples used in the bench-scale experiment had been passed earlier through the UV reactor with the lamp off, and had UVT absorbance values of 0.162 and 0.009, corresponding to UVT of 68.9% and 98%, respectively. The higher absorbance resulted from the addition of coffee solution. A small aliquot of the *B. subtilis* stock solution was added to each water sample and its concentration before and after exposure was determined based on the enumeration procedure noted in Appendix A.1. Exposed samples were stored in the dark in 20 mL vials at 4 ºC until analyzed. The UV dose is a function of the exposure time following the results of the spreadsheet. Every exposure was made in duplicate and random order to minimize technical and human errors and biases. The collimated beam apparatus for this experiment was equipped with a programmable timer, which activated a shutter automatically after the programmed time was elapsed. The full procedure for UV dose calculation is detailed in Appendix A.2 while the measurements for the Petri factor determination are presented in Appendix A.3. The UV dose-response curve for *B. subtilis* ATCC® 6633™ in this particular experiment is shown in Figure 3-8, where N_0 is the number of viable spores before exposure and N is the number of viable spores after exposure (both in CFU/mL). Raw data and calculations are given in Appendix A.4.

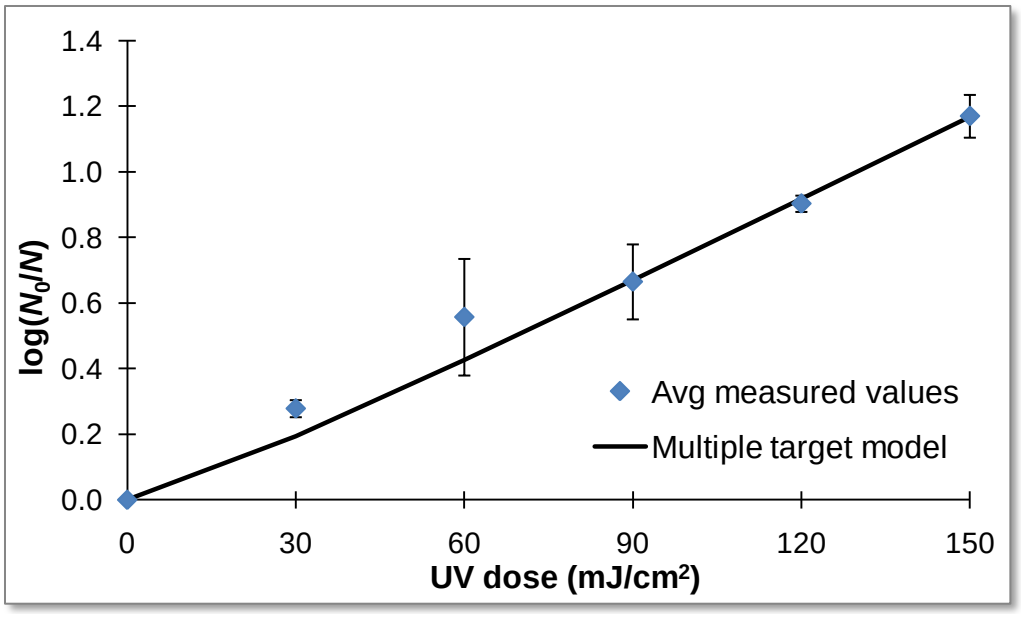

Figure 3-8 UV dose-response curve for the validation of the UV unit

Prior to obtaining the UV dose-response curve a check on the combination of UV dose-response curves (that is, for both UVTs) was performed, as stated by the USEPA (2006). The test verified that the difference between both regression coefficients was not statistically significant at the 95% confidence level. The application of this test is exemplified by Mann *et al*. (2009), and the procedure is presented in Appendix A.4. Hence, both UV dose-response curves could be combined. Accounting for the very low UV sensitivity of the *B. subtilis* strain used in this study, as well as for the fact that at 'low' doses the UV dose-response curve might exhibit a shoulder, the spore inactivation was modeled using a non-linear, multiple target model (Chen *et al*., 2009), which is shown as Equation 3-4.

$$\frac{N}{N_0} = 1-(1-10^{-kF})^{n_c} \qquad (3\text{-}4)$$

where N_0 is the number of viable spores before exposure and N is the number of viable spores after exposure (both in CFU/mL), k is the first-order inactivation

constant (cm^2/mJ), F is the UV dose (mJ/cm^2), and n_c is the number of critical targets (unitless). The constant k was determined by finding the regression coefficient of the lineal portion of the log inactivation curve and had a value of 0.0084 cm^2/mJ [standard error (SE) = 0.0011 cm^2/mJ]. This is a much lower value than those reported by other researchers at 254 nm (Chen *et al.*, 2009, Mamane *et al.*, 2005). The number of critical targets n_c was found by taking the inverse logarithm of the regression intercept and had a value of 1.25 (SE = 0.14).

After the determination of the UV dose-response curve, the uncertainty of the UV-dose response (U_{DR}) curve at 95% confidence level was calculated following the recommendations of the USEPA (2006). This procedure is also presented in Appendix A.4, and it was concluded that U_{DR} was greater than 15% for a 95% confidence interval at a UV dose producing a 1-log inactivation. Therefore, such uncertainty had to be added to the whole uncertainty of the validated UV dose (see Appendix A.4).

Once the UV dose-response curve and its uncertainty were established, the REDs were determined for the full-scale experiment. They were computed by plugging in the value of the mean log inactivation in Equation 3-4. A full set of the raw data and calculations is presented in Appendix A.5; however, a summary of the determined REDs is presented in Table 3-5, sorted by flow rate and then for UVT. The last column contains the values of the maximum theoretical UV doses in the reactor for all the conditions explored during the test, as computed by the UVCalc® software.

Table 3-5 Determination of experimental and modeled REDs for the full-scale test. Validation of the designed UV unit

Flow rate (L/s)	Absorbance	UVT (%)	Average RED (mJ/cm^2)	Avg RED SD (mJ/cm^2)	UVCalc® estimated UV dose (mJ/cm^2)
0.52	0.155	70	37.3	2	73
0.52	0.07	85.1	68.1	10	94.5
0.52	0.009	97.9	88.2	6.8	115.9
1.01	0.151	70.6	37.4	13	37.7
1.01	0.074	84.3	34.3	6	47.6
1.01	0.004	99.1	80	0.4	60.2
1.32	0.161	69	45.7	2.2	28.2
1.32	0.064	86.3	28.3	20	37.9
1.32	0.007	98.4	69.4	2.1	45.9
0.52	0.162	68.9	0.0*	0	0

* This was a blank run, meaning that the UV lamp was off

It is worth noting that the low UV sensitivity of the bacterial strain used in the experiment has an effect not only on the uncertainty but also on the value of the REDs themselves. For example, the difference between the counts in the influent and the effluent during the blank run is not completely statistically significant. Applying statistical approaches, the difference is statistically significant at the 95% level of confidence using the two-sample *t*-test (P-value = 0.0863), but it is not if the *z*-test is used instead (P-value = 0.0496; see raw data in Appendix A.5). However, if the measured values of log inactivation are plugged into Equation 3-4, an average RED of around 24 mJ/cm^2 would come up as a result, which, of course, is illogical for a non-operational UV reactor. The above discussion

highlights the fact that extreme care has to be exercised when collecting and analyzing the samples in a UV reactor.

According to the USEPA (2006), the determined RED must be adjusted to account for the different UV sensitivities between challenge and target microorganisms. The validation factor (*VF*) is then computed following Equation 2-1. However, in order to estimate *VF*, the RED bias (B_{RED}) and the validation uncertainty (U_{Val}) must be found first and put into Equation 2-1, so that the estimate of the validated UV dose (D_{Val}) can proceed (see Appendix A.5). The low UV sensitivity of the bacteria used in this experiment meant that the RED bias is high, and so is the uncertainty when determining the validated dose. Therefore, with the lowest RED measured, the validated UV dose results in a certain inactivation of 0.5 logs for both *Giardia* and *Cryptosporidium*. The uncertainty for virus removal is also high, so no log inactivation is apparent. From the model and the biodosimetry test results themselves, it is clear that the UV reactor is able to deliver a higher UV dose to reach a higher log inactivation for both protozoa and viruses. In light of this, it is suggested that future biodosimetry tests be carried out using a more UV-sensitive strain of *B. subtilis*, having a first-order inactivation constant (*k*) value closer to those reported in literature. The determined MUVIs, based on the results of the biodosimetry test and the maximum theoretical UV doses obtained from the UVCalc® software, are presented in Table 3-6 and Figure 3-9. The vertical bars in Figure 3-9 indicate the standard deviation.

Table 3-6 Coefficients of maximum UV inactivation of the UV reactor for the conditions assessed during the biodosimetry test

Flow rate (L/s)	UVT (%)	Average RED (mJ/cm^2)	UVCalc® UV dose (mJ/cm^2)	MUVI
0.52	70.0	37.3	71.5	0.52
0.52	85.0	68.1	92.6	0.74
0.52	98.0	88.2	113.8	0.78
1.01	70.7	37.4	37.7	0.99
1.01	84.3	34.3	47.6	0.72
1.01	99.1	80.0	60.2	1.33
1.32	69.0	45.7	33.3	1.37
1.32	86.4	28.3	44.9	0.63
1.32	98.3	69.4	54.2	1.28

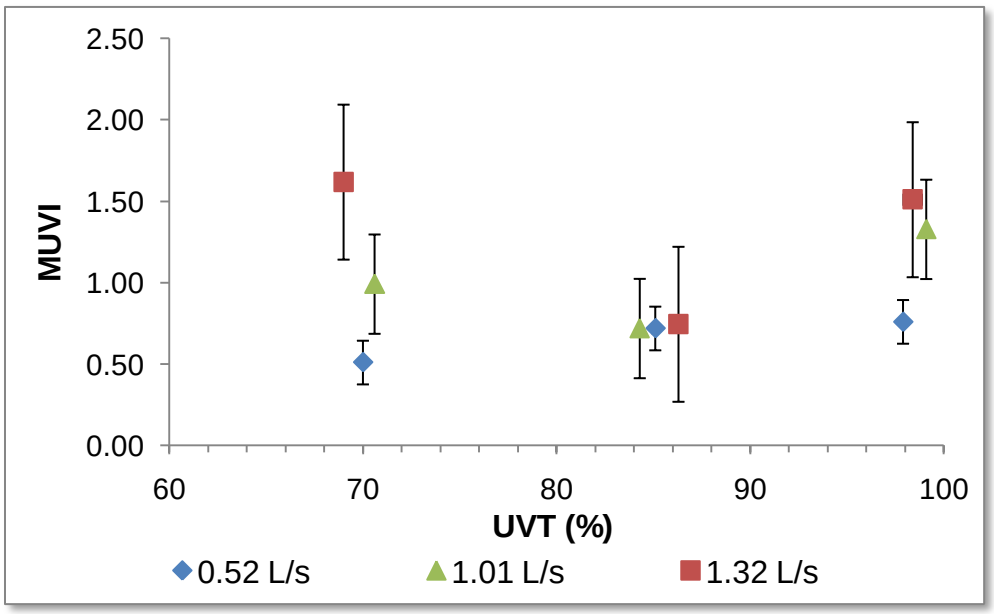

Figure 3-9 Coefficients of maximum UV inactivation for the UV reactor; error bars show standard deviations

Ideally, the MUVI should increase as the flow rate increases, since the change in the turbulence should affect the hydraulic pattern; this clearly is the case for the UVTs of about 70% and about 98%. Moreover, for the same flow rate, the MUVI

should increase as the UVT increases. However, the overall trend is that the MUVI seems to have its lowest value at a UVT of around 85%, especially for the flow rates of 1.01 and 1.32 L/s. Explanations for this fact may lie in the method for determining the flow rate in the full-scale biodosimetry test, the UV sensitivity of the challenge organism, and the collection and analysis of the samples taken from the full-scale setup. All of these factors may add some uncertainty to the calculation of both the maximum theoretical UV doses (with UVCalc®) and the average REDs, as discussed below.

The values of the MUVI greater than one, especially for the highest flow rate, may result from the low UV sensitivity of the spore strain used in this experiment and hence the high uncertainty in the values of the determined REDs. Later in the document, it is detailed how the low UV sensitivity of a challenge microorganism results in high REDs when computed using UV dose distributions. Also, the biodosimetry test is not a flawless process and some errors are usually introduced during the measurement of the flow rate and the collection or analysis of the samples. For example, the volumetric flow rate is an average measurement and does not take into account variations, however small, in the hydraulic head, as was the case in this experiment. Since the in and out samples were collected based on an average HRT resulting from such flow rate measurements, the volume element intended for analysis might have not been accurately sampled. A more complete picture of the UV reactor hydraulics, including the interaction of CFD and fluence-rate distribution models, is laid out later in this document.

4. COMPUTATIONAL FLUID DYNAMICS (CFD) MODELING OF THE UV UNIT

4.1 Introduction to computational fluid dynamics

By definition, fluid dynamics deals with the properties of substances, such as gas or water, that are in motion or 'flow', hence the term 'fluids' (Pedley, 1997). The fundamentals of fluid dynamics are based on the concepts outlined by the *conservation laws* applied to mass, energy, and momentum (Hirsch, 2007). The equations of Navier-Stokes are basically the application of Newton's Laws to moving, viscous fluids, in which mass, energy, and momentum must be conserved. These equations are non-linear, time-dependent differential equations with five unknowns: the three components of velocity (*x*, *y*, and *z*) and two thermodynamic magnitudes, such as pressure and density or pressure and temperature (Hirsch, 2007; Pedley, 1997). On the other hand, since a fluid cannot pass through the interface between itself and another medium, boundary conditions, which include the normal components of the fluid velocity, must be specified (Pedley, 1997).

From the above, one can see the difficulty in solving the differential equations resulting from the application of the Navier-Stokes equations, together with the specification of boundary conditions and the physical disturbances of the flow, such as turbulence, when they appear (see below). This is where computational fluid dynamics (CFD) comes in, as it is based on a series of mathematical techniques that reduce the complexity of the equations to be solved. These

techniques may include linearization and/or reduction of the physical dimensionality (Hirsch, 2007).

4.1.1 What is CFD?

CFD is basically a compiled computing code that has as its final objective to solve the set of Navier-Stokes equations applied to a given fluid in a determined physical space (boundary conditions). Three accepted methods for solving these equations are the finite difference method (FDM), the finite volume method (FVM), and the finite element method (FEM); of these, the FVM is currently the one used most in commercial CFD codes (Hirsch, 2007).

CFD modeling of UV reactors is gaining importance, since it can be used to predict the path of a particle inside the reactor. Moreover, when it is coupled with fluence-rate models, it may predict the approximate UV dose that a microorganism will receive inside the reactor (Bolton and Cotton, 2008). Nevertheless, this approach is not currently approved for validation of UV reactors by the USEPA (USEPA, 2006). Hulsey *et al*. (2007), note that numerical UV disinfection models should include three principal components: a turbulence/flow model, a fluence-rate distribution model and a microbial transport model. A description of a turbulence model and its implications in CFD modeling is provided below.

4.1.2 Turbulence and other hydraulic variables

Turbulence is defined by Hirsch (2007) as "a spontaneous instability of the flow, whereby all quantities take up a statistical (chaotic) behaviour". In a physical-mathematical sense, turbulence appears when the Reynolds (*Re*) number exceeds

a certain value. The *Re* number is defined as the relation between the product of the fluid velocity and its predominant dimension (length, wide, depth) and its kinematic viscosity (Hirsch, 2007). It is widely accepted that there are three flow regimes in circular pipes depending on the value of *Re* number: laminar ($Re < 2000$), critical ($2000 \leq Re \leq 4000$) and turbulent [$Re > 4000$ (Concha, 2008)]. For all practical aspects, non-turbulent flow almost never occurs (Hirsch, 2007; Pedley, 1997).

Currently, two families of approaches are used to model turbulence. Hirsch (2007) defines them as the Large Eddy Simulation (LES) and the Reynolds Averaged Navier-Stokes equations (RANS). Hulsey *et al*. (2007) establish that the approach used most in commercial models is the two-equation model, in which, in addition to solving RANS equations, balances are written for the turbulent kinetic energy k and the turbulent energy dissipation rate ε. Despite the intensive use of mathematical manipulation and computing resources when modeling turbulence, Hulsey *et al*. (2007) claim that the choice of the turbulence model has hardly any effect on the predicted microbial inactivation, with a variability of only 8% and minimal differences in the predicted fluence distribution.

4.1.3 Application of CFD to closed pipes (e.g., UV reactors)

The application of CFD to UV reactors is related principally to the existence of boundaries for the flow. Along these boundaries, the thin sub-layer, which has viscous flow behaviour, creates a new type of flow inside circular pipes – boundary layer flow (Hirsch, 2007). This, together with the shear and wake flows, might make the selection of the correct turbulence model challenging (Hulsey *et*

al., 2007). Pedley (1997) asserts that when the fluid of interest is water and its interface is limited by air, the boundary layer conditions may be neglected. Hulsey *et al*. (2007) define as essential boundary conditions those at the inlet and outlet of the reactor, as well as the wall boundaries. In the inlet, such conditions are defined by k and ε. The *no-slip* condition is usually recommended for boundary conditions of walls at rest, that is, whose velocity is zero (Pedley, 1997).

4.2 Third-party CFD codes – ANSYS-CFX

CFD codes that are developed by companies or personnel, other than those directly involved in the modeling task, are called 'third-party CFD codes'. Commercially, there are many CFD codes that may perform hydraulic modeling of UV reactors. One of those is CFX, which is the one used in this project and is described below.

4.2.1 Overview of the CFX code

CFX is a CFD software developed by ANSYS, Inc. (Canonsburg, PA). The release 11.0 structure is based on five modules, each of which performs a given task and passes the information on to other modules. These modules include software for mesh generation, a physics pre-processor, a solver and its manager program, and a post-processor. The pre-processor is where the domains and boundary and physical conditions are defined. The post-processor is in charge of report generation, visual result interfaces and customization (ANSYS, 2006a).

4.2.2 Mathematical framework

As with other CFD codes, this software solves a set of equations in order to find the values of physical fluid variables under certain physical conditions. The general mathematical background of its formulation is presented in Table 4-1 (ANSYS, 2006c), as related to the modeling of UV reactors. Particle transport modeling is carried out with a Lagrangian approach instead of using an extra Eulerian phase, by solving a set of differential equations in time for the position, velocity, temperature, and masses of species of each particle. Particle tracking in turbulent flows is performed considering two components of the fluid velocity (mean and fluctuating) and a random path. This results in an instantaneous fluid velocity (ANSYS, 2006b).

Table 4-1 Mathematical background of the CFD software CFX

Transport equations	Additional variable equations supported	Boundary conditions	Turbulence models	Discretization and solution
• Continuity • Momentum • Total energy • Thermal energy	• Transport • Poisson • Diffusive transport • Algebraic	• Inlet (supersonic /subsonic) • Outlet (supersonic /subsonic) • Opening • Wall • Symmetry plane	• Eddy viscosity models (Zero-equation, Two-equation, Eddy viscosity transport) • Reynolds stress models • Large eddy simulation • Scale-adaptive simulation	• Discretization: finite control volumes using a mesh • Solution: linear equation solution [Multigrid (MG) accelerated Incomplete Lower Upper (ILU) factorization, algebraic multigrid]

4.2.3 Study cases

Although CFX has not been used as widely as other codes in the modeling of UV reactors, there are two experiences worth mentioning. Romero-Vargas *et al*. (2006) applied CFD modeling in the assessment performance of a photocatalytic reactor for air treatment, using CFX (v5.7.1). The results of the simulations helped them to improve the reactor performance by modifying the original reactor shape from a rectangular shape to a cylindrical one. Also, the simulated change of a wire-mesh for a perforated plate resulted in a more homogeneous distribution of the mass flow rate and contact time.

Wright and Hargreaves (2001) modeled the performance of a UV reactor treating water and wastewater using the CFX software (v5.0). They used this model to verify the changes in the fluence-rate distribution inside a UV reactor based on various configurations of the inlet and outlet piping. They noted that the choice of turbulence model between the standard κ–ε, the RNG κ–ε, and the Differential Reynolds Stress model did not impact significantly on the simulation outcome. They also found that the best UV dose distribution came from the configuration of a reactor in which the inlet and outlet piping are axis-offset and located closest to the reactor ends.

4.3 Fluence-rate distribution model – UVCalc®

Fluence-rate distribution models include several approaches, such as multiple point source summation (MPSS), multiple segment source summation (MSSS), line source integration (LSI), modified LSI (RAD-LSI), discrete ordinate (DO), and view factor. The MSSS approach is a variation of the MPSS approach in

which the lamp is modeled as a series of cylindrical segments instead of point sources. This algorithm is the basis for the commercially available software UVCalc® (Bolton and Cotton, 2008; Liu *et al.*, 2004).

Bolton (2000) presented a detailed description of the application of the MPSS model to calculate fluence-rate distributions, in which the effects of refraction and reflection on the calculated fluence rates are included. In another work, Rahn *et al*. (2006) applied the iodide/iodate actinometer method to determine the fluence-rate distribution in a UV reactor. They observed that the fluence rates calculated by the MSSS approach agree well to those obtained experimentally.

UVCalc®, developed by Bolton Photosciences Inc., is a commercial software package that estimates the fluence rate in a UV reactor based on the MSSS approximation. At first, the model was based on the MPSS method, but it was modified to work with the MSSS approach, because of some inconsistencies between the modeled and measured fluence rates at the ends of the lamp. This model is the only one that has been verified experimentally (Bolton, 2008) and has also been widely applied to model UV reactors in conjunction with CFD codes (Blatchley *et al.*, 2008; Hulsey *et al.*, 2007; Liu *et al.*, 2007; Bohrerova *et al.*, 2005; Ducoste *et al.*, 2005; Jin *et al.*, 2005; Liu *et al.*, 2004). Unlike other commercial models, this model is able to determine the fluence-rate distribution for medium-pressure UV lamps.

4.3.1 Mathematical background of UVCalc®

The conceptual basis of this software is outlined in detail by Bolton (2000). The lamp is considered to be formed by a series of finite cylindrical elements, where

the light is emitted only from the cylinder surface edge and is dependent on the cosine of the angle between the unit normal vector and the direction vector (Liu *et al*., 2004). In the MPSS and MSSS approaches, the fluence rate can be estimated using the expression presented in Equation 4-1 (Bolton, 2000), provided the UV absorbance is zero (UVT = 100%). The fluence rate is a then a function of the radial (H) and longitudinal (x) distance from the lamp, and the effects of refraction/ reflection and absorbance are neglected.

$$E_o(x,H) = \frac{P_\Phi}{4\pi L x}\left[\arctan\left(\frac{L/2+H}{x}\right)+\arctan\left(\frac{L/2-H}{x}\right)\right] \qquad (4\text{-}1)$$

where E_o is the fluence rate (W/m^2), P_Φ is the total UV power output (W) at the wavelength of interest and L is the length of the lamp between electrodes (m).

In the MPSS approach, the power output of each point source is equal to P_Φ/n, where n is the number of point sources (or segment sources in the case of the MSSS approach). It is considered that n = 1001 is a good approximation to the results given by Equation 4-1, again, for a medium with a zero UV absorbance (Bolton, 2000). The UV dose (fluence) is obtained by multiplying the volume-averaged fluence rate by the hydraulic residence time of the liquid in the reactor. This procedure assumes that the reactor behaves as a perfect plug flow reactor with perfect radial mixing and zero longitudinal mixing. As this is seldom the case in 'real' reactors, the distribution of the residence time may be then found by using CFD simulation or tracer studies.

4.4 Coupling ANSYS-CFX with the fluence-rate model

Frequently throughout the document, it has been stressed that there is a need and usefulness to couple fluence rate and CFD models in order to obtain a better picture of the UV reactor performance. A process to implement a CFD model for the designed UV reactor using ANSYS-CFX (v11.0) is discussed below, followed by coupling it with a fluence-rate model, namely UVCalc® 3D.

4.4.1 Inputting information to ANSYS-CFX

The CFD modeling of any device necessarily involves the definition of boundary conditions, namely at its physical boundaries. The geometry was generated using the built-in geometry editor of the ANSYS-CFX, DesignModeler. Once completed, the geometry was exported to the mesh generation software, CFX-mesh. The process of mesh generation is iterative and results in an unstructured surface mesh (faces) and a volume mesh [tetrahedral, prisms, and pyramids (ANSYS, 2007)]. Since the resolution of the mesh might have an effect on the results of the program, an iterative process was performed to verify the differences that arise from each resolution. Dramatic changes (75 and 100% more) in the numbers of elements and nodes led to only minor changes in the numeric results of basic dimensions (velocity, pressure and turbulent eddy viscosity), usually under 10%. Therefore, given the computational costs of higher mesh resolutions, it was decided to run the program with the initial resolution (311,377 elements and 62,204 nodes). Following this process, the file was exported to the physical pre-processor of CFX, CFX-Pre. In this simulation, only

the inlet and outlet boundary conditions were defined – wall type is the default boundary condition.

For the inlet boundary condition, a subsonic flow regime was selected. The UV unit is fed from an overhead tank, which is supposed to keep a constant head during its operation. As a consequence, the 'static pressure' option was selected with a value of 196.4 Pa. Since the flow is fully developed when it reaches the wall boundary condition, the 'zero gradient' option was selected for the flow direction, implying that the velocity gradient perpendicular to the boundary is zero (ANSYS, 2006b). The turbulence is considered to be fully developed, and this option also applies to the turbulence condition. The wall surface is smooth (PVC), so this was the selected option for the wall boundary condition. The 'no-slip' condition was selected, since the walls have a zero velocity and do not exert any influence on the flow (ANSYS, 2006b). For the outlet boundary conditions, a subsonic flow and an average static pressure of zero over the whole outlet (this being a free discharge) were specified. The physical conditions of the spores had also to be specified for particle modeling.

The trajectories of the spores were modeled using the Lagrangian particle tracking multiphase model because of the more detailed computation of the flow field and residence time (ANSYS, 2006b). The following physical properties were specified for the spore material, as derived from one of the principal components of a *B. subtilis* spore core, namely, pyridine-2,6-dicarboxylic acid (Setlow, 2007): thermodynamic state = solid; density = 1020 kg/m^3; molar mass = 167.12 kg/kmol; specific heat capacity = 155.15 J/kg·K. An average diameter of 1.2 μm

with an area factor of 0.73 was established for all particles. The area factor accounts for the rod-like shape of the average spore (Chada *et al*., 2003).

A 'zero slip' velocity was selected at the inlet, since it was assumed that the particles had the same velocity as that of the continuous fluid. As the spores were considered to enter the inlet at random locations, the number of positions was set at 250 in order to compute as many trajectories as possible with the computational resources at hand. No mass flow rate of spores was considered, as this is deemed irrelevant in one-way coupling conditions, such as the present one (ANSYS, 2006b). After inputting all this data, the input file was written and processed in the software solver (ANSYS CFX-Solver). After runs slightly over one hour (in a 2 GB RAM, 2.8 GHz Intel™ dual-processor desktop PC), the results were ready to be analyzed in the software graphic post-processor (ANSYS CFX-Post).

4.4.2 Coupling the CFD and fluence-rate models

Once the processing of input data was completed, the post-processor software produced the results of the physical variables for the selected boundary conditions. An example of the results of the velocity field in the UV reactor is shown in Figure 4-1. The velocity increases at those sites where the flow encounters obstacles, especially after the inlet valve and the inlet piping. These conditions of peak velocity do increase the turbulence and, therefore, improve the mixing and increase the overall effective UV dose.

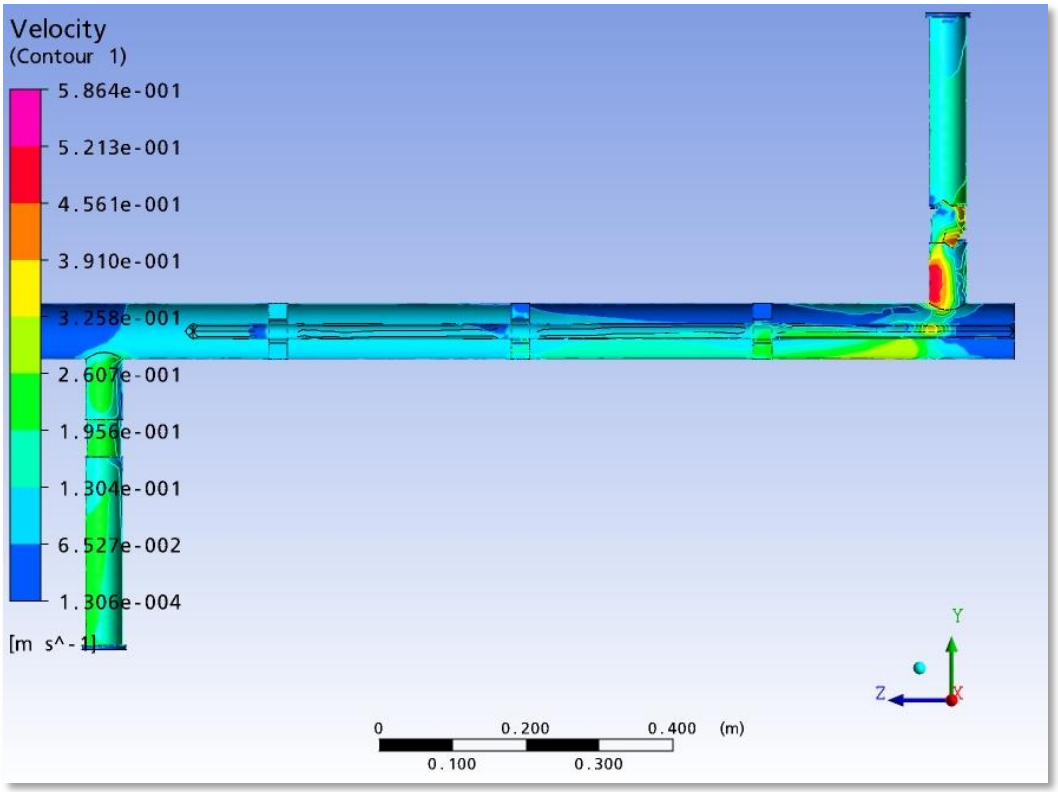

Figure 4-1 Example of a CFD simulation of the velocity distribution in the UV unit

The fluence rate, as calculated by the software UVCalc® 3D (Bolton Photosciences Inc., Edmonton, AB), was added to the CFX report containing the travel time of each particle (derived from the particle tracking). UVCalc® 3D is very similar to the one-dimensional version mentioned in Section 4.3, with the difference being that it can handle up to 100 low pressure UV lamps parallel to flow (or not parallel) and be coupled with CFD programs (BPI, 2010).

Coupling of the CFX and UVCalc® 3D software packages results in the UV dose distribution within the reactor for the conditions explored. The UV dose distribution is obtained from the frequency of the cumulative UV doses received by each particle travelling through the reactor, as calculated by the 'histogram' feature of Microsoft Excel's Data Analysis pack. Since every specific trajectory is

different, it is clear that every particle will receive a different UV dose when travelling through the reactor. For each of the different combinations of flow rate and UVT tested during the biodosimetry test, a different UV dose distribution results. For example, Figure 4-2 shows the UV dose distribution for three different flow rates: 1.32, 1.01 and 0.52 L/s and three similar UVTs (98.3, 99.1 and 98% respectively). As seen there, the peak UV doses shift to the right as the flow rate decreases, although the UV dose distribution arguably becomes more homogenous as the flow rate increases.

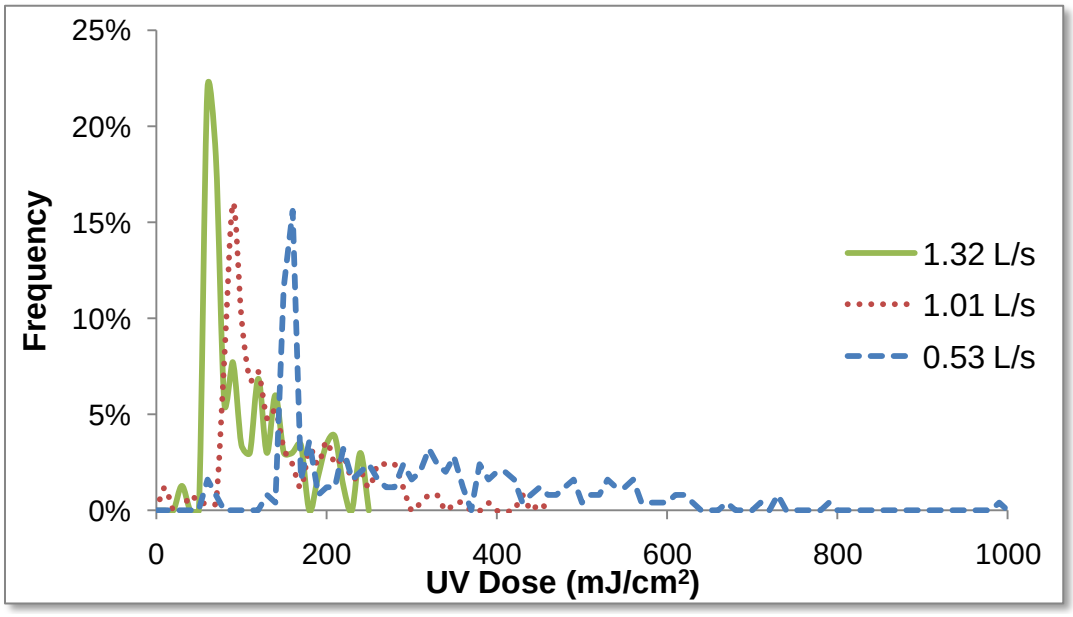

Figure 4-2 UV dose distributions for various flow rates and UVT ~ 98%

Graphically, it is also possible to map the cumulative UV dose that each particle is receiving as it travels through the reactor and the fluence-rate distribution within the UV reactor under a specific set of conditions. In Figure 4-3, an example of the cumulative UV dose inside the UV reactor is displayed. It is clear from the below figure that the higher UV doses appear mainly at the end of the travel of the particles through the reactor, near the reactor outlet.

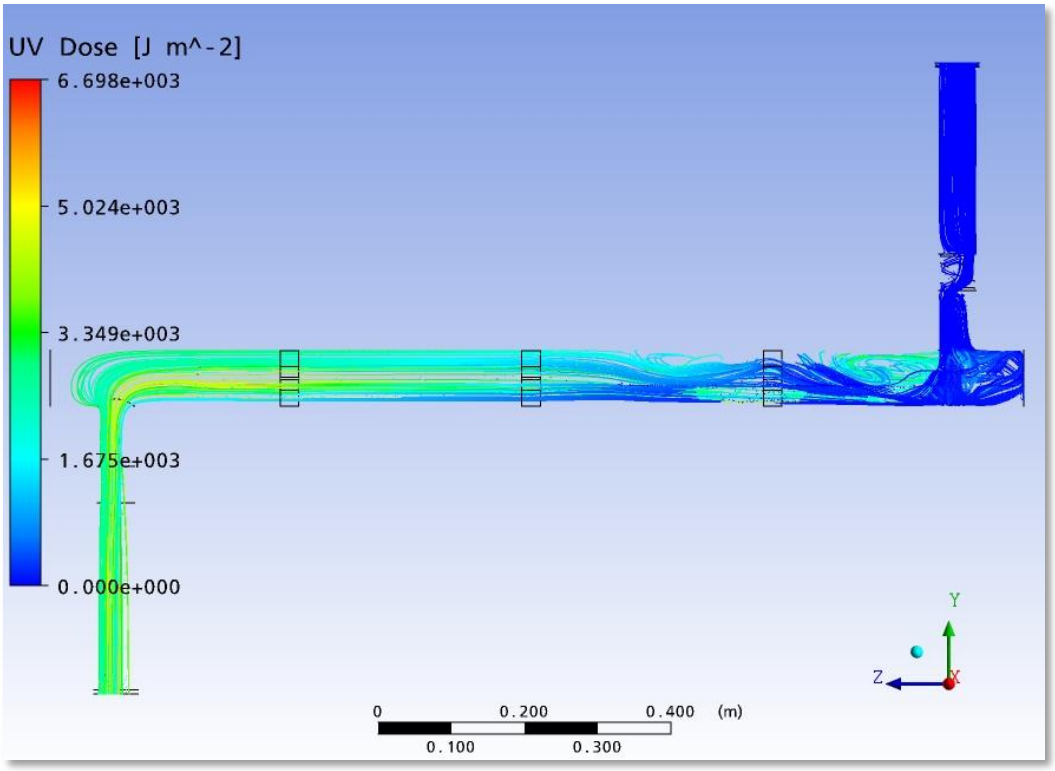

Figure 4-3 Cumulative UV dose within the UV reactor for a flow rate of 0.52 L/s and a UVT of 98%

The product of the value of the fluence rate in each volume element times the travel time in seconds of each particle traversing that particular volume element yields the UV dose contribution from that volume element. By applying this procedure for every volume element that particle (spore) traverses, the cumulative UV dose received by each particle can be computed and plotted, as presented in Figure 4-2. It is a fact that each particle follows a different trajectory; it is also that the fluence-rate distribution may change as a result of changes in the UVT, for example. In view of this, Cabaj *et al*. (1993) suggest calculating the RED as the mean UV dose distribution weighted with the UV dose-response curve of the microorganism (biodosimeter), as shown in Equation 4-2.

$$\mathrm{RED}(G_{\mathrm{D}}, k, D_{\mathrm{s}}) = \frac{1}{k} \cdot \log\left(\frac{\int_0^{D_{\mathrm{s}}} G_{\mathrm{D}}(D)\mathrm{d}D + \int_{D_{\mathrm{s}}}^{\infty} 10^{k(D-D_{\mathrm{s}})} G_{\mathrm{D}}(D)\mathrm{d}D}{\int_0^{\infty} G_{\mathrm{D}}(D)\mathrm{d}D} \right) + D_{\mathrm{s}} \qquad (4\text{-}2)$$

where D is the UV dose (mJ/cm^2), $G_{\mathrm{D}}(D)$ is the frequency density of that dose received by the organisms leaving the reactor (cm^2/mJ), k is the first-order inactivation constant (cm^2/mJ), and D_{s} is the 'shoulder' dose, that is, up to which is assumed not to have a germicidal effect (mJ/cm^2). When computing the multi-target model (Section 3.6), D_{s} was determined as the negative logarithm of the critical number of targets (n_c) divided by k, and had a value of 11.5 mJ/cm^2. The resulting REDs, as computed from the software coupling, are shown in Table 4-2, which is in turn compared with the results of biodosimetry and the theoretical maximum UV dose from the stand-alone UVCalc® Ver. 1.

Table 4-2 Comparison of the REDs and UV doses obtained by each approach for the conditions of the validation

Flow rate (L/s)	UVT (%)	UV Dose (mJ/cm^2)			MUVI	RED ratio	Modeled MUVI
		Bio-dosimetry RED	UVCalc®	CFX-UVCalc® 3D RED	Bio-dosimetry /UVCalc®	Biodosimetry /CFX-UVCalc® 3D	CFX-UVCalc® 3D RED/ UVCalc®
0.52	70.0	37.3	73	113.9	0.52	0.33	1.56
0.52	85.1	68.1	94.5	152.1	0.74	0.45	1.61
0.52	98.0	88.2	115.9	189.7	0.78	0.46	1.64
1.01	70.7	37.4	37.7	69.3	0.99	0.54	1.84
1.01	84.3	34.3	47.6	91.3	0.72	0.38	1.92
1.01	99.1	80	60.2	120.6	1.33	0.66	2.00
1.32	69.0	45.7	28.2	53	1.37	0.86	1.88
1.32	86.4	28.3	37.9	72.3	0.63	0.39	1.91
1.32	98.3	69.4	45.9	89.5	1.28	0.78	1.95

In light of the very low UV sensitivity of the *B. subtilis* spores used in this study, the approaches which involve its UV dose-response curve in the calculation of the UV doses – namely biodosimetry and joint fluence-rate/CFD models – tend to yield very high UV dose (or RED) values. Cabaj et al. (1993) observed this in their study, where they also included the breadth of the UV dose distribution as a factor in the value of the RED. In this study, the UV doses computed from the joint CFD/fluence-rate distribution model were always higher than the theoretical values calculated by the UVCalc® Ver. 1, even by as much as twice.

In Section 3.4.3, the coefficient of maximum UV inactivation (MUVI) was defined and explained and in Table 3-6 the MUVIs for the conditions present during the biodosimetry test were computed. Those same MUVIs were put into Table 4-2, alongside the RED ratios computed based on the REDs from the biodosimetry test and the UV doses obtained from the joint CFX/UVCalc® 3D model. Modeled MUVIs, that is, the ratio between the UV doses determined from fluence-rate distribution models and those determined using joint CFD-fluence-rate distribution models are shown in the last column of Table 4-2. From what is observed in Table 4-2, the RED ratios follow basically the same trend followed by the MUVIs, that is, their lowest values are obtained for a UVT of around 85% and their values tend to increase as the flow rate increases (see Section 3.6). The modeled MUVIs should be less than unity; however, the low UV sensitivity of the spores used in the biodosimetry tests skews the biodosimetry REDs to higher values. This can be seen more clearly in Figure 4-4 where the MUVIs obtained for four different UV dose-response curves of the same organism are presented.

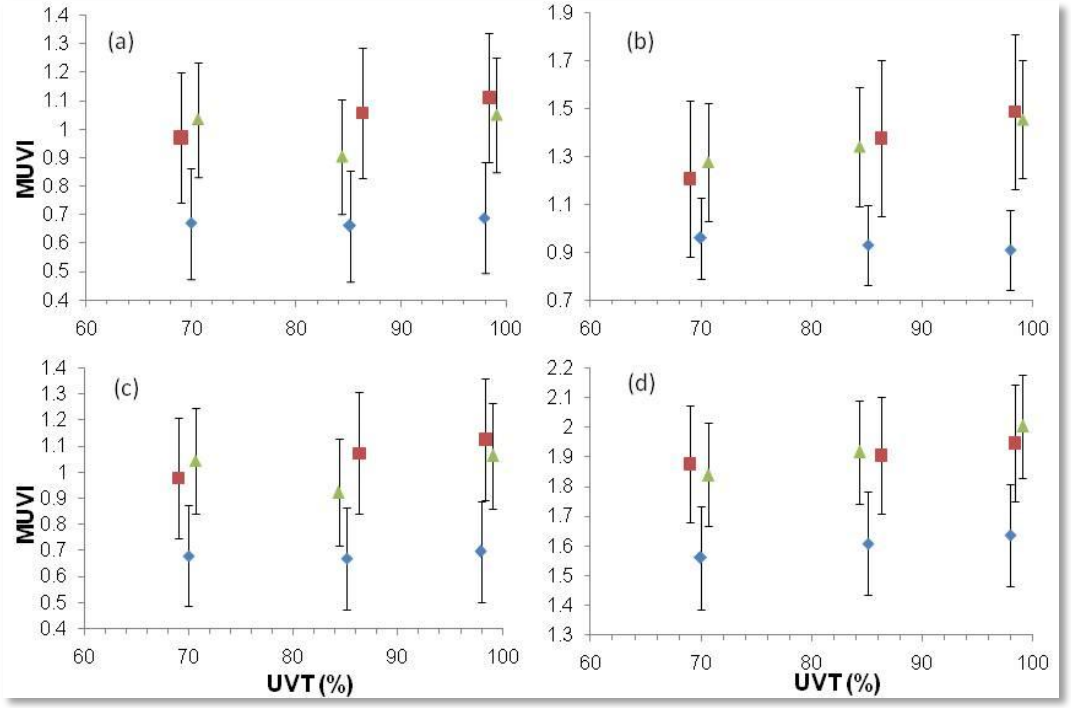

Figure 4-4 MUVIs for flow rates of 0.52 (♦), 1.01 (▲), and 1.32 L/s (■) and four UV dose-response curves: k = 0.089, D_s = 9.9 (a); k = 0.038, D_s = 12.35 (b); k = 0.086, D_s = 6.01 (c); and k = 0.008, D_s = 11.53 (d)

The MUVIs shown in Figure 4-4 came from the REDs computed by inputting the multi-target model parameters (k, D_s) of four different UV-dose response curves, and the UV dose distributions obtained from the CFX-UVCalc® 3D model, into Equation 4-2. The model parameters in Figure 4-4a are those reported by Chen *et al*. (2009) at 254 nm; those in Figure 4-4b resulted from an assessment carried out at some point during this study; the ones in Figure 4-4c resulted from the November 2010 experiment, shown in Figure 3-7, for pH = 7 and t = 144 h; and the model parameters in Figure 4-4d resulted from the joint CFD-fluence-rate distribution model, hence these MUVIs are equal to the modeled MUVIs shown in Table 4-2. Regardless of the factors contributing to the UV sensitivity of the spores, it is interesting to note how the MUVI values in Figure 4-4a and Figure

4-4c are so similar, never exceeding 2% between each other; for those UV dose-response curves, the values of the first-order inactivation constant (k) are practically the same. However, for less UV-sensitive organisms, such as those depicted in Figure 4-4b and Figure 4-4d – with much lower values of k – the resulting MUVIs exceed as much as 1.5 and 2.4 times the average of the MUVI values shown in Figure 4-4a and Figure 4-4c, respectively. Overall, MUVI values tend to increase with an increasing flow rate and UVT, except for the 0.52 L/s flow rate, where the MUVI values are rather steady for all UVTs. This suggests that MUVIs close to unity are not easy to achieve with this flow rate, even if the UVT is increased.

The marked differences in the values of the MUVI may be the result of using the lower end of the UV dose distributions to calculate the REDs of highly UV-resistant organisms. The above results in a high uncertainty with respect to the behaviour of the UV-dose response curve at greater log inactivations. Such uncertainty also reflects in the high values of the validation factor (VF), and thus the validated doses (D_{Val}) delivered by the UV reactor, as explained in Section 3.6 and computed in Appendix A.5. Therefore, it is suggested that when dealing with highly UV-resistant organisms the UV doses used to determine the UV-dose response curve be as large as possible, so to achieve log inactivations reached with 'normal' spores, that is, around 4-log or 99.99%. By doing this, a lower uncertainty may also be expected, as well as lower values of VF and D_{Val}.

The very high REDs given by the joint CFX/UVCalc® 3D model for the highly UV-resistant spores, which result in high MUVI values, may not

necessarily be an accurate depiction of the hydraulic conditions of the reactor. So, for the sake of accuracy, it is strongly recommended that any experiment that intends to derive the MUVIs for a specific set of conditions be carried out using bacteria (or viruses) with a higher UV susceptibility than that of the spores used in this study. This is the only way that the modeled MUVIs can be safely used to calibrate the precision of the actual MUVIs. This would also allow developing accurate models to evaluate the hydraulic performance of UV reactors without having to build prototypes or carrying out lengthy biodosimetry tests.

Another aspect that deserves mention, however, is the measurement of the flow rate in the full-scale reactor. As mentioned earlier, the method used for this purpose was the volumetric measure of flow. Although this is a fairly accurate method to determine flow rates, it should be noted that in a flow-through reactor fed by an overhead tank the flow rate may change depending on the hydraulic head in the tank. If this head is steady, there should not be any problems; however, the conditions of this study made it difficult to achieve this, so there might be a chance for fluctuation in the flow rate going through the reactor, depending on the head change. In order to avoid this, it is highly recommended to measure instantaneous flow rates with the aid of an accurate flow meter, such as a sonar-based flow meter.

5. IMPLEMENTING UV DISINFECTION IN A LOW-INCOME COMMUNITY

Previous sections have illustrated the tests and models used to evaluate the performance of a UV unit in laboratory. These include biodosimetry tests and CFD and fluence-rate distribution modeling. Once completed, the assessed UV unit and a commercially-available UV unit (TrojanUVMax™, Model A, Trojan Technologies, London, ON) were taken to the field to evaluate their work under 'real' conditions. It should be emphasized that any kind of modeling (CFD, fluence-rate distribution) was not carried out for the commercial UV unit, since commercial units usually undergo extensive testing and modeling before their release for use. Here, the description of the implementation process in the field is presented.

5.1 Assessing the performance of the UV units

As pointed out earlier, the UV unit was set to be installed in the rural community of Cerro Grande in Bolivia; a lack of essential utilities by its inhabitants led to the design of a solar power system for the UV unit. The change of conditions in the community that took place around August 2009, concerning the brand-new water distribution system, was documented in Section 3.1.4. It was this change of conditions that affected the operation of the designed UV unit during part of the time that it was in field. Specifically, the UV unit had been planned to be hooked up to the outlet of the manual pump depicted in Figure 3-2; however, since this well would be out of service shortly in favour of the drilled well, it was decided instead to derive a connection from the latter to the UV unit. According to the

residents, about one month after the unit was hooked up to the new water system, the turbidity flowing out of the well made it challenging for them to keep drinking the water, even if it had already been exposed to the UV treatment; moreover, the surface of the quartz sleeve was fouled with sediment deposits. The lab results from the samples taken in the UV unit, before and after UV treatment, indicate that a significant concentration of microorganisms was found in the well, as presented in Table 5-1. All parameters, except for the UVT, were analyzed at UTALAB, using the analytical methods listed in Table 3-2 (see the original reports in Appendix B). The UVT was analyzed at the UA using a spectrophotometer (Ultrospec 2100 pro, GE Healthcare Biosciences, Pittsburgh, PA).

Table 5-1 Laboratory results for grab samples taken before and after the UV unit in the community of Cerro Grande

Parameter	Units	Date	Values		Bacterial log inactivation
			Inlet	Outlet	
Total coliforms	MPN/100 mL	Jan-15/10	4300	240	1.3
		Jan-18/10	93	43	0.3
		Jan-20/10	2300	9	2.4
Fecal coliforms	MPN/100 mL	Jan-15/10	4300	240	1.3
		Jan-18/10	93	9	1.0
		Jan-20/10	2300	9	2.4
Turbidity	NTU	Jan-18/10	5.6	-	N.A.
		Jan-20/10	14.8	-	N.A.
UVT at 254 nm	%	Jan-18/10	34.3	-	N.A.
		Jan-20/10	35.8	-	N.A.

The values of coliform bacteria were reported in MPN/100 mL because the high turbidity of the samples prevented the use of membranes and hence the report of CFU/100 mL units. Because of the high turbidity and UVT values, the quartz sleeve fouling, and a clear lack of maintenance, only small log inactivation numbers could be achieved with the UV treatment. However, and in spite of this, the bacterial log reductions were always above zero, reaching a maximum of 2.4 and a minimum of 0.3. This leads to a recommendation to install a pre-treatment system prior to the point of entry (or inlet) to the UV unit, if high values of turbidity are to be common along with, of course, frequent maintenance. According to reports of the locals, the turbidity in other wells has usually cleared out in a matter of days; for this particular well, the turbidity had not cleared out after two months.

One option for pre-treatment is granular filtration. This may be carried out through a Bio Sand filter (BSF), which is promoted by the NGO COBAGUAL (see Section 3.1.1). This is an intermittent filter that develops a layer of microorganisms (*smutzdecke*) on top of the granular media, which, in turn, helps in the removal of microbiological and chemical contaminants. Studies suggest a clean bed filtration rate between 1 and 4 m/h, with the depth of filtrating media ranging between 0.4 and 0.5 m (Kubare and Haarhoff, 2010). A maximum value of 30 NTU is recommended for the influent turbidity.

Another option for pre-treatment may be the use of aloe (*Aloe barbandensis* Miller) gel, which allegedly renders the water clear by promoting the settling of dissolved solids. This form of water treatment is widely practiced in the rural

parts of Southern Bolivia, according to the local residents. Although hard evidence is difficult to obtain on this regard, Zhou *et al*. (2007) suggest a greater settling potential for aloe and kelp, as compared to zeolite, when used as absorbents of algal inhibitors. The chemical composition of the gel is what could make it comparable to commercial coagulants, such as alum, although more research is required to draw definitive conclusions on its physico-chemical and germicidal properties.

Concerning the commercial UV unit, it was installed on a side pipe from the water main coming down from the reservoir. This unit can safely treat a flow of up to 11.4 L/min (3 GPM), according to the manufacturer's datasheet. With the water requirements computed in Section 3.2.1, more than 500 persons could be served by this system, but it should be noted that the presence of taps might increase the actual consumption.

5.2 Conditions in the community for the implementation of the technology

The limited time that the designed UV unit remained on site was not enough to verify the effects of its implementation in the long term. However, a quick glance over the community exposed several risk factors that may lead to outbreaks of waterborne diseases, such as a lack of water treatment, the use of uncovered containers for the storage of water, raising of animals, presence of latrines (and their lack of maintenance), and reported signs of water contamination. A significant outbreak is not recalled by the residents or the nurse, but he and his predecessors have not kept proper track of the health records, hence the claims of

waterborne diseases cannot be substantiated. The fact is that although the water does have some level of microbiological pollution, it does not result in significant disease outbreaks, except for mild, isolated cases, mainly during the wet season (according to the nurse's account), affecting young children especially. This may be explained, in part, to a lower degree of virulence for diseases in greatly endemic areas. That factor has been attributed to the suggested reduced virulence of pathogens, as in the case of *Vibrio cholerae* (Ewald *et al*., 1998) or to the innate immunity against organisms such as *Giardia* (Lane and Lloyd, 2002; Faubert, 2000).

As for the feasibility of implementing a water treatment system that renders the water free from pathogens, people seem to be willing to pay for it but in accordance to their income. A suggested figure of US$2 (Bs.$14) per month may seem low but this is equivalent to nearly 6% of the average monthly salary of rural workers and almost 3% of the legal minimum monthly wage in Bolivia (see Section 3.1.3). A lack of economic resources can be offset by in-kind contributions, such as labour, as has been the case in many of the projects carried out in the community. Given the cooperative scheme in place in the community, a water treatment system that minimizes O&M costs and maximizes local labour during construction will always be favoured.

5.3 Cost analysis and life cycle assessment

Cost is a variable that traditionally has been regarded as a barrier to achieve a larger implementation of UV-based water treatment systems in developing countries. In fact, at least in Bolivia, this kind of equipment has been used mainly

by industrial customers, according to a local retailer. The costs analyzed here come from an assumed UV unit which includes a 50-W UV lamp and is able to treat flow rates up to 0.5 L/s (8 GPM). When applicable, the solar power system is assumed to have a 60 W output and a 65 Ah battery capacity. A factor of 1.58 times the cost of the equipment in North America is applied to include costs of taxes, importation, nationalization and retail profit. The costs of land are not taken into account.

5.3.1 Capital costs

These costs refer to the initial investment for the system, including equipment and materials, labour and tools. Several scenarios may arise as a result of combinations of the following three factors: the need for water pre-treatment, the presence of an electrical grid, and the presence of a distribution system for piped water. The need for water pre-treatment arises from high turbidity values, which may be rather permanent, and call for a system (usually a granular filter) that is able to reduce them. In off-grid locations, an alternative (solar) power system for the UV system is obviously required.

The presence (or absence) of a distribution system of piped water has to do with the method of hooking up the UV unit to the water source. Where such a network does not exist, water from the source should be collected in a reservoir prior to UV treatment; otherwise, it could be installed directly in-line with the network main. The treated water might then be stored in reservoirs connected in series or in parallel, depending on the community needs (Figure 5-1).

Alternatively, a large reservoir may be used instead of several reservoirs. Plastic 200-L barrels, with a lid, may be employed as reservoirs.

In some long-established wells a UV sensor may not be required for the UV reactor. But, in those sources where turbidity does fluctuate, a UV sensor connected to an alarm is highly suggested in order to warn the operator about this condition. Between four and five barrels might be needed to supply water during the usual two periods per day of water fetching, that is, in the morning and shortly after noon. It also should be noted that a plastic UV reactor chamber was quoted in a specialized workshop in Bolivia, including labour and accessories.

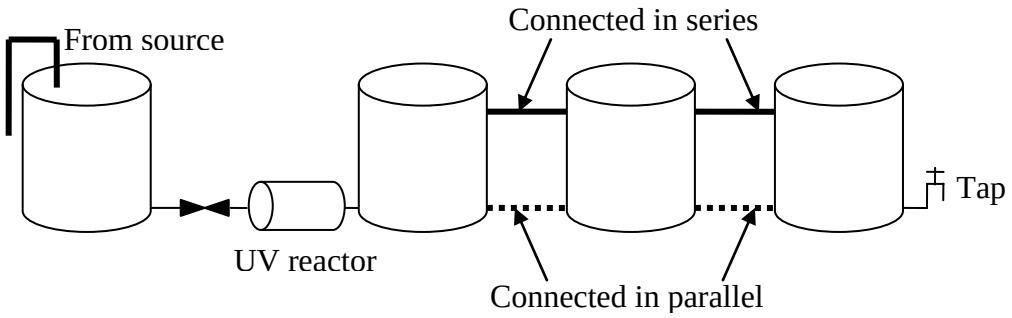

Figure 5-1 Configuration for the reservoirs when no piped water is available

The capital costs for the various components are described below using an average exchange rate of Bs.$7 per US$1.

- UV system (includes reactor, UV lamp, quartz sleeve and ballast) = US$943
- Solar power system (includes solar panel, inverter, regulator and battery) = US$1,539
- Solar power system (for DC UV lamps, inverter and battery not included) = US$975

- Plastic reservoirs (includes accessories) = US$323
- Wood (wooden structures of support) = US$56
- Alarm system (includes radiation detector, UV sensor, relay and alarm) = US$551
- BioSand filter [extrapolated from the cost for a household unit given by Hirsche and Jayanthan (2007)] = US$714
- Labour (for the installation of the components and the building of structures; includes tools) = US$56

The costs for the options of components are summarized in Table 5-2.

5.3.2 O&M costs

It has been mentioned previously in the document that O&M costs depend on several factors. However, two significant factors are spare parts and labour requirements. In the case of a UV unit, the principal spare part, which needs to be replaced on a periodic basis, is the UV lamp. Moreover, if solar power systems are to be used, the battery should also be listed. Regardless of the technology, the O&M of any water treatment system will require manual labour, whose dedication and qualifications depends mainly on the sophistication of the technology and the size of the system. Below, the O&M requirements for the alternatives outlined in the previous section are given. The O&M costs, which are presented in Table 5-2, were computed with an hourly rate of US$0.47 for the labour (derived from the minimum legal monthly wage in Bolivia), plus an additional 5% to account for tool wear. In on-grid locations, the cost of electrical

energy is taken as US$0.09 [Bs.$0.62 according to INE (2009)] per kilowatt hour (kWh).

Table 5-2 Comparison of the various costs of the alternatives

Pre-treatment		Grid		Network		Alarm		Capital costs (US$)	O&M costs/year (US$)	LCCs (US$)	US $/m^3	Min. No. of users
Yes	No	Yes	No	Yes	No	Yes	No					
✓		✓		✓			✓	1,713	216	440	0.07	27
✓		✓			✓		✓	2,092	189	538	0.18	30
✓			✓	✓			✓	3,252	230	836	0.27	44
✓			✓		✓		✓	3,631	232	933	0.12	48
✓			✓		✓		✓	3,067*	182	788	0.10	40
	✓	✓		✓		✓		1,550	248	398	0.16	27
	✓	✓		✓			✓	999	236	257	0.13	20
	✓		✓	✓		✓		3,089	262	794	0.27	43
	✓		✓	✓			✓	2,538	240	652	0.23	37
	✓	✓			✓	✓		1,929	221	496	0.18	29
	✓	✓			✓		✓	1,378	209	354	0.14	23
	✓		✓		✓	✓		3,468	264	892	0.29	47
	✓		✓		✓		✓	2,917	252	750	0.25	41
	✓		✓		✓		✓	2,353*	202	605	0.20	33

*These correspond to the alternatives where DC UV lamps are used

- UV system: this system requires replacing the UV lamp every year, regardless of the actual time of the operation. For systems installed downstream of a granular filter, the off-line chemical cleaning (OCC) of the quartz sleeve (see Section 2.7.1) is assumed to be performed every

month. For systems with no previous treatment, the OCC is assumed to be performed every week. The estimated time of the cleaning procedure is 1.5 h and about 125 mL of acetic acid is required per event. Additionally, it is assumed that the quartz sleeve will be replaced every five years.

- Solar power system: the O&M requires only the removal of dust and particles from the panel, which is estimated to take 1 h every two months. The battery is assumed to require no service (sealed) and to be replaced every three years, if installed.
- Plastic reservoirs: the only O&M task required for this component is cleaning, assumed to take two hours every six months.
- Alarm system: this system requires no maintenance other than the OCC of the UV sensor, with the same frequency as that of the quartz sleeve. The estimated time is 0.5 h.
- BioSand filter: according to Kubare and Haarhoff (2010), a typical BSF only requires its top layer to be stirred and the resulting dirty water to be collected. For a small community filter this may take 2 h every two months. The increase of the head loss may signal a need for sand cleaning, which is assumed to be performed every three months and to last 4 h. But, if turbidity values get very high, very frequently, a better option to consider would be a roughing filter which, nonetheless, is assumed to have the same O&M requirements as those of the BSF.

The resulting O&M costs for the various combinations of components are again summarized in Table 5-2.

5.3.3 Life cycle costs (LCCs)

As with any other project, the useful life of a water treatment system is limited. This is why, after some years of operation, those facilities have to undergo modifications, upgrading or replacement of all or several of their parts. Most of the components of a UV system, and the solar power system if installed, have a long useful life span, in the order of decades. Since the life spans for the individual components are different, a lifetime of 20 years is assumed for the whole system, in order to homogenize the LCCs. These costs include the money that users have to pay for the replacement or upgrading of the system components at the end of their useful life, converted to present value. They also include the annual payment of the loan, if any was incurred in to pay for the system, converted to present value.

As seen in Table 5-2, the yearly O&M costs are a fraction of the capital costs, so a greater economic effort must be expended by the users at the beginning of the operation of the system. Therefore, the users would have to resort to external credits in order to obtain funding for the implementation of the system; it would be then up to them to pay off the loan during the life time of the system. The present value factor can be computed using Equation 5-1, as presented by Celik *et al*. (2008); the annual payment may then be computed by dividing the amount to finance by this factor.

$$\frac{P}{A} = \frac{1-(1+I)^{-N}}{I} \qquad (5\text{-}1)$$

where *P/A* is the present value factor (unitless), *N* is the number of years and *I* is the interest rate (%). The interest rate (*I*) may take various values depending on the kind of debt. For example, for the mortgage payment the rate to use would be the prime lending rate; on the other hand, for the replacement of the equipment the rate to use would be the net discount rate, that is, the nominal discount rate minus the inflation rate (Celik *et al*., 2008). The values of these rates, as reported in the CIA's World Factbook, are 13.9% for the prime lending rate, 13% for the commercial bank prime lending rate and 4.3% for the inflation rate (CIA, 2010). Since there is no heavy infrastructure that may remain in place after the lifetime of the components expires, salvage values are not taken into account. Yearly LCCs are presented in Table 5-2.

5.3.4 Costs of producing treated water

After assembling all the costs relative to the implementation of a UV-based disinfection system, the cost of each cubic meter of treated water can be found. The calculation was made for the total number of m^3 that is produced during the year, assuming a production of six hours per day in locations with no grid or network, and continuously in those locations with both a grid and network. Additionally, in the locations with both a grid and network a percentage of unaccounted-for water in the network is assumed, to account for loss of revenue (Hassanein and Khalifa, 2008; MSOP, 2004). The percentage of unaccounted-for

water in Latin American utilities is estimated to be about 38% (Hassanein and Khalifa, 2008). The costs of each treated m^3 are presented in Table 5-2.

For those alternatives where the flow is constant, and hence the daily water production is higher, the unit costs of the treated water are lower (Table 5-2). This is in agreement with the concept of economy of scale where the costs are lowered for higher demands as the costs are amortized among more users. A similar observation was made by Cotton *et al*. (2001) where they concluded that the unit cost of treated water is reduced as the size of the system increases. In their study, they determined a value of US$0.54/$m^3$ in the smallest plant (0.02 ML/d). This is a higher value than the highest value reported in Table 5-2, but it should be noted that this plant would also have higher technological requirements in its design, building and operation than any of the systems discussed here.

From Table 5-2 it is also clear that the highest unit cost of treated water (US$ 0.29/m^3) appears for the option of no pre-treatment, no grid, no network and alarm. With the water requirements computed for a situation of no network available, the daily flow rate treated by the UV unit would satisfy the demand of 360 persons or 60 users (one user understood as one single household); the cost of the water treated during one month is close to US$94. Knowing that the users are willing to pay up to US$2 per month to treat their water, it results that 60 users can contribute with US$120 per month, which is US$26 in excess of the actual value required per month. In other words, for this community of 60 users, the monthly fee to disinfect their water with the most expensive UV-based option revised is US$1.57. With a monthly fee of US$2, the equilibrium point, that is,

when the number of users is enough to cover the costs of producing the water for them is reached with the minimum number of users shown in Table 5-2. It can be observed then that the systems evaluated here can be sustainable with as few as 20 users or with 48 users in the worst-case scenario, that is, when pre-treatment is required and there is no grid or network available.

6. CONCLUSIONS AND RECOMMENDATIONS

The performance of the devised UV unit was verified using the approach currently approved by the USEPA, namely biodosimetry, in addition to mathematical models (fluence-rate distribution and CFD) and their combination. What can be inferred from the results of these simulations and experiments is that the concept of 'maximum UV inactivation' of a UV reactor is valuable, as it affords to assess its hydraulic behaviour, and therefore its efficiency, using the results of biodosimetry. By having a good agreement between the results of CFD modeling and the ones recorded by biodosimetry tests the effects of hydraulic changes in the UV reactor efficiency can be modeled accurately. This serves as a way to optimize the design, decrease construction costs, evaluate options of O&M and (retro) fit the implementation of a UV disinfection system to any particular conditions. However, if the CFD modeling is to be used as a design tool, it would be advisable to affect its results for a security factor of around 1.2, unless a calibration of the CFD model is achieved. This calibration could be carried out by means of tracer or particle image velocimetry (PIV) studies.

Amongst the implementation of a locally devised UV disinfection system in a low-income region, one of the most significant costs goes to the validation of the unit. Since the costs and procedures of importing an inoculum can be prohibitive, it is advisable then to look for challenge organisms that may be cultured in local labs, and yet not be too expensive to hamper the development of this technology in low-income countries. However, a cost analysis is always recommended prior to undertaking this procedures as, in some cases, it might result less expensive to

import a fully-equipped, already-validated UV unit than creating locally a new one.

From the cost analysis, it is observed that the calculated costs for the O&M costs of the UV-based technology are within the range of the costs reported by other researchers (see Section 2.4). In accordance with their findings, it is concluded that this technology is affordable for low-income communities, even under conditions of lack of electricity, piped distribution networks and an adequate feed water quality. This allows the implementation of this technology elsewhere like, for example, in remote First Nations communities in Northern Canada. Some of these communities enjoy having in place piped water infrastructure, while other smaller communities where the water has to be manually fetched from wells or ponds may greatly benefit from having a stand-alone disinfection system. Further research is suggested on the topic of water pre-treatment, especially for those water sources with a very high turbidity. In those cases, the research may be focused on the design and performance of high-rate, locally-built roughing filters and the use of alternative coagulants/flocculants such as aloe vera, widely used in Southern Bolivia and described earlier in the document.

The use of DC UV lamps, which do not require additional infrastructure of battery and inverter, was included among the costs analysis (Table 5-2). However, this is a technology that has to be carefully reviewed, as the sturdiness of a DC UV lamp with respect to fluctuating input has not been extensively studied. Since this is an option with a significant effect on the capital and O&M costs, let alone

the sustainability of the system, more research is thus suggested. Also, the issue of the disposal of used UV lamps deserves attention, because of their mercury content. As long as new technologies, which do not generate hazardous waste – such as UV LEDs (Chatterley and Linden, 2010) – are not currently affordable, the disposal of used UV lamps in low-income communities requires further research.

Given the small time window in which this project was developed, especially in its field stage, a more thorough evaluation of the impact of the technology on the villagers' health could not be completed. As mentioned in Section 5.2, people under conditions of constant exposure to pathogenic organisms develop effective immune systems against those organisms. This might seem to be the case of this community, since there have not been many reports of outbreaks, although when they did occur they seemed to affect young children mainly. Interestingly, the samples taken from the water sources in the community always showed some kind of microbiological contamination, above the national guidelines. This is why it is suggested to verify the impact of UV-based technologies with more exhaustive clinical and field testing. By doing this, the actual source of disease may be tracked down and even the perception of skeptic persons may be changed.

Finally, another issue that is worth researching is the community mobilization towards the realization of this kind of project. Although the scope of such a research falls rather in the social sciences field, it is also true that engineering development-related projects usually include views of different disciplines to gain a greater impact. And, unlike technologies already in place in rural Bolivia, such

as SODIS or BSFs, UV-based disinfection systems are to be applied at the community level rather than at household level. Therefore, even though it is more challenging to engage the whole community at once than on a house-by-house basis, the impact of the project could be, undoubtedly, much wider.

BIBLIOGRAPHY

Abu-Hamdeh NH (2000). Photovoltaic system design for a village of farmers in Jordan Badia. *Applied Engineering in Agriculture* **16**: 3, 297 – 302.

Alawaji S, Smiai SM, Rafique S, and Stafford B (1995). PV-Powered water pumping and desalination plant for remote areas in Saudi Arabia, *Applied Energy* **52**: 2-3, 283 – 289.

Andrady AL, Torikai A, and Fueki K (1989). Photodegradation of rigid PVC formulations. I. Wavelength sensitivity to light-induced yellowing by monochromatic light, *Journal of Applied Polymer Science* **37**: 4, 935 – 946.

Annaratone D. 2010. *Engineering heat transfer*. Berlin, Germany: Springer-Verlag.

ANSYS (2006a). ANSYS CFX Introduction – ANSYS CFX Release 11.0, ANSYS Europe, Ltd., Canonsburg, PA.

ANSYS (2006b). ANSYS CFX-Solver modeling guide – ANSYS CFX Release 11.0, ANSYS Europe, Ltd., Canonsburg, PA.

ANSYS (2006c). ANSYS CFX-Solver theory guide – ANSYS CFX Release 11.0, ANSYS Europe, Ltd., Canonsburg, PA.

ANSYS (2007). CFX Mesh help – ANSYS Release 11.0, SAS IP, Inc., Canonsburg, PA.

Argaw N (2003). Renewable energy in water and wastewater treatment applications – Period of performance: April 1, 2001 – September 1, 2001, National Renewable Energy Laboratory, Golden, CO. Available at: www.nrel.gov/docs/fy03osti/30383.pdf

AUC (2009). Germicidal ultraviolet lamps Ster-L-Ray, Atlantic Ultraviolet Corporation, Hauppauge, NY. Available at: http://www.ultraviolet.com/pdflib/981039.pdf

Bishop RH. 2002. *The mechatronics handbook*. Boca Raton, FL: The Instrumentation, Systems, and Automation Society, CRC Press LLC.

Blatchley III ER, Shen C, Scheible OK, Robinson JP, Ragheb K, Bergstrom DE, Rokjer D (2008). Validation of large-scale, monochromatic UV disinfection systems for drinking water using dyed microspheres, *Water Research* **42**: 3, 677 – 688.

Bohrerova Z, Bohrer G, Mohanraj SM, Ducoste J, and Linden K (2005). Experimental measurements of fluence distribution in a UV reactor using fluorescent microspheres, *Environmental Science and Technology* **39**: 22, 8925 – 8930.

Bohrerova Z, Mamane H, Ducoste J, and Linden K (2006). Comparative inactivation of *Bacillus subtilis* spores and MS2 coliphage in a UV reactor: Implications for validation, *Journal of Environmental Engineering* **13**: 12, 1554 – 1561.

Bolton JR (2000). Calculation of ultraviolet fluence rate distribution in an annular reactor: Significance of refraction and reflection. *Water Research* **34**: 13, 3315 – 3324

Bolton JR (2004). Germicidal fluence (UV dose) calculations for a low pressure UV lamp, Bolton Photosciences Inc., Edmonton, AB.

Bolton JR (2008). Manual for UVCalc® version 1.0, Bolton Photosciences Inc., Edmonton, AB.

Bolton JR and Cotton CA. 2008. *The ultraviolet disinfection handbook*. Denver, CO: American Water Works Association.

Bolton JR and Linden K (2003). Standardization of methods for fluence (UV dose) – Determination in bench-scale UV experiments, *Journal of Environmental Engineering* **129**: 3, 209 – 215.

BP Solar (2003). 135 watt photovoltaic module BP 3135 data sheet, BP p.l.c., London, UK. Available at: http://www.bp.com/liveassets/bp_internet/solar/bp_solar_usa/STAGING/local_assets/downloads_pdfs/product_data_sheet_bp_3135.pdf

BPI (2010). Announcement – UVCalc® software now online, Bolton Photosciences Inc, Edmonton, AB. Retrieved from http://www.boltonuv.com/sites/default/files/UVCalcWebAnnouncement.pdf on April 19, 2010.

Brownell SA, Chakrabarti AR, Kaser FM, Connelly LG, Peletz RL, Reygadas F, Lang MJ, Kammen DM, and Nelson KL (2008). Assessment of a low-cost, point-of-use, ultraviolet water disinfection technology, *Journal of Water and Health* **6**: 1, 53 – 65.

Burch JD and Thomas KE (1998). Water disinfection for developing countries and potential for solar thermal pasteurization, *Solar Energy* **64**: 1-3, 87 – 97.

Cabaj A, Sommer R, and Schoenen D (1993). Biodosimetry: Model calculations for U.V. water disinfection devices with regard to dose distributions, *Water Research* **30**: 4, 1003 – 1009.

Celik AN, Muneer T, and Clarke P (2008). Optimal sizing and life cycle assessment of residential photovoltaic energy systems with battery storage, *Progress in Photovoltaics: Research and Applications* **16**: 1, 69 – 85.

Chada VGR, Sanstad EA, Wang R, and Driks A (2003). Morphogenesis of *Bacillus* spore surfaces, *Journal of Bacteriology* **185**: 21, 6255 – 6261.

Chatterley C and Linden K (2010). Demonstration and evaluation of germicidal UV-LEDs for point-of-use water disinfection, *Journal of Water and Health* **8**: 3, 479 – 486.

Chen S and Ravallion M (2008). The developing world is poorer than we thought, but no less successful in the fight against poverty, The World Bank, Development Research Group, Washington DC. Available at: http://www-wds.worldbank.org/external/default/WDSContentServer/IW3P/IB/2010/01/21/000158349_20100121133109/Rendered/PDF/WPS4703.pdf

Chen RZ, Craik SA, and Bolton JR (2009). Comparison of the action spectra and relative DNA absorbance spectra of microorganisms: Information important for the determination of germicidal fluence (UV dose) in an ultraviolet disinfection of water, *Water Research* **43**: 20, 5087 – 5096.

Chevefrils G, Caron E, Wright H, Sakamoto G, Payment P, Barbeau B, and Cairns B (2006). UV dose required to achieve incremental log inactivation of bacteria, protozoa and viruses, *IUVA News* **8**: 1, 38 – 45.

CIA (2010). The World Factbook, Central Intelligence Agency, Washington DC. Retrieved from https://www.cia.gov/library/publications/the-world-factbook/geos/bl.html on May 6, 2010.

Concha F (2008). Settling velocities of particulate systems 15: velocities in turbulent Newtonian flows, *International Journal of Mineral Processing* **88**: 3-4, 89 – 93.

Cotton CA, Owen DM, Cline GC, and Brodeur TP (2001). UV disinfection costs for inactivating *Cryptosporidium*, *American Water Works Association Journal* **93**: 6, 82 – 94.

Dejung S, Fuentes I, Almanza G, Jarro R, Navarro L, Arias G, Urquieta E, Torrico A, Fernández W, Iriarte M, Birrer C, Stahel WA, and Wegelin M (2007). Effect of solar water disinfection (SODIS) on model microorganisms under improved and field SODIS conditions, *Journal of Water Supply: Research and Technology – AQUA* **56**: 4, 245 – 256.

Ducoste J and Linden K (2005). Determination of ultraviolet sensor location for sensor set-point monitoring using computational fluid dynamics, *Journal of Environmental Engineering and Science* **4**, S33 – S43.

Ducoste J, Linden K, Rokjer D, and Liu D (2005). Assessment of reduction equivalent fluence bias using computational fluid dynamics, *Environmental Engineering Science* **22**: 5, 615 – 628.

ETRESH (2010). Clear-sky radiation models, Education and Training on Renewable Energy Systems for Housing, Edinburgh Napier University, Edinburgh, UK. Retrieved from http://www.etresh.eu/downloads.htm on February 23, 2010.

Ewald PW, Sussman JB, Distler MT, Libel C, Chammas WP, Dirita VJ, Salles CA, Vicente AC, Heitmann I, and Cabello F (1998). Evolutionary control of infectious disease: Prospects for vectorborne and waterborne pathogens, *Memorias do Instituto Oswaldo Cruz* **93**: 5, 567 – 576.

Faubert G (2000). Immune response to *Giardia duodenalis*, *Clinical Microbiology Reviews* **13**: 1, 35 – 54.

First MW, Banahan KF, and Dumyahn TS (2007). Performance of ultraviolet germicidal irradiation lamps and luminaries in long-term service, *Leukos* **3**: 3, 181 – 188.

Fox RB, Isaacs LG, and Stokes S (1963). Photolytic degradation of poly(methy1 methacrylate), *Journal of Polymer Science: Part A-General Papers* **1**: 3, 1079 – 1086.

Gadgil A (1998). Drinking water in developing countries, *Annual Review of Energy and the Environment* **23**: 1, 253 – 286.

Gadgil A, Greene D, Drescher A, Miller P, and Kibata N (1998). Low cost UV disinfection system for developing countries: Field tests in South Africa, *Proceedings of the First International Symposium on Safe Drinking Water in Small Systems*, Washington DC, May 10 – 13.

Gadgil A and Shown LJ (1995). To drink without risk: The use of ultraviolet light to disinfect drinking water in developing countries, The Solar Cooking Archive. Retrieved from: http://solarcooking.org/ultraviolet1.htm on May 2, 2008.

GMAG (2006). Plan de desarrollo municipal – 2006-2010; Volumen I: Diagnóstico municipal, Gobierno Municipal de Ascensión de Guarayos, Plan Internacional, Proyecto de Desarrollo Concurrente Regional II, Ascensión de Guarayos, Bolivia. Available at: http://guarayos.gob.bo/pdm.htm

Guest RK (2004). *Bacillus spp.* spore production – A short guidance manual, Department of Civil and Environmental Engineering, University of Alberta, Edmonton, AB.

Guzmán-Ortiz M (2010, January 30). La energía solar. *El Diario*. Retrieved from: http://www.eldiario.net/noticias/2010/2010_01/nt100130/1_05opn.php on February 9, 2010.

Hassanein AAG and Khalifa RA (2008). Financial and operational performance assessment of water/wastewater utilities: Comparative study, *Journal of Infrastructure Systems* **14**: 4, 283 – 292.

Haysom A (2006). A study of the factors affecting sustainability of rural water supplies in Tanzania, Cranfield University, Silsoe, UK. Available at: http://www.wateraid.org/documents/plugin_documents/rural_water_supplies_in_tanzania.pdf

Hijnen WAM, Beerendonk EF, and Medema GJ (2006). Inactivation credit of UV radiation for viruses, bacteria and protozoan (oo)cysts in water: A review, *Water Research* **40**: 1, 3 – 22.

Hirsch C. 2007. *Numerical computation of internal and external flows: an introduction to CFD – second edition*. Oxford, UK: Butterworth-Heinemann.

Hirsche T and Jayanthan J (2007). More than just a drop in the bucket..., Newsletter of the Bolivian-Canadian Clean Water Network **1**: 1, 4. Available at: http://bccwater.weebly.com/uploads/1/1/1/0/1110828/bcc_water_newsletter_1.pdf

Hulsey R, Ducoste J, and Linden K. 2007. *UV disinfection for large water treatment plants*. Denver, CO: American Water Works Association Research Foundation.

INE (2009). Anuario estadístico 2008, Instituto Nacional de Estadística, La Paz, Bolivia. Available at: http://www.ine.gov.bo/pdf/Anuario_2008/Anuario2008.pdf

Jin S, Linden K, Ducoste J, and Liu D (2005). Impact of lamp shadowing and reflection on the fluence rate distribution in a multiple low-pressure UV lamp array, *Water Research* **39**: 12, 2711 – 2721.

Kubare M and Haarhoff J (2010). Rational design of domestic biosand filters, *Journal of Water Supply: Research and Technology—AQUA* **59**: 1, 1 –15.

Lane S and Lloyd D (2002). Current trends in research into the waterborne parasite *Giardia*, *Critical Reviews in Microbiology* **28**: 2, 123 – 147.

Larsen WC and Brownell SA (2001). UV water treatment in Haiti – A continuing success story, *IUVA News* **3**: 1, 32.

Lin LS, Johnston CF, and Blatchley ER (1999a). Inorganic fouling at quartz/water interfaces in ultraviolet photoreactors – I. Chemical characterization, *Water Research* **33**: 15, 3321 – 3329.

Linden K (2008). Ultraviolet irradiation: An age-old emerging technology for water treatment, Frontiers of Engineering: Reports on Leading-Edge Engineering from the 2007 Symposium, 117 – 124.

Liu D, Ducoste J, Jin S, and Linden K (2004). Evaluation of alternative fluence rate distribution models, *American Water Works Association Journal* **53**: 6, 391 – 408.

Liu D, Wu C, Ducoste J, and Linden K (2007). Numerical simulation of UV disinfection reactors: Evaluation of alternative turbulence models, *Applied Mathematical Modelling* **31**: 9, 1753 – 1769.

Luque A and Hegedus S. 2003. *Handbook of photovoltaic science and engineering*. Hoboken, NJ: John Wiley and Sons, Inc.

Mamane H, Linden K, Cabaj A, and Sommer R (2005). Spectral sensitivity of *Bacillus subtilis* spores and MS2 coliphage for validation testing of ultraviolet reactors for water disinfection, *Environmental Science & Technology* **39**: 20, 7845 – 7852.

Mann R, Brazier J, and Tsuchiya A (2009). A comparison of patient and general population weightings of EQ-5D dimensions, *Health Economics* **18**: 3, 363 – 372.

McGuire MJ (2006). Eight revolutions in the history of US drinking water disinfection, *American Water Works Association Journal* **98**: 3, 123 – 149.

MSOP (2004). Norma Boliviana NB 689: Instalaciones de agua – Diseño para sistemas de agua potable, Ministerio de Servicios y Obras Públicas, Viceministerio de Servicios Básicos, La Paz, Bolivia. Available at: http://www.minagua.gov.bo/vapsb/biblioteca/DOCS/NORMAS%20TECNICAS/NB%20689%20AguaPotable%20-%20dic2004/NB689%20AguaPotable%20NORMA.pdf

MWH. 2005. *Water treatment: Principles and design, second edition*. Crittenden JC, Trussell RR, Hand DW, Howe KJ, and Tchobanoglous G (eds.). Hoboken, NJ: John Wiley and Sons, Inc.

Nagai N, Matsunobe T, and Imai T (2005). Infrared analysis of depth profiles in UV-photochemical degradation of polymers, *Polymer Degradation and Stability* **88**: 2, 224 – 233.

Nalluri C and Featherstone RE. 2009. *Nalluri & Featherstone's civil engineering hydraulics: Essential theory with worked examples*. Ames, IA: Wiley-Blackwell. 58 – 92 pp.

NSF (2004). NSF consumer information: Residential Plumbing, National Sanitation Foundation. Retrieved from: http://www.nsf.org/consumer/plumbing/index.asp?program=Plumbing on February 14, 2010.

Pedley TJ (1997). Introduction to fluid dynamics, *Scientia Marina* **61**: Suppl. 1, 7 – 24.

Peng J, Qiu Y, and Gehr R (2005). Characterization of permanent fouling on the surfaces of UV lamps used for wastewater disinfection, *Water Environment Research* **77**: 4, 309 – 322.

RAEL (2006). The UV-tube project, Renewable and Appropriate Energy Laboratory, University of California at Berkeley. Retrieved from: http://rael.berkeley.edu/old-site/uvtube/uvtubeproject.htm on June 23, 2008.

Rahn R, Bolton JR, and Stefan M (2006). The iodide/iodate actinometer in UV disinfection: Determination of the fluence rate distribution in UV reactors, *Photochemistry and Photobiology* **82**: 2, 611 – 615.

Rashid MH. 2007. *Power electronics handbook: Devices, circuits and applications*. Burlington, MA: Elsevier Academic Press. 565 – 591 pp.

Reid R (1998). Status of water disinfection in Latin America and the Caribbean, *Proceedings of the Regional Symposium on Water Quality: Effective Disinfection*, CEPIS-OPS, Lima, Peru. 1 – 13 pp.

Romero-Vargas Castrillón S, Ibrahim H, de Lasa H (2006). Flowfield investigation in a photocatalytic reactor for air treatment (Photo-CREC–air), *Chemical Engineering Science* **61**: 10, 3343 – 3361.

Setlow P (2007). I will survive: DNA protection in bacterial spores, *TRENDS in Microbiology* **15**: 4, 172 – 180.

Shi W, Zhang J, Shi X-M, and Jiang G-D (2008). Different photodegradation processes of PVC with different average degrees of polymerization, *Journal of Applied Polymer Science* **107**: 1, 528 – 540.

Sobsey MD, Handzel T, and Venczel L (2003). Chlorination and safe storage of household drinking water in developing countries to reduce waterborne disease, *Water Science and Technology* **47**: 3, 221 – 228.

SODA (2004). Climate: Averages, normals, and typical years, Solar Radiation Data, Armines / MINES ParisTech, Centre Energétique et Procédés (CEP), Sophia-Antipolis, France. Retrieved from: http://www.soda-is.com/eng/services/climat_free_eng.php on February 23, 2010.

Solsona F and Méndez JP (2002). Water disinfection, CEPIS-PAHO-WHO-EPA, Lima, Peru. 92 – 102 pp. Available at: http://www.bvsde.paho.org/bvsacg/fulltext/desinfeccioneng/chapter4.pdf

Targýt S (2004). What is good engineering practice? ASRAY Lift Guide Rails. Available at: http://www.asray.com/_files/content/be74eb562e1d9c98aa937b1091d7f5bce5d641c9.pdf

Tham Y, Muneer T, and Davison B (2009). A generalized procedure to generate clear-sky radiation data for any location, *International Journal of Low-Carbon Technologies* **4**: 1, 205 – 212.

Torikai A and Hasegawa H (1998). Wavelength effect on the accelerated photodegradation of polymethylmethacrylate, *Polymer Degradation and Stability* **61**: 2, 361 – 364.

TuTiempo.net (2010). Historical weather: Ascención de Guarayos, Bolivia, TuTiempo.net. Retrieved from: http://www.tutiempo.net/en/Climate/Ascencion_De_Guarayos/851750.htm on February 23, 2010.

UNDP (2009). Human development report 2009 – Overcoming barriers: Human mobility and development. United Nations Development Programme, New York, NY. Available at: http://hdr.undp.org/en/media/HDR_2009_EN_Complete.pdf

USEPA (1999). Alternative disinfectants and oxidants guidance manual, Report EPA 815-R-99-014, U.S. Environmental Protection Agency, Office of Water, Washington DC. Available at: http://www.epa.gov/ogwdw000/mdbp/alternative_disinfectants_guidance.pdf

USEPA (2006). Ultraviolet disinfection guidance manual for the final long term 2 enhanced surface water treatment rule, Report EPA 815-R-06-007, U.S. Environmental Protection Agency, Office of Water, Washington DC. Available at: http://www.epa.gov/safewater/disinfection/lt2/pdfs/guide_lt2_uvguidance.pdf

Vidal A and Díaz AI (2000). High-performance, low-cost solar collectors for disinfection of contaminated water, *Water Environment Research* **72**: 3, 271 – 276.

WHO (2000). Global water supply and sanitation assessment 2000 report, World Health Organization and United Nations Children's Fund. Retrieved from: http://www.who.int/docstore/water_sanitation_health/Globassessment/GlobalTOC.htm on May 10, 2008.

WHO (2008). World health statistics 2008, World Health Organization, Geneva, Switzerland. Available at: http://www.who.int/whosis/whostat/EN_WHS08_Full.pdf

Wong MB. 2009. *Plastic analysis and design of steel structures*. Boston, MA: Butterworth-Heinemann. 2 – 54 pp.

Wright NG and Hargreaves DM (2001). The use of CFD in the evaluation of UV treatment systems, *Journal of Hydroinformatics* **3**: 2, 59 – 70.

Yates MV (2008). Adenoviruses and ultraviolet light: An introduction, *Ozone: Science and Engineering* **30**: 1, 70 – 72.

Zhou LH, Zheng TL, Wang X, Ye JL, Tian Y, and Hong HS (2007). Effect of five Chinese traditional medicines on the biological activity of a red-tide causing alga—*Alexandrium tamarense*, *Harmful Algae* **6**: 3, 354 – 360.

APPENDICES

A. PROCEDURES IN THE VALIDATION PROCESS

Appendix A.1 Production and assay of *B. subtilis* spores

The *B. subtilis* production involved four stages: pre-culture, production, purification, and enumeration. All glassware, equipment, and solutions were sterilized by autoclaving at 121 ºC for 15 min (MDT Castle steam sterilizer, ETL Testing Laboratories Inc., Cortland, NY). Pre-culture was carried out by inoculating a hydrated vial of *B. subtilis* stock solution into an 8 mL test tube containing nutrient medium [8 mg/L nutrient broth (Difco nutrient broth, Becton, Dickinson, and Company, Sparks, MD), 0.25 mg/L $MgSO_4 \cdot 7H_2O$ (ACS-480, BDH Chemicals, Toronto, ON), and 1 mg/L KCl (P217-500, Fisher Chemicals, Fisher Scientific, Fair Lawn, NJ)]. After 24 h incubation at 37 ºC (Precision 31483 gravity convection incubator, GCA Corporation, Chicago, IL), the culture was in log-growth phase and the next stage could proceed.

For the production stage, modified Schaeffer's medium was prepared by sterilizing the nutrient medium and adjusting to pH 8.0 (measured with Accumet Research AR20 pH/conductivity meter, Fisher Scientific). A stock solution of 1 μM $FeSO_4$ (BDH Chemicals Inc., Toronto, ON), 10 μM $MnCl_2$ (BDH Chemicals Ltd., Poole, UK), and 1.0 μM $CaCl_2$ (C79-500, Fisher Chemicals, Fisher Scientific, Fair Lawn, NJ) was prepared. Aliquots of this stock solution were added to the medium using sterile 0.20 μm syringe filters (Whatman Puradisc 25 mm, Whatman International Ltd., Florham Park, NJ). Once prepared, baffled flasks containing approximately 250 mL of Schaeffer's medium were inoculated with culture (about 1/300 in volume) in log-growth phase. Later, they were placed in an incubator shaker (Innova 4080, New Brunswick Instruments Co., Edison, NJ) operating at 180 rpm and 37 ºC, for more than two weeks.

Purification was performed right after the production stage was finished. The contents of the flasks were centrifuged (Sorvall RC-5B refrigerated superspeed centrifuge, Mandel Scientific Company Ltd., Guelph, ON), at 7500 RCF and 4 ºC for 20 min. The supernatant was repeatedly removed and replaced by sterile

deionized (DI) water (Synergy UV ultrapure water systems, Millipore Corporation, Billerica, MA) until the supernatant was clear. Afterwards, the solution was set in a water bath operating at 75 ºC for about one hour, to eliminate vegetative bacteria. In the end, the suspension was stored in 50% ethanol solution at 4 ºC for later use. Successive batches of purified spores were added to the stock solution to increase the titre of spores.

Enumeration was performed using the pour plate method. First, a number of test tubes containing nutrient medium and 1.6% agar (BP1423-500 granulated, Fisher BioTech, Fair Lawn, NJ) were sterilized and set in a water bath at 50 ºC. Later, successive 10^{-1} dilutions were performed by transferring 1 mL of the stock solution of spores to a 9 mL tube with sterile DI water, and from that to another 9 mL tube, until completing a 10^{-6} or 10^{-7} dilution. From the dilution of interest, 1 mL was transferred to a sterile 100 mm Petri dish (Fisherbrand, Fisher Scientific), as well as the contents of one tube with nutrient medium. Mixing took place by softly swirling the Petri dish around 20 times. The Petri dish contents were then set for drying in a biological safety cabinet (Model 1284, Class II A/B3, Forma Scientific Co., Marietta, OH), for about 4 to 5 min. *B. subtilis* colonies could be counted after incubation at 37 ºC for almost 24 h. This approach was used not only for the enumeration of spores in the stock solution, but also for the enumeration of spores before and after UV irradiation, and it was always made on duplicate at least.

The Schaeffer-Fulton staining method was employed to verify the existence of *B. subtilis* spores during the production phase. To this end, a solution of 5% aqueous malachite green (A779-500, Fisher Chemicals, Fisher Scientific, Fair Lawn, NJ) was prepared. A smear of the culture was put to dry in a microscope slide (Fisherbrand, Fisher Scientific), then flooded with the malachite solution and flamed. Subsequently, it was rinsed with water and flooded again with 1% aqueous safranin stain (Protocol, Fisher Scientific Co., Kalamazoo, MI). When air-dry, the slide was placed under the microscope (Stereomaster II, Fisher Scientific). Spores should appear green-stained whereas vegetative bacteria should appear red-stained. When an important proportion of green-stained,

spread-out colonies were viewed, the purification process was considered complete.

Appendix A.2 UV dose calculations for the bench-scale experiment

Date of this Version 06-May-04

Germicidal Fluence (UV Dose) Calculations for a Low Pressure UV Lamp

Programmed by Jim Bolton - Bolton Photosciences Inc., 628 Cheriton Cres., NW, Edmonton, AB, Canada T6R 2M5
Tel: 780-439-4709 (home); 519-741-6283 (cellular); Fax: 780-439-7792; Email: jbolton@boltonuv.com
Comments and/or questions are welcome

Note that this Spreadsheet includes the new "Divergence Factor", which has been found to be necessary due to the fact that the beam "diverges" as it passes through the solution.

Note: This Spreadsheet should only be used if the suspension depth in the "Petri" dish is less than 2 cm.
For suspensions with depths greater than 2 cm, use the Spreadsheet "Fluence = MP - deep.xls

DO NOT CHANGE ANY CELLS OTHER THAN THE CELLS WITH A YELLOW BACKGROUND

INSTRUCTIONS AND NOTES

1. Set up a "quasi" collimated beam apparatus. If possible, do not use a "collimating tube", but rather use circular "masks" to define the beam. Make sure that safety measures are taken to protect workers from exposure to the UV from the lamp. EYE PROTECTION IS AN **ABSOLUTE** REQUIREMENT.
2. Place the detector head of the UV radiometer on a horizontal surface, containing a 0.5 cm x 0.5 cm grid, such that the "calibration plane" (see the Calibration Sheet provided by the manufacturer of the Radiometer) is at the level of where the top of the solution will be during exposures to the UV.
3. Determine the "Petri Factor" using the procedure given in the "Petri Factor" Worksheet.
4. Measure the absorption coefficient (1 cm absorbance) at 254 nm for the water to be irradiated and insert into Cell **C43**. Make sure that the instrument is balanced with distilled water in the same cuvette.
5. Insert the solution volume into Cell **F34**.
6. Insert the distance from the center of the UV lamp to the surface of the water in the Petri Dish into cell **F36**.
7. Insert the center meter reading into cell **G46**.
8. Insert the desired Fluences (UV Doses) into cells **E55 to E61**.
9. Remove the radiometer detector head and place a Petri Dish (or other container), containing the cell suspension, on a stirring motor placed so that the top of the solution is at the same level as that of the "calibration plane" of the detector head. Add a very small stir bar and make sure that the stirring rate is such that there is no vortex.
10. Expose samples in the UV beam for the times calculated in rows **55 to 61**. Do at least three exposures for each time and in random order.
11. The "example" Worksheet shows how to analyze the data and obtain the Fluence (UV Dose) Response Curve.

solution volume =	15 mL
water path length =	0.76 cm
distance from UV lamp to top of water surface =	26.9 cm
Divergence Factor =	0.9724

absorption coefficient cm^{-1}	total absorbance (A)	Water Factor (WF)	WF X DF
0.1620	0.124	0.8701	0.8461

Radiometer reading at the center of Petri Dish =	0.328	mW/cm^2
Petri factor = 0.898		
True irradiance across the Petri dish =	0.294	mW/cm^2
Reflection factor = 0.975		
Water factor *		
Divergence factor = 0.846		
Average Germicidal Irradiance throughout the water volume =	0.243	mW/cm^2

Time for a Fluence (UV Dose) of	1	mJ/cm^2 =	4.123	s				
Time for a Fluence (UV Dose) of	30	mJ/cm^2 =	123.7	s	=	2 min	4	s
Time for a Fluence (UV Dose) of	60	mJ/cm^2 =	247.4	s	=	4 min	7	s
Time for a Fluence (UV Dose) of	90	mJ/cm^2 =	371.1	s	=	6 min	11	s
Time for a Fluence (UV Dose) of	120	mJ/cm^2 =	494.7	s	=	8 min	15	s
Time for a Fluence (UV Dose) of	150	mJ/cm^2 =	618.4	s	=	10 min	18	s
Time for a Fluence (UV Dose) of	180	mJ/cm^2 =	742.1	s	=	12 min	22	s
Time for a Fluence (UV Dose) of		mJ/cm^2 =	0.0	s	=	0 min	0	s

Note: the exposure times should be at least 30 s. If they are calculated to be shorter, arrange the irradiation platform further away from the UV lamp so that the irradiance will be smaller.

Figure A-1 Snapshot of the "Fluence Calculations" worksheet for the validation of the UV unit (UVT = 68.9%)

Appendix A.3 Estimation of the Petri factor for the bench-scale experiment

Experimental procedure according to Bolton (2004):

a) Draw a 0.5 cm x 0.5 cm grid and place the centre of the grid at the centre of the collimated beam.

b) Measure the Irradiance (with a radiometer) every 0.5 cm in the x and y directions and place the readings into columns C and H below. It is only necessary to take readings out to 0.5 cm beyond the radius of the Petri dish (or other container to be used). The units do not matter since ratios are calculated.

c) Input the Petri dish 'inner' diameter. Measure carefully with a plastic mm ruler or better with a pair of callipers.

d) The Petri factor is calculated and automatically transferred to the "Fluence Calculations" Worksheet.

Table A-1 UV irradiance distribution across the Petri dish for a low pressure UV lamp

A	B	C	D	F	G	H	I
x	y	Meter reading	Ratio	x	y	Meter reading	Ratio
0	-4.0	0	0.000	-4.0	0	0	0.000
0	-3.5	19	0.000	-3.5	0	22	0.000
0	-3.0	24	0.882	-3.0	0	26	0.765
0	-2.5	27	0.918	-2.5	0	27	0.788
0	-2.0	28	0.953	-2.0	0	28	0.812
0	-1.5	30	0.965	-1.5	0	30	0.847
0	-1.0	31	0.988	-1.0	0	32	0.882
0	-0.5	32	1.000	-0.5	0	33	0.953
0	0.0	33	1.000	0.0	0	33	1.000
0	0.5	33	0.965	0.5	0	32	1.000
0	1.0	32	0.929	1.0	0	31	0.953
0	1.5	31	0.882	1.5	0	30	0.906
0	2.0	31	0.824	2.0	0	28	0.871
0	2.5	29	0.800	2.5	0	27	0.847
0	3.0	27	0.741	3.0	0	25	0.824
0	3.5	24	0.000	3.5	0	19	0.000
0	4.0	0	0.000	4.0	0	0	0.000
						Petri dish diameter (cm) =	5.0

Appendix A.4 Determination of the UV dose-response curves and statistics

Table A-2 Raw data and calculation of the log inactivation for the bench-scale experiment

UVT (%)	Fluence (mJ/cm^2)	CFU counts			Geometric mean	N_0 (CFU/ mL)	N (CFU/ mL)	log (N_0/N)
		Dilution factor	Replicates					
			#1	#2				
98.0	0	1.0E+04	17	30	2.26E+05	2.17E+05	2.17E+05	0.000
98.0	0	1.0E+03	204	229	2.16E+05			
68.9	0	1.0E+04	9	9	9.00E+04	9.04E+04	9.04E+04	0.000
68.9	0	1.0E+03	81	101	9.04E+04			
98.0	30	1.0E+04	11	7	8.77E+04	2.17E+05	1.10E+05	0.297
98.0	30	1.0E+03	120	104	1.12E+05			
68.9	30	1.0E+04	4	9	6.00E+04	9.04E+04	4.97E+04	0.260
68.9	30	1.0E+03	55	43	4.86E+04			
98.0	60	1.0E+03	52	39	4.50E+04	2.17E+05	4.50E+04	0.683
98.0	60	1.0E+02	TNTC	TNTC	N/A			
68.9	60	1.0E+03	40	28	3.35E+04	9.04E+04	3.35E+04	0.432
68.9	60	1.0E+02	TNTC	TNTC	N/A			
98.0	90	1.0E+03	33	46	3.90E+04	2.17E+05	3.90E+04	0.746
98.0	90	1.0E+02	TNTC	TNTC	N/A			
68.9	90	1.0E+03	19	19	1.90E+04	9.04E+04	2.36E+04	0.584
68.9	90	1.0E+02	226	255	2.40E+04			
98.0	120	1.0E+02	264	257	2.60E+04	2.17E+05	2.60E+04	0.921
98.0	120	1.0E+01	TNTC	TNTC	N/A			
68.9	120	1.0E+02	109	127	1.18E+04	9.04E+04	1.18E+04	0.886
68.9	120	1.0E+01	TNTC	TNTC	N/A			
98.0	150	1.0E+02	130	134	1.32E+04	2.17E+05	1.32E+04	1.216
98.0	150	1.0E+01	TNTC	TNTC	N/A			
68.9	150	1.0E+02	67	69	6.80E+03	9.04E+04	6.80E+03	1.124
68.9	150	1.0E+01	TNTC	TNTC	N/A			
98.0	180	1.0E+01	TNTC	TNTC	N/A	2.17E+05	N/A	N/A
98.0	180	1.0E+01	TNTC	TNTC	N/A			
68.9	180	1.0E+00	TNTC	TNTC	N/A	9.04E+04	N/A	N/A
68.9	180	1.0E+00	TNTC	TNTC	N/A			

SUMMARY OUTPUT								
Regression Statistics								
Multiple R	0.96607919							
R Square	0.933309							
Adjusted R Square	0.91663625							
Standard Error	0.06747405							
Observations	6							
ANOVA								
	df	*SS*	*MS*	*F*	*Significance F*			
Regression	1	0.2548542	0.2548542	55.97811	0.001706417			
Residual	4	0.018211	0.0045527					
Total	5	0.2730652						
	Coefficients	*tandard Erro*	*t Stat*	*P-value*	*Lower 95%*	*Upper 95%*	*Lower 95.0%*	*Upper 95.0%*
Intercept	0.09697777	0.1377308	0.7041109	0.520194	-0.28542432	0.47937987	-0.2854243	0.47937987
X Variable 1	-0.00841385	0.0011246	-7.481852	0.001706	-0.01153615	-0.0052915	-0.0115361	-0.0052915

Figure A-2 Regression analysis of the bench-scale experiment as computed by Microsoft Excel

USEPA (2006) establishes that when two (or more) different water qualities are to be assessed in the bench-scale experiment, a check must be performed in order to define whether the resulting UV dose-response curves can be combined. This check consists in finding out if the regression coefficients are significantly different, statistically, at a 95% confidence level. Because two different samples are tested in this study, that check is performed following the example given in Mann *et al*. (2009), according to the Equation A-1 below.

$$z = \frac{\beta_{68.9} - \beta_{98}}{\sqrt{(\mathrm{SE}_{68.9})^2 + (\mathrm{SE}_{98})^2}} \qquad \text{(A-1)}$$

where z is the z-score statistical test, $\beta_{68.9}$ is the regression coefficient for the water sample with UVT = 68.9%, β_{98} is the regression coefficient for the water sample with UVT = 98%, $\mathrm{SE}_{68.9}$ is the standard error for the water sample with UVT = 68.9% and SE_{98} is the standard error for the water sample with UVT = 98%. So if the calculated value of z is less than 1.96 then the difference is not statistically significant at the 95% confidence level. From Microsoft Excel, $\beta_{68.9}$ yielded a value of 0.0073, β_{98} gave a value of 0.0069, $\mathrm{SE}_{68.9}$ obtained a value of 0.0005, and SE_{98} a value of 0.0009. By solving Equation A-1 with these values, a value of 0.33 was obtained for z, hence the curves are not significantly different at the 95% confidence level and thereby can be combined.

After proving the UV dose-response curves combinable, the following step was to determine the uncertainty of the collimated beam data (U_{DR}), as noted in USEPA (2006). To this end, U_{DR} should not be more than 15% the value of the UV dose producing 1-log inactivation if the interval confidence is found using statistical techniques; otherwise, it should be added to the whole uncertainty of the validated dose. Since the confidence intervals were found using Regression in the Data Analysis pack of Microsoft Excel, the UV dose producing 1-log inactivation resulted in 118.9 mJ/cm^2. The upper bound of the 95% confidence interval was a UV dose of 189 mJ/cm^2, and the lower bound gave a value of 86.7 mJ/cm^2, all of which resulted in an uncertainty of 37.1%. Therefore, U_{DR} > 15% and it should be added to the whole uncertainty of the validated dose, as outlined in the U_{Val} decision tree for the UV intensity setpoint approach (USEPA, 2006). The procedure is explained in the section below.

Appendix A.5 Determination of the RED and validated dose from the full-scale experiment

Table A-3 Raw data and calculation of the log inactivation for the full-scale experiment

Absor-bance	UVT %	Flow rate L/s	Raw Data Inlet				Raw Data Outlet				Log Inactivation			Average RED mJ/cm^2	RED SD mJ/cm^2
			Dilution factor	CFU Counts			Dilution factor	CFU Counts			Log(In) - Log(Out)				
				#1	#2	#3		#1	#2	#3	#1	#2	#3		
0.004	99.1	1.01	1.0E+03	22	23	31	1.0E+02	58	61	83	0.58	0.58	0.57	80.0	0.4
			1.0E+02	TNTC	TNTC	TNTC	1.0E+01	TNTC	TNTC	TNTC					
0.155	70.0	0.52	1.0E+03	24	26	31	1.0E+02	147	163	180	0.21	0.20	0.24	37.3	2.0
			1.0E+02	TNTC	TNTC	TNTC	1.0E+01	TNTC	TNTC	TNTC					
0.151	70.7	1.01	1.0E+03	22	38	39	1.0E+03	13	14	18	0.11	0.33	0.28	37.4	13.4
			1.0E+02	TNTC	TNTC	TNTC	1.0E+02	174	183	208					
0.007	98.3	1.32	1.0E+03	28	29	30	1.0E+02	87	97	100	0.51	0.48	0.48	69.4	2.1
			1.0E+02	TNTC	TNTC	TNTC	1.0E+01	TNTC	TNTC	TNTC					
0.009	98.0	0.52	1.0E+04	12	17	18	1.0E+02	313	316	370	0.58	0.69	0.66	88.2	6.8
			1.0E+03	120	155	169	1.0E+01	TNTC	TNTC	TNTC					
0.064	86.4	1.32	1.0E+03	35	68	80	1.0E+02	329	331	370	0.03	0.31	0.33	28.3	20.4
			1.0E+02	TNTC	TNTC	TNTC	1.0E+01	TNTC	TNTC	TNTC					
0.074	84.3	1.01	1.0E+03	16	21	21	1.0E+02	113	118	137	0.15	0.25	0.19	34.3	6.0
			1.0E+02	TNTC	TNTC	TNTC	1.0E+01	TNTC	TNTC	TNTC					
0.070	85.0	0.52	1.0E+03	28	35	49	1.0E+02	110	120	131	0.41	0.46	0.57	68.1	10.1
			1.0E+02	TNTC	TNTC	TNTC	1.0E+01	TNTC	TNTC	TNTC					
0.161	69.0	1.32	1.0E+03	36	40	40	1.0E+03	19	20	22	0.31	0.29	0.27	45.7	2.2
			1.0E+02	TNTC	TNTC	TNTC	1.0E+02	176	208	214					
0.162	68.9	0.52*	1.0E+03	8	12	13	1.0E+03	9	12	12	0.23	0.06	0.09	24.2	10.7
			1.0E+02	119	125	136	1.0E+02	66	107	110					

* This was a blank run, meaning that the UV lamp was off

USEPA (2006) recommends obtaining B_{RED} by comparing the highest UV sensitivity (mJ/cm^2/log I) of the replicates, at the lowest UVT, with the tables G.1 to G.17 from the document. These tables present the UV sensitivities of *Cryptosporidium* and *Giardia*, and the required UV doses and expected log inactivation for different UVT. The UV sensitivity is calculated by dividing the RED at the lowest UVT between each log inactivation of the replicates. The lowest recorded UVT was 69 %, which includes log inactivations of 0.31, 0.29, and 0.27, with an associated RED of 45.7 mJ/cm^2. Said log inactivations result in UV sensitivities of 148.5, 160.1, and 168.9 mJ/cm^2 per log, respectively. B_{RED} is then looked for in the tables G.1 to G.17 of USEPA (2006) with the highest sensitivity, that is, 168.9 mJ/cm^2 per log. By looking at Table G.1, corresponding to a 4.0 log inactivation of *Cryptosporidium*, with that sensitivity value and 69% UVT, a B_{RED} value of 2.73 is obtained. This value will be recalled later when the other parameters have been calculated. U_{Val} must be found following the correct equation. For this, the decision tree shown in Figure 5.4 of USEPA (2006) is employed. Assuming a UV sensor uncertainty less than 10% (as it is brand-new), and knowing that the value of U_{DR} is certainly greater than 15%, it is then true that $U_{Val} = (U_{SP}^2 + U_{DR}^2)^{1/2}$. U_{SP} is found then by solving Equation A-2.

$$U_{SP} = \frac{t \times SD_{RED}}{RED} \times 100\% \qquad \text{(A-2)}$$

where U_{SP} is the uncertainty of the set-point RED (%), t is the t-statistic for the number of replicates, SD_{RED} is the highest standard deviation of the average log inactivation (mJ/cm^2) and RED is the UV dose corresponding to SD_{RED} (mJ/cm^2).

For three replicates, at a 95% confidence level, the t-statistic is 3.18 (USEPA, 2006). From Table A-3, it becomes apparent that the highest SD_{RED} would correspond to 20.4 mJ/cm^2 and an associated RED of 28.3 mJ/cm^2. Plugging these values in Equation A-2 produces a U_{SP} value of 229.6%, hence U_{Val} = 232.5%. Next, the validation factor (VF) is computed by inputting B_{RED} and U_{Val} into Equation 2-1, yielding a VF value of 9.08. The validated dose (D_{Val}) is obtained by dividing the least determined RED by VF (D_{Val} = RED/VF). From Table A-3,

the value of RED to be used is 28.3 mJ/cm^2, resulting in a value of D_{Val} of 3.1 mJ/cm^2.

In any case, the validated dose should be greater than the actual required UV dose to achieve the log inactivation used when computing B_{RED}. For example, since a 4-log inactivation was used to estimate B_{RED}, D_{Val} should be higher than the value pointed out in Table G.1 of USEPA (2006). The UV dose required to achieve a 4-log inactivation of *Cryptosporidium* is 22 mJ/cm^2, as seen in that table. This value is higher than the calculated value of D_{Val}, so the estimates of B_{RED}, *VF*, and D_{Val} have to be repeated over and over until the required UV dose is smaller than the validated dose. After successive iterations, the resulting final values of these parameters are found in Table G.8 of USEPA (2006) and are as follows: B_{RED} = 4.9; U_{SP} = 229.6%; U_{DR} = 37.1%; U_{Val} = 232.5%; *VF* = 16.29; and D_{Val} = 1.7 mJ/cm^2. In the same table, it is stated that the required UV dose to achieve a 0.5-log inactivation of *Cryptosporidium* is 1.6 mJ/cm^2, which is lower than the validated dose. In other words, at the minimum RED delivered by this UV reactor (28.3 mJ/cm^2), at least 0.5-log inactivation of *Cryptosporidium* may be expected with the type of challenge organism used in the biodosimetry test.

Likewise, the final values of these parameters, but for inactivation of *Giardia* instead, are found in Table G.16 and are as follows: B_{RED} = 5.16; U_{SP} = 229.6%; U_{DR} = 37.1%; U_{Val} = 232.5%; *VF* = 17.16; and D_{Val} = 1.7 mJ/cm^2. In the same table, it is stated that the required UV dose to achieve a 0.5-log inactivation of *Giardia* is 1.5 mJ/cm^2, so at the minimum RED delivered by the reactor, at least 0.5-log inactivation of *Giardia* may also be expected with the type of challenge organism used during the biodosimetry test.

B. LABORATORY RESULTS

UNIVERSIDAD AUTÓNOMA "GABRIEL RENE MORENO"
"Unidad Técnica de Apoyo a los Laboratorios"

UTALAB
Servicios Laboratoriales y Medioambientales

INFORME DE ENSAYOS

Nombre del Laboratorio	:	**Universidad Autónoma "Gabriel René Moreno"**
Identificación del Informe	:	1327/2008
Nombre del cliente	:	MARIO ALBERTO ZAPATA
Solicitado por	:	MARIO ALBERTO ZAPATA
Muestra Nº 1800	:	ANALISIS DE AGUA
Lugar de muestreo	:	Pozo Bomba Manual
Ubicación de la toma de muestra	:	MUNICIOIO DE GUARAYOS (COMUNIDAD CERRO GRANDE)
Muestra tomada por	:	MARIO ALBERTO ZAPATA
Fecha de recepción de muestras	:	16/12/2008 **Hrs.:** 09:54
Fecha de muestreo	:	15/12/2008 **Hrs.:** 12:00
Fecha de entrega	:	19/12/2008 **Hrs.:** 17:00
Teléfono	:	1780885737

Nº	PARAMETROS	UNIDADES	METODOS DE ANALISIS	LIMITES DE DETECCION	VALORES MAXIMOS ADMISIBLES	RESULTADO DE ANALISIS
1	Alcalinidad Total c. CaCO3	mg/l	Titulación (2320-B)	2,0	370,0	492,0
2	Coliformes Fecales	UFC / 100ml	Filtro de Menbrana (9222-B)	2.0	<2.0	< 2.00 E + 00
3	Coliformes Totales	UFC / 100ml	Filtro de Menbrana (9922-D)	2.0	< 2.0	5.9 E + 01
4	Sólidos Suspendidos Totales a 105°C	mg/l	Gravimetría (2540-D)	1,0	60.0	7,0
5	Sólidos Totales a 105°C	mg/l	Gravimetría (2540-B)	1,0	1560	1336,0
6	Turbidez	NTU	Nefelométrico (2130-B)	0,01	5	0,39

** Métodos Normalizados para Aguas Potables y Residuales : APHA, AWWA Y WPCF, Ed. 1992

Luis Medinaceli Gutierrez
RESPONSABLE TECNICO
U.T.A.L.A.B - U.A.G.R.M.

UNIVERSIDAD AUTONOMA GABRIEL RENE MORENO
U.T.A.L.A.B.
Santa Cruz - Bolivia

Este informe es un original único identificado como 1327/2008. Cualquier enmienda, corrección o raspadura invalida este documento

¡Contribuyendo al desarrollo regional y a la preservación del Medio Ambiente!

Av. Centenerio Esq. 2do. Anillo (Campus Universitario) Telf./Fax: (591-3) 334-8419 * 332/1277 * E/mail: utalab@cotas.com.bo
Santa Cruz - Bolivia

Figure B-1 Lab results from the sample taken in the outlet of the manual pump in Cerro Grande, December 15, 2008

UNIVERSIDAD AUTÓNOMA "GABRIEL RENE MORENO"
"Unidad Técnica de Apoyo a los Laboratorios"
UTALAB
Servicios Laboratoriales y Medioambientales

INFORME DE ENSAYO

Página 1 de 1

Nombre del Laboratorio	:	Universidad Autónoma "Gabriel René Moreno"
Identificación única del informe	:	46/2010
Nombre del cliente	:	MARIO ALBERTO ZAPATA
Solicitado por	:	Mario Alberto Zapata
Muestra N º 42	:	Análisis de Agua de Pozo
Lugar de Muestreo	:	Entrada al Filtro de Arena
Ubicación de la toma de la muestra	:	Asención de Guarayos
Muestra tomada por	:	Mario Alberto Zapata
Fecha recepción de la muestra	:	15 /01 / 2010, Hrs. 17:30
Fecha de muestreo	:	16 /01 / 2010, Hrs. 10:40
Fecha de entrega	:	29 / 01 / 2010, Hrs. 17:00
Teléfono	:	1780885737

Nº	PARAMETROS	UNIDADES	METODOS DE ANALISIS *	LIMITES DE DETECCION	VALORES MXIMOS ADMISIBLES	RESULTADO DE ANALISIS
1	Coliformes Fecales	NMP / 100 ml	Tubos Múltiples (9221 - C)	2,0	< 2,0	4,3 E + 03
2	Coliformes Totales	NMP / 100 ml	Tubos Múltiples (9221 - B)	2,0	< 2,0	4,3 E + 03
3	Turbidez	NTU	Nefelométrico (2130 - B)	0,01	5.0	0,55

Ing. Roman Gutiérrez Tito
JEFE TECNICO
UTALAB UAGRM

UNIVERSIDAD AUTONOMA GABRIEL RENE MORENO
U.T.A.L.A.B.
Santa Cruz - Bolivia

Contribuyendo al desarrollo regional y a la preservación del Medio Ambiente!

Este informe es un original único identificado como 46/10. Cualquier enmienda o corrección o reemplazo invalida este documento.
Av. Cementerio Esq. 2do. Anillo (Campus Universitario) Telf./Fax: (591-3) 334-8179 - 3382121 E-Mail: utalab@cotas.com.bo
Santa Cruz - Bolivia

Figure B-2 Lab results from the sample taken before the UV treatment in Cerro Grande, January 15, 2010

UNIVERSIDAD AUTÓNOMA "GABRIEL RENE MORENO"
"Unidad Técnica de Apoyo a los Laboratorios"
UTALAB
Servicios Laboratoriales y Medioambientales

INFORME DE ENSAYO

Página 1 de 1

Nombre del Laboratorio	:	Universidad Autónoma "Gabriel René Moreno"
Identificación única del informe	:	47/2010
Nombre del cliente	:	MARIO ALBERTO ZAPATA
Solicitado por	:	Mario Alberto Zapata
Muestra N º 43	:	Análisis de Agua de Pozo
Lugar de Muestreo	:	Salida al Filtro de Arena
Ubicación de la toma de la muestra	:	Asención de Guarayos
Muestra tomada por	:	Mario Alberto Zapata
Fecha recepción de la muestra	:	15 /01 / 2010, Hrs. 17:30
Fecha de muestreo	:	16 /01 / 2010, Hrs. 10:40
Fecha de entrega	:	29 / 01 / 2010, Hrs. 17:00
Teléfono	:	1780885737

Nº	PARAMETROS	UNIDADES	METODOS DE ANALISIS *	LIMITES DE DETECCION	VALORES MXIMOS ADMISIBLES	RESULTADO DE ANALISIS
1	Coliformes Fecales	NMP / 100 ml	Tubos Múltiples (9221 - C)	2,0	< 2,0	2,4 E + 02
2	Coliformes Totales	NMP / 100 ml	Tubos Múltiples (9221 - B)	2,0	< 2,0	2,4 E + 02
3	Turbidez	NTU	Nefelométrico (2130 - B)	0,01	5.0	0,39

Ing. Roman Gutiérrez Tito
JEFE TECNICO
UTALAB UAGRM

UNIVERSIDAD AUTONOMA GABRIEL RENE MORENO
U.T.A.L.A.B.
Santa Cruz - Bolivia

Contribuyendo al desarrollo regional y a la preservación del Medio Ambiente!

Av. Centenario Esq. 2do. Anillo (Campus Universitario) Tel./Fax: (591-3) 334-8419 - 332-1277 E-mail: utalab@cotas.com.bo
Santa Cruz - Bolivia

Figure B-3 Lab results from the sample after the UV treatment in Cerro Grande, January 15, 2010

UNIVERSIDAD AUTÓNOMA "GABRIEL RENE MORENO"
"Unidad Técnica de Apoyo a los Laboratorios"

UTALAB
Servicios Laboratoriales y Medioambientales

INFORME DE ENSAYO

Página 1 de 1

Nombre del Laboratorio	:	Universidad Autónoma "Gabriel René Moreno"
Identificación única del informe	:	48/2010
Nombre del cliente	:	MARIO ALBERTO ZAPATA
Solicitado por	:	Mario Alberto Zapata
Muestra N ° 44	:	Análisis de Agua de Pozo
Lugar de Muestreo	:	Entrada al Filtro de Arena
Ubicación de la toma de la muestra	:	Ascención de Guarayos
Muestra tomada por	:	Mario Alberto Zapata
Fecha recepción de la muestra	:	18 /01 / 2010, Hrs. 16:20
Fecha de muestreo	:	19 /01 / 2010, Hrs. 10:50
Fecha de entrega	:	29 / 01 / 2010, Hrs. 17:00
Teléfono	:	1780885737

Nº	PARAMETROS	UNIDADES	METODOS DE ANALISIS *	LIMITES DE DETECCION	VALORES MXIMOS ADMISIBLES	RESULTADO DE ANALISIS
1	Coliformes Fecales	NMP / 100 ml	Tubos Múltiples (9221 - C)	2,0	< 2,0	9,3 E +01
2	Coliformes Totales	NMP / 100 ml	Tubos Múltiples (9221 - B)	2,0	< 2,0	9,3 E +01
3	Turbidez	NTU	Nefelométrico (2130 - B)	0,01	5.0	///////

Ing. Roman Gutiérrez Tito
JEFE TECNICO
UTALAB UAGRM

UNIVERSIDAD AUTONOMA GABRIEL RENE MORENO
U.T.A.L.A.B.
Santa Cruz - Bolivia

Contribuyendo al desarrollo regional y a la preservación del Medio Ambiente!

Este informe es un original único identificado como 48/10. Cualquier enmienda, corrección o raspadura invalida este documento.

Av. Centenario Esq. 2do. Anillo (Campus Universitario) Telf./Fax: [illegible] .com.bo
Santa Cruz - Bolivia

Figure B-4 Lab results from the sample taken before the UV treatment in Cerro Grande, January 18, 2010

UNIVERSIDAD AUTÓNOMA "GABRIEL RENE MORENO"

"Unidad Técnica de Apoyo a los Laboratorios"

UTALAB

Servicios Laboratoriales y Medioambientales

INFORME DE ENSAYO

Página 1 de 1

Nombre del Laboratorio : Universidad Autónoma "Gabriel René Moreno"
Identificación única del informe : 49/2010
Nombre del cliente : MARIO ALBERTO ZAPATA
Solicitado por : Mario Alberto Zapata
Muestra N ° 45 : Análisis de Agua de Pozo
Lugar de Muestreo : Salida al Filtro de Arena
Ubicación de la toma de la muestra : Ascención de Guarayos
Muestra tomada por : Mario Alberto Zapata
Fecha recepción de la muestra : 18 /01 / 2010, Hrs. 16:20
Fecha de muestreo : 19 /01 / 2010, Hrs. 10:50
Fecha de entrega : 29 / 01 / 2010, Hrs. 17:00
Teléfono : 1780885737

Nº	PARAMETROS	UNIDADES	METODOS DE ANALISIS *	LIMITES DE DETECCION	VALORES MXIMOS ADMISIBLES	RESULTADO DE ANALISIS
1	Coliformes Fecales	NMP / 100 ml	Tubos Múltiples (9221 - C)	2,0	< 2,0	9,00 E + 00
2	Coliformes Totales	NMP / 100 ml	Tubos Múltiples (9221 - B)	2,0	< 2,0	4,3 E + 01
3	Turbidez	NTU	Nefelométrico (2130 - B)	0,01	5.0	///////

Ing. Roman Gutiérrez Tito
JEFE TECNICO
UTALAB UAGRM

UNIVERSIDAD AUTONOMA GABRIEL RENE MORENO
U.T.A.L.A.B.
Santa Cruz - Bolivia

Contribuyendo al desarrollo regional y a la preservación del Medio Ambiente!

Este informe es un original único identificado como 48/10 . Cualquier enmienda, corrección o raspadura invalida este documento

Av. Centenario Esq. 2do. Anillo (Campus Universitario) Telf.Fax: ...com.bo
Santa Cruz - Bolivia

Figure B-5 Lab results from the sample taken after the UV treatment in Cerro Grande, January 18, 2010

UNIVERSIDAD AUTÓNOMA "GABRIEL RENE MORENO"
"Unidad Técnica de Apoyo a los Laboratorios"
UTALAB
Servicios Laboratoriales y Medioambientales

INFORME DE ENSAYO

Página 1 de 1

Nombre del Laboratorio	:	Universidad Autónoma "Gabriel René Moreno"
Identificación única del informe	:	50/2010
Nombre del cliente	:	MARIO ALBERTO ZAPATA
Solicitado por	:	Mario Alberto Zapata
Muestra N ° 46	:	Análisis de Agua de Pozo
Lugar de Muestreo	:	Entrada al Filtro de Arena
Ubicación de la toma de la muestra	:	Ascención de Guarayos (Comunidad de Cerro Grande)
Muestra tomada por	:	Mario Alberto Zapata
Fecha recepción de la muestra	:	21 /01 / 2010, Hrs. 16:20
Fecha de muestreo	:	20 /01 / 2010, Hrs. 11:10
Fecha de entrega	:	29 / 01 / 2010, Hrs. 17:00
Teléfono	:	1780885737

Nº	PARAMETROS	UNIDADES	METODOS DE ANALISIS *	LIMITES DE DETECCION	VALORES MXIMOS ADMISIBLES	RESULTADO DE ANALISIS
1	Coliformes Fecales	NMP / 100 ml	Tubos Múltiples (9221 - C)	2,0	< 2,0	2,3 E + 03
2	Coliformes Totales	NMP / 100 ml	Tubos Múltiples (9221 - B)	2,0	< 2,0	2,3 E + 03
3	Turbidez	NTU	Nefelométrico (2130 - B)	0,01	5.0	5,61

Ing. Roman Gutiérrez Pinto
JEFE TECNICO
UTALAB UAGRM

UNIVERSIDAD AUTONOMA GABRIEL RENE MORENO
U.T.A.L.A.B.
Santa Cruz - Bolivia

Contribuyendo al desarrollo regional y a la preservación del Medio Ambiente!

Este informe es un original único identificado como 48/10. Cualquier enmienda, corrección o escritura invalida este documento.

Av. Cañoto N° 1892 Esq. 2do. Anillo (Campus Universitario Piraí) Fax: (591-3) 3336570 utalab@uagrm.com.bo
Santa Cruz - Bolivia

Figure B-6 Lab results from the sample taken before the UV treatment in Cerro Grande, January 20, 2010

UNIVERSIDAD AUTÓNOMA "GABRIEL RENE MORENO"
"Unidad Técnica de Apoyo a los Laboratorios"
UTALAB
Servicios Laboratoriales y Medioambientales

INFORME DE ENSAYO

Página 1 de 1

Nombre del Laboratorio	:	Universidad Autónoma "Gabriel René Moreno"
Identificación única del informe	:	50/2010
Nombre del cliente	:	MARIO ALBERTO ZAPATA
Solicitado por	:	Mario Alberto Zapata
Muestra N ° 46	:	Análisis de Agua de Pozo
Lugar de Muestreo	:	Entrada al Filtro de Arena
Ubicación de la toma de la muestra	:	Ascención de Guarayos (Comunidad de Cerro Grande)
Muestra tomada por	:	Mario Alberto Zapata
Fecha recepción de la muestra	:	21 /01 / 2010, Hrs. 16:20
Fecha de muestreo	:	20 /01 / 2010, Hrs. 11:10
Fecha de entrega	:	29 / 01 / 2010, Hrs. 17:00
Teléfono	:	1780885737

Nº	PARAMETROS	UNIDADES	METODOS DE ANALISIS *	LIMITES DE DETECCION	VALORES MXIMOS ADMISIBLES	RESULTADO DE ANALISIS
1	Coliformes Fecales	NMP / 100 ml	Tubos Múltiples (9221 - C)	2,0	< 2,0	9.00 E 00
2	Coliformes Totales	NMP / 100 ml	Tubos Múltiples (9221 - B)	2,0	< 2,0	9.00 E 00
3	Turbidez	NTU	Nefelométrico (2130 - B)	0,01	5.0	14,81

Ing. Roman Gutierrez Tito
JEFE TECNICO
U.T.A.L.A.B

UNIVERSIDAD AUTONOMA GABRIEL RENE MORENO
U.T.A.L.A.B.
Santa Cruz - Bolivia

Contribuyendo al desarrollo regional y a la preservación del Medio Ambiente!

Santa Cruz - Bolivia

Figure B-7 Lab results from the sample taken after the UV treatment in Cerro Grande, January 20, 2010